NONINVASIVE DIAGNOSIS OF ACUTE COMPARTMENT SYNDROMES USING ULTRASOUND AND MECHANICAL VIBRATION: FEASIBILITY STUDY

by

AARON DELLAH

A thesis submitted to the Department of Mechanical Engineering

in conformity with requirements for

the degree of Master of Science (Engineering)

Queen's University

Kingston, Ontario, Canada

September, 1998

Abstract

Acute compartment syndrome is a rare limb-threatening condition characterized by the fluidic pressurization of muscle compartments bound by inextensible tissues. The etiology and current diagnostic techniques for compartment syndromes were reviewed and morbidity, time dependency and clinical uncertainty were identified as the factors warranting the need for a non-invasive diagnostic technique. Following a review of the literature and analysis of existing and proposed new techniques, the "mechanical response technique" using a vibratory stimulus and ultrasound imaging was selected for the feasibility study.

A simple mechanical model was designed to simulate a compartment syndrome. The model consisted of two concentric cylinders pressurized with water representing a muscle compartment inside a limb-like structure. Compartment pressures were varied and the model was subjected to mechanical vibration. The motion of the compartment walls was monitored with ultrasound imaging. A pilot study was performed to determine which parameters were best suited for measuring compartment motion.

A second study measured the displacement amplitude of the compartment wall closest to the source of a 5 Hertz vibration. The "limb" pressure was held constant at 7mmHg and the "compartment" pressure varied from 0 to 45mmHg relative to the limb. Displacement amplitudes were found to initially decrease with increased compartment pressure and then remain constant. The system response was approximated using a mass-spring-damper model.

The data proved that the "mechanical response" technique was a promising idea warranting further research. The success of the experiment was considered limited because of the simplicity of the mechanical model. It was recommended that a better compartment syndrome model be developed, and further improvements be made to the vibration and ultrasound data collection components of the study.

Acknowledgements

No man walks alone; the following people have shared my journey.

I would first like to thank my supervisors: Dr. Carolyn Small for her support, understanding, insight, motivation and kindness, and Dr. Dave Pichora for sharing his knowledge, experience and ideas.

I would especially like to thank Dr. Fraser Saunders for allowing me the use of his ultrasound equipment and lab space. Without his generosity and commitment, the work herein would not have been complete. I would also like to thank Pat Cledgett and , and Helen Prohaska for their patience and expertise for showing me how to operate the ultrasound equipment.

Many suggestions and ideas used in this thesis were contributed by members of the Clinical Mechanics Group including Dr. Carolyn Small, Dr. Dave Pichora, Dr. Tim Bryant, and Dr. Randy Ellis. Dr. Genevieve Dumas helped me to obtain some additional funding through Ontario Graduate Studies for which I am very thankful. Much appreciated technical assistance was provided by Dave Siu, Gerry Saunders, Barb Baker, Paul Greene, Alan McPhail, Geoff Brooks, Andy Bryson and Dr. John Garner. Finally, thanks to Gayle Laporte, Etta Cerisano, Barb Higgins, and Jacquie Paquin for keeping things running so smoothly while I was at Queens.

Many friends have helped along the way including Jason Carey, Gordon McAlary, David Kirby, Tony Yang, Olivier LeRudulier, Patricia McAllister, Egil Naesguthe, Paulo Pagot, Radu Zdero, Jeff Cassin, Mark Danby, Paul Dederer, Guy Oram, and last but not least, Katia Dyrda. Too many memories for words to do them justice, I thank you all for your help and your friendship. Reaching deeper into the past, I cannot forget to include Robert Grandmaison, Richard Nishimura, S. P. Singh, Sheryl Goodall, Stephanie Greene, Colleen Leonard, Shane Monty, Alex Meldrum, Artur Pawelec, Pawel Mlynarski, and Krzysztof Staniszewski. You have all played a leading role in my life.

Finally, no acknowledgements would be complete without expressing my love to my parents Abdellatif and Carolyn, my brother Shan, my sister Nayla, and my soul mate Patricia Moussette. Thank you for your unconditional support. I love you all.

Table of Contents

List of Figures

List of Tables

Table of Conversions

In clinical practice and related publications, the units for measuring compartment syndromes pressures are millimetres of mercury (mmHg). This thesis uses the traditional units of millimetres of mercury in favour of Pascals.

Furthermore, the construction of the testing apparatus was built using standard stock parts with U.S. Customary System (USCS) dimensions. To avoid the confusion of using two sets of units, all engineering drawing been dimensioned in USCS units and only key dimensions have been converted to SI units.

The above mentioned units can be converted to their SI equivalents by using the following conversion factors:

USCS - SI Conversions
1mmHg = 133.3 Pa
30mmHg = 4000Pa
1 inch = 25.4mm

All experimental measurements were performed in SI and are so reported.

Chapter 1: Introduction

Acute compartment syndrome is a limb-threatening condition that is difficult to diagnose and treat. This condition is characterized by the fluidic pressurization of muscle compartments bound by inextensible tissues. The shortfalls of current practice have prompted the research for developing a new, noninvasive diagnostic technique for this condition. The work presented in this thesis demonstrates the feasibility of detecting differentially pressurized compartments enclosed in a volume of fluid, through ultrasound detection of evoked vibration of the compartment wall.

A review of the literature covering the clinical aspects of compartment syndromes, current diagnostic techniques and previous attempts at noninvasive diagnosis is presented (Chapter 2). Concurrent to the literature review, brainstorming ideas for new diagnostic techniques were compiled, both existing and proposed new techniques were analyzed for their feasibility (Chapter 3). The analysis concluded that ultrasound imaging might be used to observe the mechanical response of a differentially pressurized compartment subjected to an externally applied vibration.

An experimental apparatus and methodology were developed. The apparatus included a water-filled "artificial limb", a vibration stimulus jig, and a probe holder for a commercial ultrasound imaging (Chapter 4).

The ultrasound machine's M-Mode and Doppler mode images, providing displacement and velocity data respectively against time, were used to observe the vibratory response

of the compartment walls under a range of conditions. A series of tests performed to investigate pressure dependence showed large amplitude changes at low pressures (Chapter 5).

This work shows that ultrasound imaging can remotely detect altered mechanical vibratory response in a membrane enclosing a pressurized compartment. The implications and limitations are discussed in Chapter 6. The technique looks promising, and further research is required to determine if the technique is applicable in a clinical environment. Some recommendations for future work are included in Chapter 7.

Chapter 2: Literature Review

2.1 Clinical Aspects of Compartment Syndrome

A widely accepted definition of compartment syndrome is "...a condition in which increased tissue pressure within a limited space compromises the circulation and the function of the contents of that space."[14] The most common sites for this condition are the muscle compartments of the forearm and lower leg[15,21]. The most common of the numerous causes for compartment syndrome is trauma. Regardless of the cause, all compartment syndromes are characterized by a steady increase in the interstitial fluid pressure and eventual tissue damage in the affected compartment. The current means of detecting a compartment syndrome include clinical assessment and direct (invasive) measurements of the intra-compartment pressure. Compartment syndrome is treated surgically; failure to treat a compartment syndrome can lead to tissue necrosis, contracture or amputation of the affected area.

2.1.1 Etiology

The onset of compartment syndrome requires a relatively rigid enclosure that restricts the volume of the tissues therein. Such enclosures may be bounded by noncompliant tissues, bone, or circumferential dressings such as casts or splints. The extremities are especially vulnerable to compartment syndromes because they are subdivided into well defined compartments by tough, inelastic, fibrous tissues called fascia. The areas most commonly affected by compartment syndromes are the lower leg and forearm (see Figure

2-1). Other sites reported in the literature include muscle compartments in the upper arm, thigh, hand, foot, abdomen, lumbar spine, buttocks, and eye region.[4]

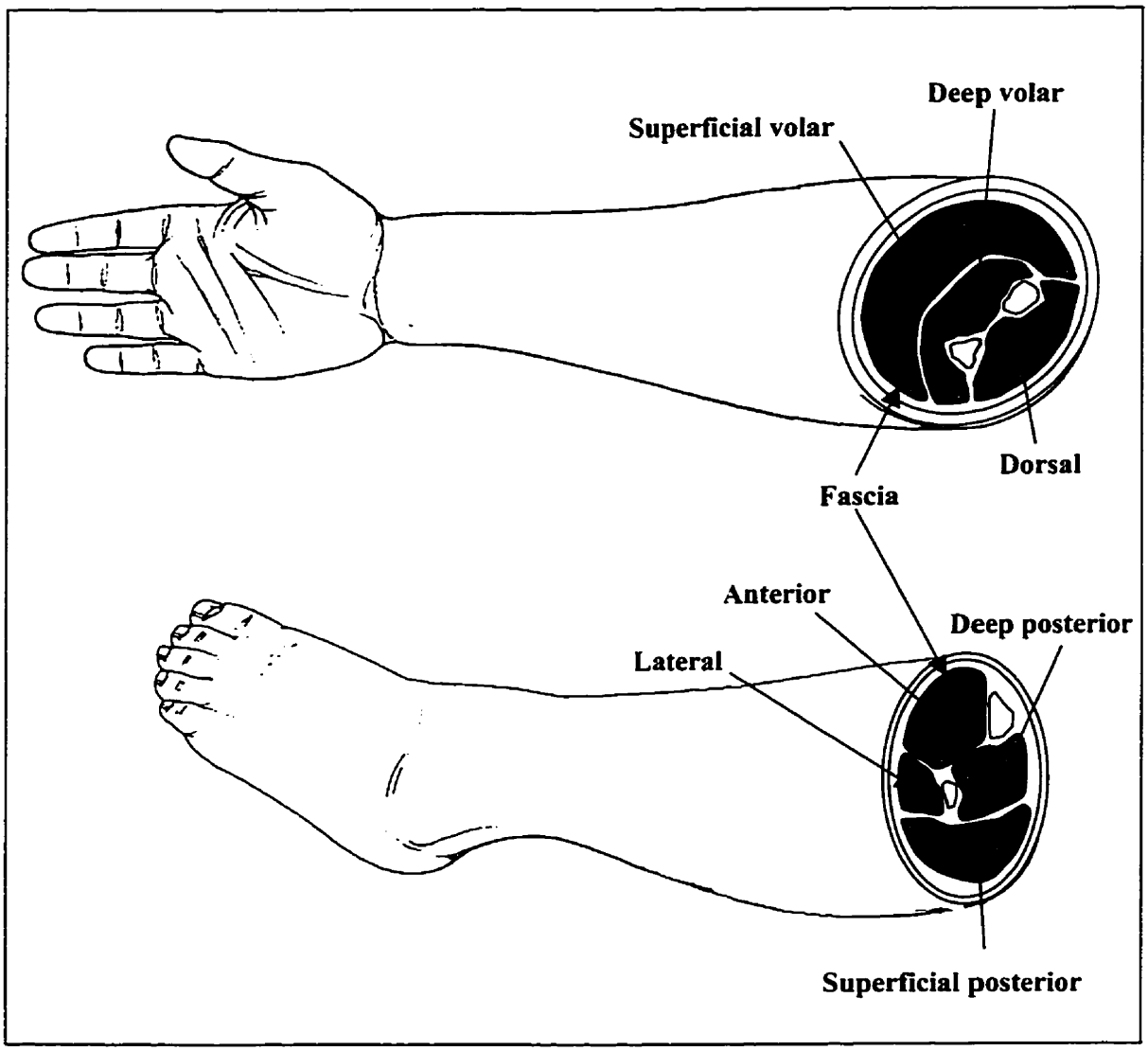

Figure 2-1 Compartments of the forearm and lower leg. (Adapted from Rorabeck[21])

The lower leg is divided into four osteo-fascial compartments: the anterior, lateral, deep posterior and superficial posterior. Of these, the anterior and lateral are most susceptible to compartment syndromes. The forearm is divided into three compartments: the dorsal,

deep volar and superficial volar. Of these, the volar compartments are most frequently affected.

Compartment syndromes result from a variety of injuries and/or abnormalities. The leading causes of compartment syndromes have been identified as fracture, soft tissue injuries, arterial injuries, limb compression, and thermal injuries including burns and frostbite (Figure 2-2).[15]

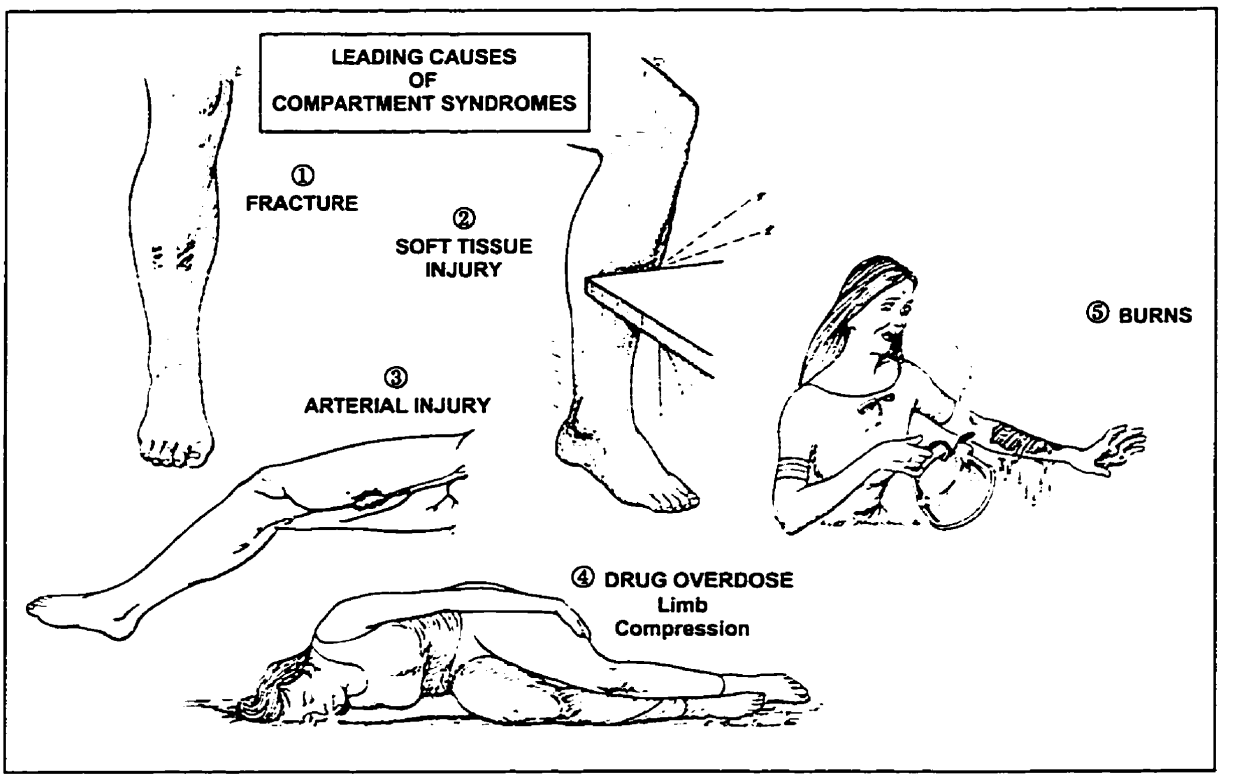

Figure 2-2 Leading causes of compartment syndromes. (From Mubarak & Hargens[15])

Two detailed lists of the causes of compartment syndromes can be found in the literature and are presented here in Table 2-1. The lists differ in their classification schemes, but both categorize their causes under two main mechanisms: decreased compartment volumes and/or increased compartment contents.

Classification of Acute Compartment Syndromes

Decreased Compartment Size
- Constrictive dressings and casts
- Closure of fascial defects
- Thermal injuries and frostbite

Increased Compartment Contents
- Primary edema accumulation
  - Postischemic swelling
    - Arterial injuries
    - Arterial Thrombosis or embolism
    - Reconstructive vascular and bypass surgery
    - Replantation
    - Prolonged tourniquet time
    - Arterial spasm
    - Cardiac catheterization and angiography
    - Ergotamine ingestion
  - Prolonged immobilization with limb compression
    - Drug overdose with limb compression
    - General anesthesia with knee-chest position
  - Thermal injuries and frostbite
  - Exertion
  - Venous disease
  - Venomous snakebite
- Primary hemorrhage accumulation
  - Hereditary bleeding disorders, e.g. hemophilia
  - Anticoagulant therapy
  - Vessel laceration
- Combination of edema and hemorrhage accumulation
  - Fractures
    - Tibia
    - Forearm
    - Elbow, e.g., supracondylar
    - Femur
  - Soft tissue injury
  - Osteotomies, e.g. tibia
- Miscellaneous
    - Intravenous infiltration, e.g., blood, saline
    - Popliteal cyst
    - Long leg brace

(a)

Etiologies of Compartment Syndrome

Increased Compartment Content

Bleeding
- Major vascular injury
- Coagulation defect
  - Bleeding disorder
  - Anticoagulant therapy

Increased capillary filtration
- Reperfusion after ischemia
  - Arterial bypass grafting
  - Embolectomy
  - Ergotamine ingestion
  - Cardiac catheterization
  - Lying on limb
- Trauma
  - Fracture
  - Convulsion
- Intensive use of muscles
  - Exercise
  - Seizures
  - Eclampsia
  - Tetany
- Burns
  - Thermal
  - Electrical
- Intra-arterial drug injection
- Orthopedic surgery
  - Tibial osteotomy
  - Hauser procedure
  - Reduction and internal fixation of fractures
- Snakebite

Increased capillary pressure
- Intensive use of muscles
- Venous obstruction
  - Phlegmasia cerulea dolens (i.e., acute inflammation and edema of the legs)
  - Ill-fitting leg brace
  - Venous ligation
- Diminished serum osmolarity(i.e. nephrotic syndrome)

Decreased Compartment Volume
- Closure of fascial defects
- Excessive traction on fractured limbs

Miscellaneous
- Infiltrated infusion
- Pressure transfusion
- Leaky dialysis cannula
- Muscle hypertrophy
- Popliteal cyst

External Pressure
- Tight casts, dressings, or air splints
- Lying on limb

(b)

Table 2-1 Causes of compartment syndromes as compiled by (a) Mubarak & Hargens[15] and (b) Matsen (in Cook[4]).

The main physiological factors contributing to the onset of compartment syndromes are external compression, edema and hemorrhaging. External compression is caused by constrictive dressings or prolonged immobilization with limb compression. The compressive forces are transmitted to the compartments, thereby increasing the intra-compartmental pressure. Edema, or swelling, refers to the accumulation of excess fluid in any body tissue and can result from fracture, soft tissue or thermal injuries. Edema can also occur after an arterial occlusion is cleared, and the restored blood flow causes post-ischemic swelling. The excess fluids related to edema result in increased intracompartmental pressure. Hemorrhaging refers to excessive discharging of blood caused by a coagulation disorder or the rupture of a blood vessel. Similar to edema, hemorrhaging increases the fluid content of the compartment, thus increasing the intracompartmental pressure.

Once a compartment syndrome is established, pressure in the affected compartment continues to rise. The traditional hypothesis states that increasing pressures decrease the longitudinal arteriovenous (A-V) pressure gradient in the compartment[8]. The decrease in the A-V pressure gradient leads to reduced flow and oxygen levels in the compartment tissues (hypoxia). The body responds to the hypoxia by releasing histamine, a vasodilator, to improve the local blood flow. However, the histamine also increases the capillary membrane permeability, which releases cellular fluids into the affected compartment. The effect of the body's reactionary measures is an acceleration of the deteriorating compartmental and A-V pressures. The outcome of this degenerative loop is a complete loss of perfusion to the compartment. The loss of perfusion leads to

ischemia which causes decreased capillary retention and failure of the sodium pump. Consequently, more fluid is released into the compartment, further increasing the compartment pressure.

Elevated pressures impair the microcirculation first at the level of the capillaries and venules which have the lowest perfusion pressure. Impaired perfusion occurs when compartment pressures exceed approximately 30 mmHg.[8] [14] Normal compartment pressures range from 7 to 10 mmHg.

2.1.2 Treatment

Compartment syndromes presenting clinical symptoms and elevated intracompartmental pressures are eligible for treatment through surgical decompression. There is no uniform agreement on the pressure threshold for diagnosing a compartment syndrome that requires treatment. Commonly accepted values for compartment pressure are +30mmHg (relative to atmospheric pressure) or –30mmHg (relative to diastolic blood pressure).

The treatment, known as fasciotomy, consists of cutting the restrictive fascia along the length of the compartment in order to relieve the pressure inside(Figure 2-3). Wounds are dressed and left to heal for 7 to 10 days before closing. A skin graft is often required to complete the closing procedure.

Medicinal treatments such as anti-coagulants and vasodilators have been used in an attempt to treat compartment syndromes. However, these only helped to perpetuate the cycle of continuously increasing compartment pressures.

The extent of irreversible tissue damage in compartment syndromes increases relative to the compartment pressure and duration of pressurization. Since no experimental studies have gone so far as to induce permanent damage in human subjects, researchers have had to rely on animal studies to obtain this information. Permanent deficits in canine models of compartment syndromes have been reported to occur at pressures as low as 40mmHg in as little as twelve hours.[22] These data stress that an early diagnosis and treatment of compartment syndromes is required in order to prevent the loss of neural or muscular functions.

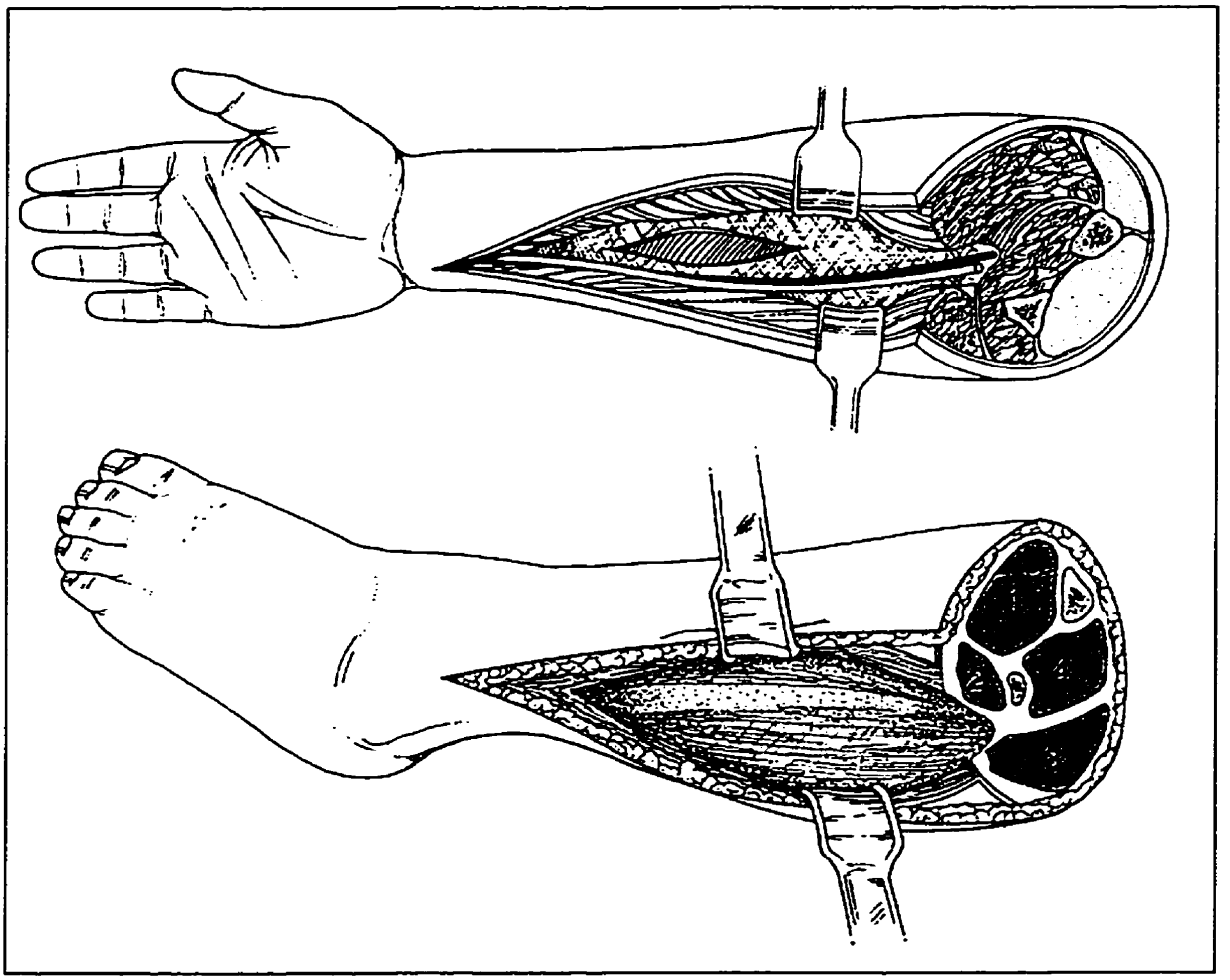

Figure 2-3 Fasciotomy of the forearm and lower leg. (From Rorabeck[21])

2.1.3 Current Diagnostic Techniques

The current practices for diagnosing compartment syndromes include clinical assessments and the measurement of intracompartmental pressures. Clinical assessments, for the most part, require a conscious, co-operative patient. Symptoms may include pain, numbness, weakness or increased stiffness in the affected area. Pain out of proportion for the patient's injuries is the first and most prominent symptom of a compartment syndrome. Muscle stiffness can be evaluated through experienced palpation and comparison of right and left limbs. Although clinical evaluations are usually the first signs of an impending compartment syndrome, some or none of the clinical symptoms may present, and all require an experienced clinician to provide an accurate evaluation. For these reasons, positive clinical assessments are usually followed by direct measurement of the compartment pressure. In the unconscious or uncooperative patient, the decision to perform the invasive pressure measurement relies solely on the physician's experience and assessment of the seriousness of the case.

Intracompartmental pressure measurements can be performed with one of several invasive catheter techniques, all of which determine the hydrostatic pressure in a small volume of fluid introduced into the suspect compartment.

The needle manometer or Whitesides technique was the first method introduced for measuring compartment pressures.[21] The set-up consists of a syringe, a mercury manometer, and a saline filled needle inserted into the compartment (Figure 2-4). The syringe is used to increase the pressure in the tubing until movement of the air-saline

meniscus is observed; the manometer reading at the onset of this movement is the intracompartmental pressure. This technique uses equipment readily available in most hospitals, but is not as reproducible as other techniques.[21]

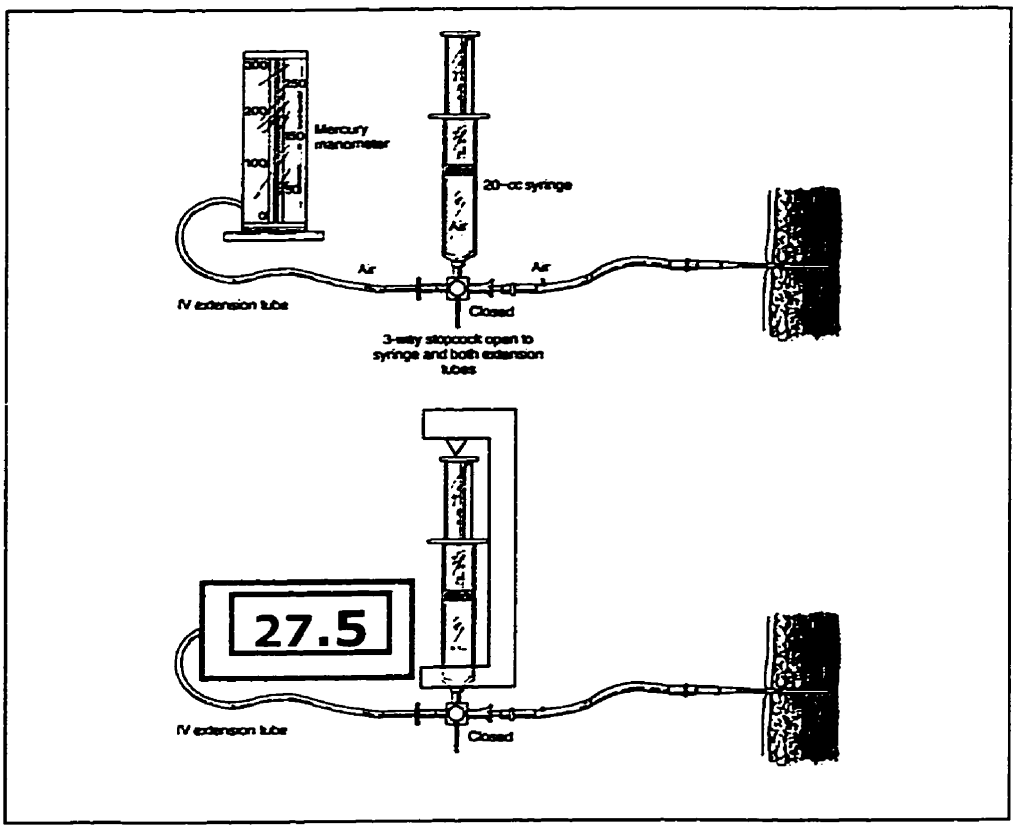

Figure 2-4 Whitesides needle manometer (above) and modified version for continuous infusion/measurement (below). (Adapted from Rorabeck[21])

In the modified needle technique (continuos infusion) the syringe is depressed mechanically, and the pressure required to infuse the saline solution is recorded as the compartment pressure. Unfortunately, the continuous infusion method tends to give artificially high readings and is susceptible to blockage due to clotting.[15,21] Furthermore, continuous infusion of fluid into the compartment aggravates the compartment syndrome. Current practice uses the wick and slit catheter techniques for long term monitoring. A wick or slit catheter is connected to a pressure transducer via saline filled IV tubing and is

inserted into the muscle compartment through a needle which is subsequently removed (Figure 2-5). Once in place, the catheter can be left in the compartment for long term intracompartmental pressure monitoring. Both the wick and slit catheters are designed to push tissues away from the tips and help maintain open passages for fluids, however, it is recommended that they be flushed with saline every six hours.[23]

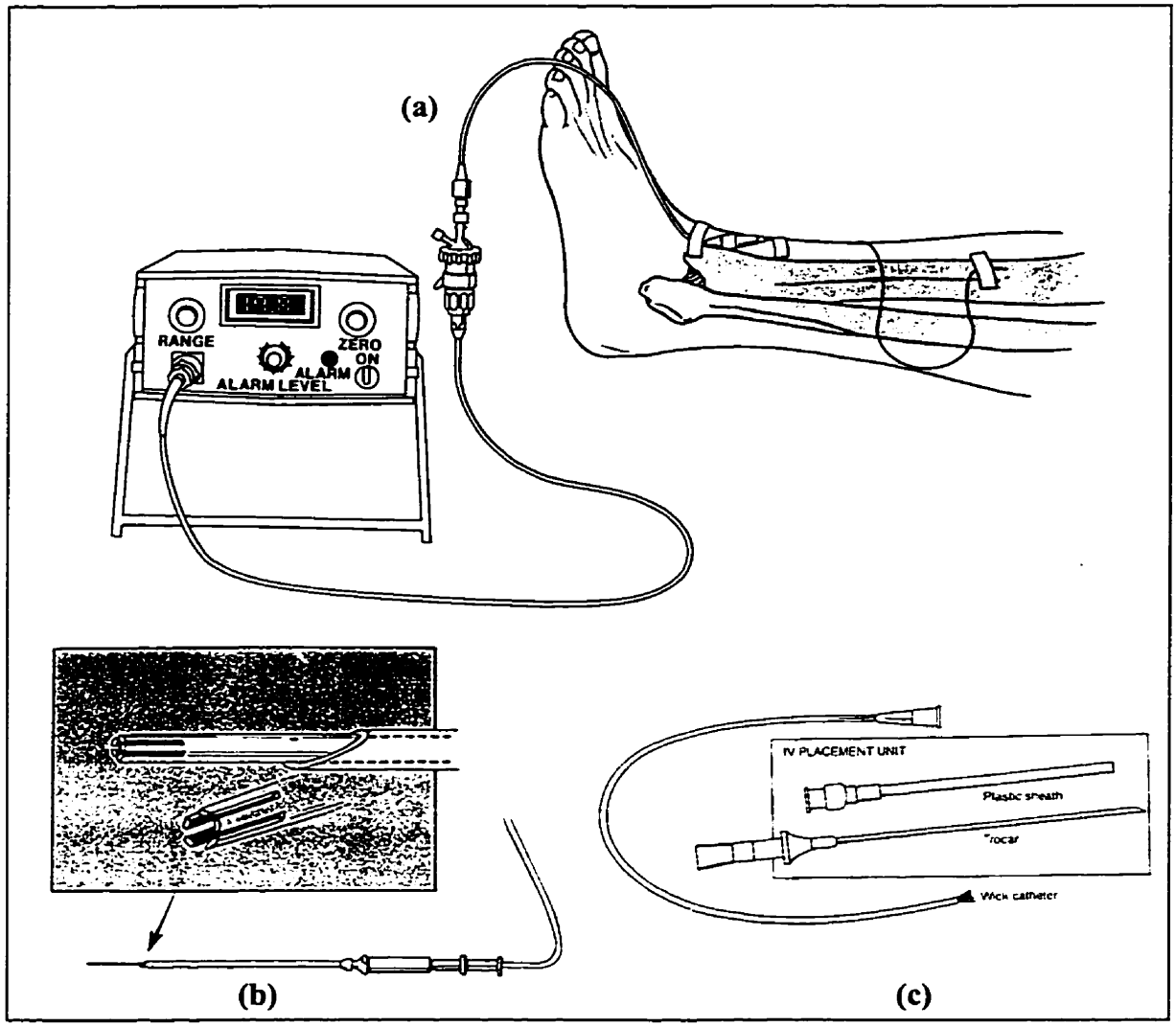

Figure 2-5 (a) Catheter techniques for (b) slit and (c) wick catheters. (Adapted from Rorabeck[21])

The latest catheter, the Solid-state Transducer Intracompartmental Catheter (S.T.I.C), measures compartment pressure via a silicone semiconductor strain gauge fitted inside a

rigid, perforated polyethylene tube (Figure 2-6). The S.T.I.C. catheter is filled with saline solution and, like its predecessors, introduced to the compartment through a needle. Compartment pressures can then be read once, or monitored continuously. Measurements from the S.T.I.C. catheter are comparable to those of the wick and slit catheter techniques.[21] Advantages of the S.T.I.C. catheter are its ease of setup and portability. The only disadvantage is its loss of accuracy over time when used for continuous monitoring.[21]

Figure 2-6 S.T.I.C catheter. (FromGood[8])

In general, all the invasive pressure measurement techniques require infusing fluid into the already pressurized compartment. Although the amount of fluid required is small, repeated and continuous infusion measurements should theoretically accelerate the rate of deterioration of the compartment. Unfortunately, without the fluid medium between the

compartment tissues and the catheter, the invasive pressure systems are unable to record the intracompartmental pressures.

2.1.4 Summary - Why a New Technique is Needed

The high morbidity and accompanying uncertainty of clinical assessments creates the necessity for an accurate means of diagnosing compartment syndromes. The current techniques create additional risk, pain, and discomfort for the patient. Furthermore, the current techniques require a physician trained to perform the procedure. An accurate, noninvasive diagnostic technique would be more suitable for continuous or repeated use, less harmful to the patient, and could be used by untrained staff as a screening test in the case of uncertainty.

2.2 Non-invasive Techniques in the Current Literature

A critical review of the literature has led to a compilation of different models used to simulate compartment syndromes, the different noninvasive diagnostic techniques used to diagnose them, and the advantages and disadvantages of these techniques. These techniques can be subdivided into five categories based on the properties that they attempt to measure: biochemical, hemodynamic, neurological, imaging, and mechanical.

2.2.1 Compartment Syndrome Models

Excluding clinical trials, four different methods for modelling compartment syndromes have been published in the literature: two invasive models used on animals and cadavers, and two non-invasive models used on humans subjects.

The most popular compartment syndrome model involves injecting excess fluid (usually blood) into an animal or cadaveric compartment until the desired compartment pressure is reached.[5,9,10,18,19,22,25,26] A similar technique reported the insertion of a fluid filled balloon into the anterior compartment of a rabbit limb.[24] Compartment pressure was controlled through balloon inflation and deflation. In both models, compartment pressures require verification with invasive measurements.

The simplest human model of compartment syndrome includes the application of external pressure via a wide pressure cuff or similar device[3,13]. A direct correlation between external and compartment pressure has been documented. A more elaborate model is exercise induced compartment syndrome in patients with chronic compartment syndromes.[2,28] This model requires invasive pressure measurements.

To date, there is no published literature describing an all mechanical simulator of compartment syndromes.

2.2.2 Biochemical Properties

Hypoxia and ischemia associated with the later stages of compartment syndromes change the biochemical composition of the tissues and fluids contained in the affected compartments. Several researchers have exploited this phenomenon in their attempt to diagnose compartment syndromes.

Breit et al.[2] demonstrated that tissue pO_2 and Hemoglobin (Hb) levels could be measured non-invasively using near-infrared spectroscopy. Their study used the pressure cuff model to simulate chronic compartment syndromes in humans and found significant ($p<0.05$) decreases in pO_2 levels and increases in Hb levels due to the application of external pressures. Despite the success of this study, the advantage of the near-infrared spectroscopy's non-invasiveness is balanced with the disadvantage that it can only provide readings relative to a patient's previously measured "normal" values. Until this problem can be overcome, its current usefulness in a clinical setting is minimal.

Heppenstall et al.[10] measured levels of inorganic phosphate (IP), phosphocreatine (CP) and pH using phosphorus nuclear magnetic resonance (P-NMR) spectroscopy. Their research used a canine blood infusion model of compartment syndromes and showed significant increases ($p<0.05$) in the IP:CP ratio, and significant decreases ($p<0.05$) in pH for all compartments whose pressure was within 20 mmHg of the mean arterial blood pressure. Unfortunately, magnetic resonance imaging is prohibitively expensive making it an unrealistic tool for diagnosing compartment syndromes.

2.2.3 Hemodynamic Properties

Increasing pressures in compartment syndromes change the dynamics of blood flow and pressures in and around the affected compartment. Studies on the pressure-flow relationships in compartment syndromes focus primarily on the arterial and venous flows to and from the compartment.

In their canine study, Gall et al.[5] used noninvasive electromagnetic and plethysmographic techniques to measure arterial and venous blood flow respectively. Results indicated a significant ($p<0.05$) drop in arterial and venous flow at compartment pressures of 80 and 40mmHg respectively. Furthermore, the analysis revealed a strong correlation ($r=-0.85$, $p<0.01$) between compartment pressures and venous blood flow. These results are confirmed in the long-term clinical study performed by Jones et al.[11] who assessed the quality of venous flow with an acoustic Doppler probe in patients suspected of having compartment syndromes. Their study found a perfect correlation between patients with compartment syndrome and abnormal venous flow, and a less than perfect correlation between patients with compartment syndrome and compartment pressures greater then 30mmHg. These results indicate that the qualitative assessment of Doppler venous flow has a higher sensitivity and specificity than invasive pressure measurements. The only fault with this study was that all the patients had initial or evolving neurological deficits indicating that the diagnosis was being performed in the late stages of the syndrome.

In addition to blood flow, Gall et al. also used plethysmography to measure venous capacitance (a measure of the maximum volume of a limb whose venous return has been

occluded) in their canine model of compartment syndromes. Their results indicated that capacitance levels were significantly ($p<0.05$) less then normal when pressures exceeded 40mmHg and had a strong correlation ($r=-0.91$, $p<0.01$) with compartment pressures.

In a pressure related study, Willey et al.[28] used a non-invasive auscultatory technique on humans to evaluate the compartment pressures in exercise induced compartment syndromes. The technique hypothesized that the anterior tibial compartment acts like a pressure cuff and occludes the anterior tibial artery. If this were the case, Korotkoff sounds distal to the tibial compartment could be produced by elevating the patient's leg (Figure 2-7). A simple formula could then used to calculate the compartment pressure from the leg height. The study found changes in compartment pressures in the pathological subjects was higher (range: 16 to 39mmHg) then the controls (range: ~2 to 9mmHg). The auscultatory technique appears to be a simple non-invasive method of diagnosing anterior tibial compartment syndromes. However, it cannot diagnose the condition in some compartments because not all compartments have arteries that run close enough to the limb surface to hear Korotkoff sounds.

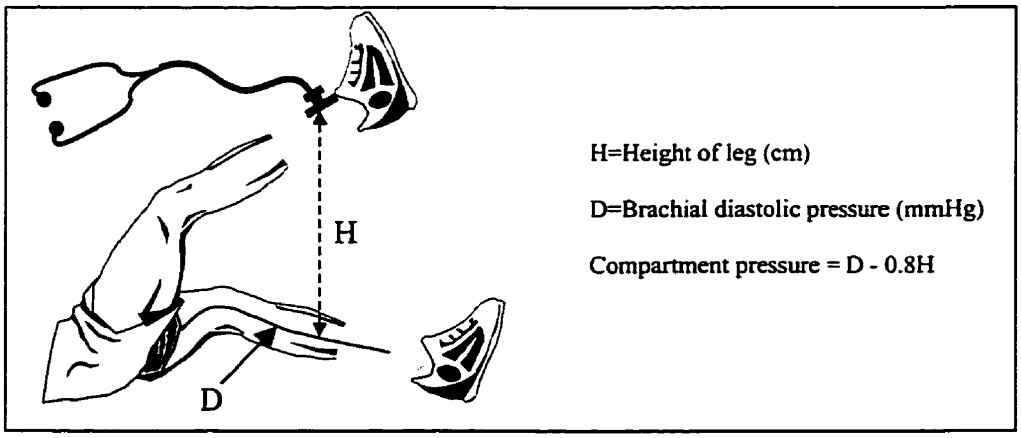

Figure 2-7 Auscultatory technique for measuring anterior tibial compartment pressure.

2.2.4 Neurological Properties

Increasing compartment pressure impairs the function of nerves in a compartment syndrome. These neurological deficits manifest themselves in animal and human studies through reductions in nerve conduction velocities, action potentials, and sensory perception.

Hargens et al.[9] and Rorabeck & Clarke[22] demonstrated this phenomenon in their canine studies of compartment syndromes. Using the blood injection model, both authors concluded that action potentials and nerve conduction velocities measured with surface electrodes decreased with increased time and pressure, and that complete nerve conduction failure occurred when pressures were 50mmHg or higher. Studies by Matsen et al[13] and Chidgey et al.[3] have produced similar results in man using an external compression model with surface electrode electromyography.

In a related field, Present et al.[18] used surface electrodes to monitor somatosensory evoked potentials(SEP) in the median, deep peroneal, and tibial nerves of monkeys with fluid injection models of compartment syndromes. The SEP waveforms were found to be "significantly" decreased with compartment pressures as low as 30mmHg and as early as 45 minutes of pressurization.

Three authors including Chidgey et al.[3], Matsen et al.[13], and Phillips et al.[17] evaluated sensory perception in humans subjected to externally applied compression of the nerve. All three shared the same conclusion that increased compartment pressure and duration of

compression decreased sensory perceptions. Phillips et al. went one step further and determined that perception of a 256 Hertz vibratory stimulus was the earliest and therefore best indicator for detecting increased compartment pressures.

Neurological deficits occur only with time, after pressurization is established. Altered neurological properties are unsuitable for early diagnosis of compartment syndromes.

2.2.5 Physical Properties

Physical factors related to compartment syndromes include compartment size and firmness. Both of these factors are attributed to the increasing amounts of fluid present in the affected compartment whose volume is constrained by bone and fascia.

Robinson et al.[20] measured both ipsi- and contra-lateral limb circumferences in six patients diagnosed with anterior compartment syndromes of the thigh before and after recovery. Their results showed no significant differences between the measurements, indicating that limb circumference alone is not a good indicator of compartment syndromes. Gershuni et al.[7] and Brahim & Zaccardelli[1] both studied the use of ultrasound for measuring the width of the anterior compartment in man and suggested that this measurement technique could be useful to help diagnose compartment syndromes. Diagnosing compartment syndromes by measuring changes in volume is difficult because volume changes are small and only occur at the very onset of pressurization.

Steinberg & Gelberman[25] used a non-invasive indentation technique to determine the "hardness" of limbs affected with compartment syndromes (Figure 2-8). In their canine, cadaveric and human clinical trials, significant correlation ($r=0.87$ to 0.99, $p<0.05$) was found between the ratio of ipsi- vs. contra-lateral compartment pressures and the ratio of ipsi- and contra-lateral "hardness". The results indicated that "hardness" is an excellent measure for diagnosing compartment syndromes.

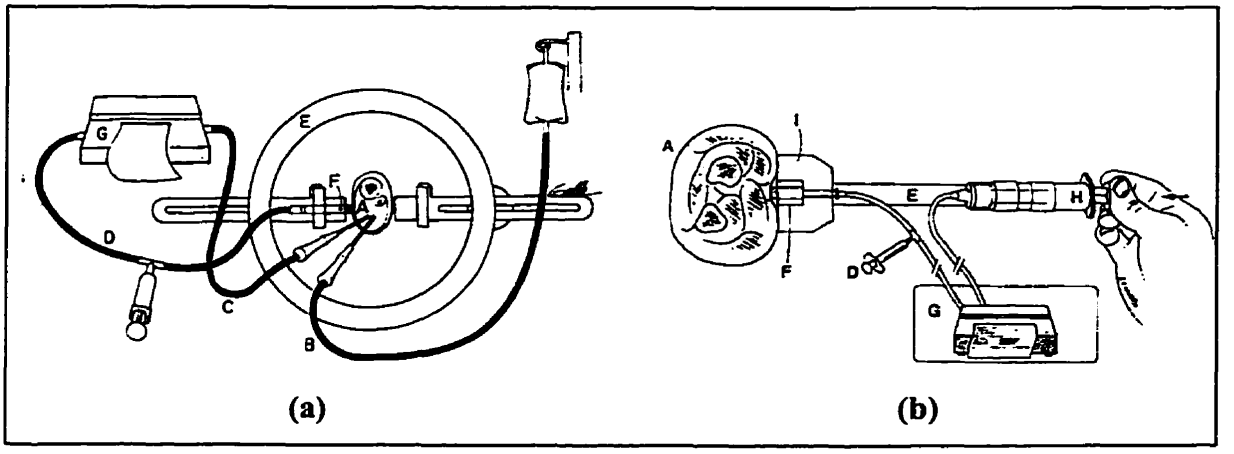

Figure 2-8 Piston probe used to measure "hardness" in (a) laboratory and (b) clinical studies. (A) Limb of dog, anatomic specimen or patient. (B) Plasma injected through 14-guage catheter. (C) Wick catheter. (D) Syringe for lowering or raising pressure in the probe F. (E) Plexiglass brace. (F) Low-friction piston-probe. (G) Flat-bed recorder. (H) Pressure of 300 mmHg is applied to the syringe H securing the platform I and probe F against the limb. (I) Platform holding probe F. (From Steinberg & Gelberman[25])

2.2.6 Imaging Properties

Three authors have indicated their use of computer aided topography (CT) scans in the diagnosis of compartment syndromes [12,16,27]. The case studies presented in all three publications indicate that CT can be used to locate moderate muscle necrosis in muscle compartments. This technique is non-invasive, but impractical due to its high cost and delayed diagnosis.

2.3 Summary

Compartment syndromes are rare, morbid pathologies that result from many possible causes. However, all compartment syndromes exhibit the same pattern of increasing pressurization. For whatever cause, fluid accumulates at low pressures until the normally "loose" tissue constraints become taut, and pressures then begin to rise. The key to early diagnosis lies in detecting compartments whose interstitial fluid pressure has been raised to the point where the fluid volume becomes constrained by bone and fascia stretched to its limit. The interstitial pressure required to achieve this limit is very low, within the range of 30mmHg (4 kPa).

Chapter 3: Theory

The motivation for this research project was the hypothesis that a reliable, quantitative, noninvasive technique for diagnosing compartment syndromes could be developed. A key component was the design and construction of an experimental model, which is described in the next chapter. This chapter deals with the selection of the most promising noninvasive measurement technique.

3.1 Proposed Diagnostic Techniques

Several brainstorming sessions produced a list of new ideas that were categorized into the same groups used in the literature review. A short description of each technique is provided below, and the advantages and disadvantages of each technique are listed in Table 3-1.

3.1.1 Stiffness

One of the first ideas for a non-invasive diagnostic technique for compartment syndrome was to build a modified tonometer that could measure the indentation stiffness of a limb surface. The idea was based on the hypothesis that a symptomatic muscle compartment would be "stiffer" than a normal muscle. Sensitivity due to population variances in tissue stiffness could be controlled through comparisons to contralateral limbs. Such a device, similar to the one designed by Steinberg & Gelberman[25], would measure the force-displacement characteristics of a tissue indentor.

PROPOSED TECHNIQUES	PROS	CONS
Physical Properties:		
Stiffness	Ease of use; Simplicity	Insensitive to deep compartments; Previously done[25]
Circumferential Stiffness	Ease of use; Simplicity; Possibly sensitive to deep compartments	No compartment specificity
Limb Circumference	Very easy and repeatable; No equipment required; Cheap	Requires animal or human subjects; No compartment specificity; Insensitive to late stage compartment syndromes; Cannot discriminate swelling
Mechanical Response	Compartment specificity	Need external stimulation; Need means of monitoring tissue motion
Neurological Properties:		
Nerve Conduction Velocity		Requires animal or human subjects; Late diagnosis
Hemodynamic Properties:		
Localized Blood Pressure		Difficult to design appropriate mechanical model
Blood Flow - Plethysmography		Difficult to design appropriate mechanical model
Blood Flow - Ultrasound	Ability to measure local flow	Difficult to design appropriate mechanical model
Blood Flow - Tracking injection		Invasive; Difficult to design appropriate mechanical model
Biochemical Properties:		
Reactive Hyperemia		Requires animal or human subjects
Blood Composition		Invasive; Requires animal or human subjects
Pulse Oximetry		Inability to access deep tissues; Requires animal or human subjects
Imaging Properties:		
Ultrasound		Cannot detect pressure changes directly
CT Scans		Expensive; Can only visualize necrotic tissue
MRI		Expensive; Can only visualize necrotic tissue
Temperature:		
Temperature - Metabolic	Simplicity	Requires animal or human subjects
Temperature - Cooling rate	Simplicity	Difficult to design appropriate mechanical model

Table 3-1 Summary of diagnostic ideas, pros and cons

3.1.2 "Circumferential Stiffness"

Previous methods of quantifying tissue stiffness focus on applying force to a single point on the limb surface. Another approach to this technique could involve the application of a compressive force around the circumference of the limb with a device similar to a blood pressure cuff. Such a cuff could be inflated with a constant flow rate while the pressure required to maintain that flow rate was monitored. The pressure-flow characteristics of this compression could be used to define a "circumferential tissue stiffness" which would presumably be different between normal and symptomatic limbs.

3.1.3 Limb Circumference

The monitoring of limb circumference was another method suggested for diagnosing compartment syndrome. This would simply involve using a measuring tape to periodically measure the limb circumference of patients suspected of having a compartment syndrome. A correlation could then be drawn between the rate of increasing limb circumference to increasing pressure. The suggestion was based on the hypothesis that early stages of compartment syndrome might generate changes in the limb circumference significant enough to make a diagnosis. However, the measurement alone would not be able to discriminate swelling from compartment syndromes.

3.1.4 Mechanical Response to Impulse or Vibration

The "mechanical response" suggestion involves observing the mechanical response of a muscle compartment stimulated by an external impulse or vibration. The suggestion was borne from the idea that a pressurized muscle compartment would be more likely to move as a solid mass whereas a normal compartment would tend to deform like a jelly. Two types of mechanical stimulus were discussed: impulse and vibration, corresponding to the transient and steady state responses of the compartment respectively. It was noted that Gao et al.[6], are developing techniques for measuring tissue properties with the use of mechanical vibration and ultrasound imaging and that their findings could be useful in developing a similar technique for diagnosing compartment syndromes.

3.1.5 Nerve Conduction Velocity

The measurement of nerve conduction velocities to diagnose compartment syndromes was briefly considered, primarily because these measurements can be performed non-invasively. This could have been performed using surface electrode electromyography (EMG) on a human or animal model of compartment syndrome.

3.1.6 Localised Blood Pressure

It was suggested that a compartment syndrome might have an affect on the local arterial blood pressure of a limb. The rationale for this suggestion stemmed from the idea that a symptomatic compartment could compress nearby arteries, thereby reducing the blood pressure downstream. One suggested means of detecting whether or not this phenomena

occurred would be to use a modified blood pressure cuff to measure the arterial blood pressure at several locations along the length of the limb. However, this technique might not be practical in a trauma situation.

3.1.7 Blood Flow

Since later stages of compartment syndromes are characterized by a localized reduction in blood flow to the affected area, it was suggested that the measurement of this flow could lead to a possible diagnosis. Three means of measuring blood flow were discussed: plethysmography, Doppler ultrasound, and the tracking of an injected substance.

3.1.8 Reactive Hyperemia

Reactive hyperemia refers to the change in skin colour when a light pressure is applied and then removed from a skin surface. Since this phenomenon is related to local blood flow, it was suggested that the monitoring of this colour change could help diagnose compartment syndrome. The hypothesis proposed that locally decreased perfusion due to a compartment syndrome would cause an increase in the time required for the skin to return to its normal colour.

3.1.9 Blood Composition

Although invasive, monitoring changes in blood composition to diagnose compartment syndrome was briefly discussed because it could be incorporated into routine blood tests. Possible indicators discussed included decreased oxygen (due to low perfusion), and

increased lactate levels (due to muscle necrosis). It was noted that both these indicators would only be present in the later stages of a compartment syndrome, therefore research would have to be done to find a more appropriate blood test.

3.1.10 Pulse Oximetry

Pulse oximetry was also suggested as a tool for diagnosing compartment syndromes through the monitoring of blood oxygen levels. This technique, based on detecting low oxygen levels in symptomatic compartments, would include the advantages of non-invasiveness and ease of use

3.1.11 Imaging

Some discussion centred on the idea that a symptomatic compartment may have an abnormal appearance on one of the medical imaging techniques commonly used in hospitals. Techniques discussed included ultrasound, magnetic resonance and computer aided tomography (CT) imaging. Since the latter two were too costly, only ultrasound imaging was seriously considered. After some discussion and further investigation, it was decided that the minute differences of propagation speed of ultrasound through fluids at different pressures would be difficult to measure.

3.1.12 Temperature

Two hypotheses linking local temperature to the presence of compartment syndromes were discussed. The first hypothesis stated that a lack of perfusion to the limb might

cause a decrease in metabolic activity and hence a decrease in limb's overall temperature. It was suggested that this phenomenon could be measured using the thermal imaging technique known as thermography. A second hypothesis stated that a lack of perfusion would affect the ability of the limb to carry heat to or away from itself. This phenomenon could be measured by heating or cooling the limb to a set temperature and recording the time required for the limb to return to its normal state using a surface thermometer or thermography.

3.2 Evaluation of Proposed Diagnostic Techniques

After the list of new diagnostic techniques was generated, an evaluation process to decide which of these would be most suitable for further study began. Ideally, things such as cost, availability of equipment, or a lack of test subjects would not limit such a decision. Realistically, these were issues that had to be considered when deciding which among the new ideas was to be researched. In the interests of presenting all the ideas equally, two comparative analyses are presented here. The first is an objective analysis that assumes ideal research conditions. The second is a discussion regarding the less then ideal factors that influenced the final decision. The final decision was made prior to performing the "Ideal Case" analysis. This analysis is only included here to help support the validity of the final decision and to provide a list of ideas for additional research.

3.2.1 Ideal Comparative Analysis – Quality Function Deployment

Throughout the brainstorming sessions, a number of design criteria were raised which were used to judge the new diagnostic techniques (Table 3-2). A full description of these criteria can be found in Appendix A. These criteria were used to evaluate the proposed ideas in a grading scheme known as Quality Functional Deployment (QFD).

Table 3-2 Design criteria and associated weights

CRITERIA	WEIGHT
Design Criteria	**/ 30**
Noninvasive	15
Repeatable / Continuous measurements	15
Diagnostic Criteria	**/ 54**
Early diagnosis	15
Sensitive to compartment syndromes	15
Specific to affected compartment	8
Specific to compartment syndromes	8
Diagnosis of all compartments	8
Other	**/ 16**
No risk to patient	4
Easily interpreted	4
Portability	4
Inexpensive	4
Total:	**100**

Evaluation of a specific diagnostic technique started by assigning a weight to each of the design criteria based roughly on their importance. Each proposed technique was then assigned a score of 1, ½, or 0 for each criteria based on weather it fulfilled all, some, o none of the requirements of that criteria. For example, the S.T.I.C. catheter would receive a score of one for "Portability" but a score of zero for "Non-invasiveness". A final grade for each diagnostic technique was calculated by multiplying the respective scores and weights for each criteria and adding these results. The details of the QFD analysis are shown in Table 3-3.

	15 Noninvasive	15 Repeatable / Continuous	15 Early diagnosis	15 Sensitive to C.S.	8 Specific to C.S.	8 Compartment specific	8 All compartments	4 No risk to patient	4 Easily interpreted	4 Portable	4 Inexpensive	Score	Rating	Mechanical Model?
Stiffness	1	1	1	½	½	0	1	1	1	1	1	84.5	✗	✗
Circumferential Stiffness	1	1	1	½	½	0	1	1	1	1	1	84.5	✗	✗
Limb Circumference	1	1	1	½	0	0	½	1	1	1	1	76.5	✗	✗
Mechanical Response	1	1	1	½	½	1	1	½	½	½	½	82.5	✗	✓
Nerve Conduction Velocity	1	½	0	1	½	1	0	½	½	½	½	59.5	✗	✗
Localized Blood Pressure	1	1	½	1	½	1	½	1	1	1	1	88.5	✓	✗
Blood Flow - Plethysmography	1	1	½	½	½	0	½	1	1	1	1	73	✗	✗
Blood Flow - Ultrasound	1	1	½	1	½	1	1	1	1	1	1	92.5	✓	✗
Blood Flow - Tracking Injection	½	0	½	1	½	1	1	½	1	½	½	62.5	✗	✗
Reactive Hyperemia	1	1	½	½	½	½	½	1	½	1	1	74.5	✗	✗
Blood Composition	½	½	0	1	½	½	1	½	1	1	1	63.5	✗	✗
Pulse Oximetry	1	1	½	½	½	½	½	1	1	1	½	74.5	✗	✗
Ultrasound	1	½	½	½	½	1	1	1	½	½	½	70	✗	✗
CT Scans	1	½	½	½	½	1	1	0	½	0	0	60	✗	✗
MRI	1	½	½	½	½	1	1	1	½	0	0	65	✗	✗
Temperature - Metabolic	1	1	½	½	½	½	½	1	1	½	½	72	✗	✗
Temperature - Cooling rate	1	1	½	½	½	½	½	1	1	1	1	77	✗	✓
STIC Catheter	0	1	1	1	1	1	1	½	1	1	1	86.5		

Table 3-3 Evaluation scheme for new diagnostic techniques. Scores out of 100. ✓ and ✗ indicates better or worse then STIC catheter

The results indicate that only two of the newly proposed diagnostic techniques scored higher then 86.5% and would therefore be an improvement over the S.T.I.C. catheter. Unfortunately, the choice of which technique to research was subject to some limitations.

3.2.2 Real Comparative Analysis – Experimental Limitations

Although many of the ideas generated during the brainstorming sessions were good, many were quickly eliminated because they would require live animal or human subjects for experimental testing. Only two of the new techniques could be tested with a mechanical model (Table 3-4).

Technique	Score (%)	Mechanical Model
~~Blood Flow - Ultrasound~~	92	✗
~~Localized Blood Pressure~~	88	✗
STIC Catheter	86.5	
~~Stiffness~~	84.5	✗
~~Circumferential Stiffness~~	84.5	✗
Mechanical Response	82.5	✓
Temperature - Cooling rate	77	✓

Table 3-4 Feasibility table for testing new techniques with a mechanical model

For this reason, only the "Limb Heating/Cooling" and "Mechanical Response" techniques were considered. Any model constructed for the "Limb Heating/Cooling" idea would be reduced to a simple heat transfer study of a heat exchanger process. Research in this area has been extensive, so designing a model to validate the proof of concept would be redundant and may not reflect the heat hypothesized heat exchange process in actual compartment syndromes.

On the other hand, building a test apparatus for measuring the mechanical response of an inaccessible pressurized bladder would be novel to both the fields of engineering and medicine. Therefore, even the simplest model would require development from the ground up including the model design, variables to be considered, measurement techniques, and theoretical applications. Although the first prototype would probably not be an accurate model of a compartment syndrome, the development of the experimental procedure would be a useful and necessary step for future research in this area.

Research for the new compartment syndrome diagnostic technique focused on developing a compartment syndrome simulator and methodology for observing the mechanical response of a pressurized compartment due to an external stimulus.

Chapter 4: Materials and Methodology

The complete test apparatus consisted of four major components: the artificial limb, the vibrator stand, the indentor-transducer system, and the ultrasound machine. The artificial limb was designed to simulate a pressurized muscle compartment in a human limb. The vibrator was used to stimulate the artificial limb with a series of impulses and produce movement of the pressurized compartment inside the limb. The indentor-transducer system monitored the indentor frequency and impaction. The ultrasound machine was used to measure the displacements and velocities of the compartment walls in a hard copy format that was later used for data analysis. The sections to follow provide the details of each of these components.

4.1 Artificial Limb

The mechanical stimulus hypothesis stated that the mechanical response of a muscle compartment would change with increased compartment pressures. In order to test this hypothesis in a physical model, the model required two key components:

1. A variable pressure compartment to represent the compartment, and
2. A housing for the compartment representing the surrounding limb tissues

Muscle compartments do not have simple geometries. The compartment boundaries, which consist of the strong, inelastic fascial borders, may be located adjacent to other compartments, skin, and/or bones. The compartment contents consist mostly of muscle tissues with negligible amounts of artery, venous, nerve, and fatty tissues.

To simplify the geometry of the system, a unicompartmental model was designed featuring two concentric cylinders that could be independently pressurized to represent a muscle compartment in a limb (Figure 4-1).

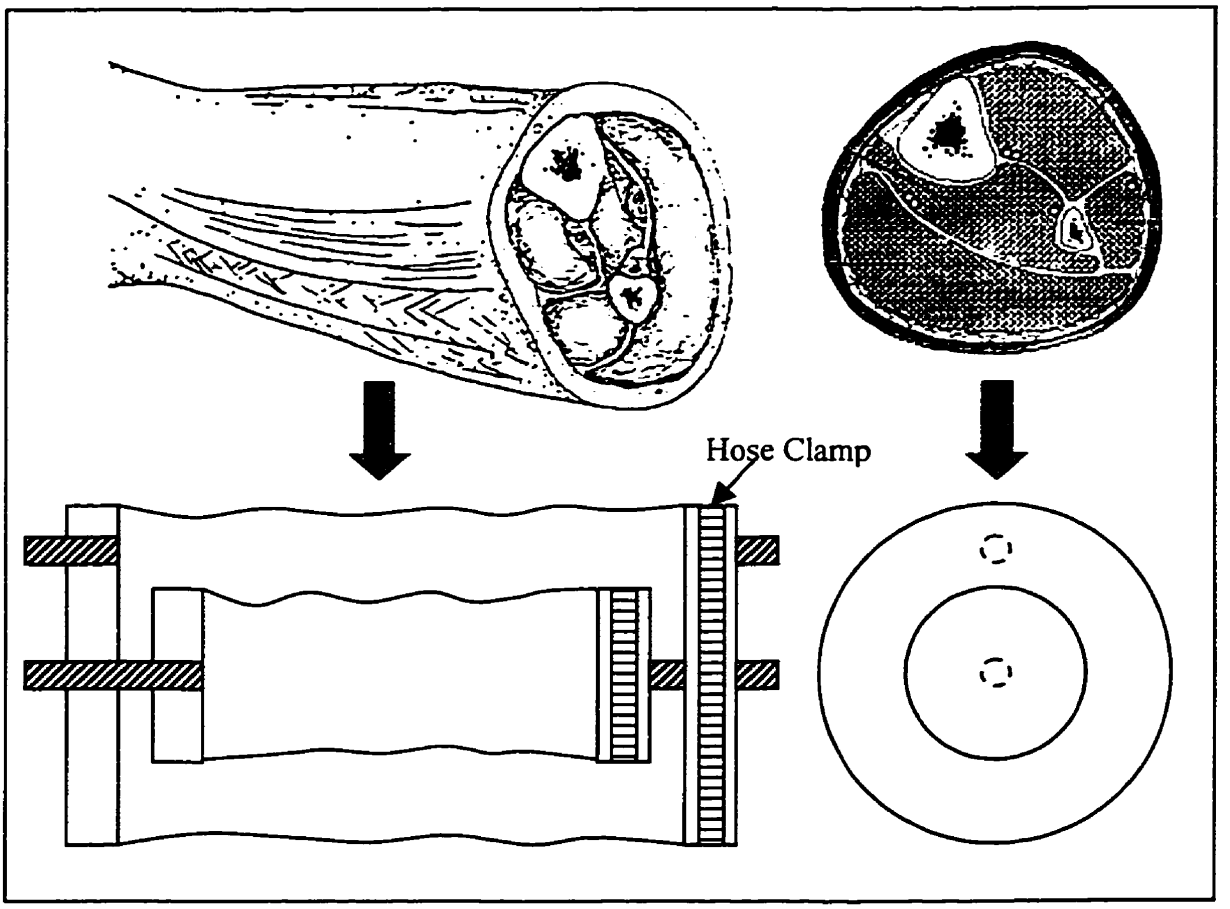

Figure 4-1 Conceptual design for unicompartmental model. (Leg from Good[8] and Rorabeck[21])

Three types of material were considered for the mechanical equivalent of fascia: rubber, plastic and animal tissues. A cylindrical form of these materials was found in the form of bicycle inner tubes, baby bottle liners, and sausage casings respectively. A sample of each of these was obtained and the following observations were made. The sausage casings were very strong, but too porous to contain a pressurized fluid (water). The bicycle inner tubes could contain a pressurized fluid, but were too elastic to represent

fascia. The plastic baby bottle liners were both inelastic and able to contain fluids and were therefore chosen to model the fascia. Similarly, plastic milk bags were used to contain the material surrounding the compartment.

Materials considered for the compartment contents and surrounding tissue were water, oil, gel (i.e. ultrasound gel), gelatin, sponge or some combination of these. Ideally, the chosen material would have the elastic properties of muscle, and the viscous characteristics of fluid. Materials considered to best imitate the elastic properties of muscle included gelatin, gel, a sponge-water mixture, and a gelatin-water mixture. None of these were used since it was uncertain whether any of them would maintain an even pressure distribution throughout the compartment. An attempt to obtain an even pressure distribution with gelatin was made by pouring the hot liquid gelatin solution into the compartment, raising the pressure to the level desired, and allowing it to solidify overnight. Although the gelatin seemed to have solidified after this process, there was no means of measuring (and hence verifying) the "pressure" in the solidified compartment. In the end, it was finally decided that water would be the initial compartment material because it was easiest to work with and it would be adequate to prove the underlying concept of the hypothesis. The artificial limb is pictured in Figure 4-2 and detailed drawings are provided in Figures 4-3 to 4-5 (membranes and hoses omitted for clarity). Complete details of the individual components and assembly procedure can be found in Appendix B.

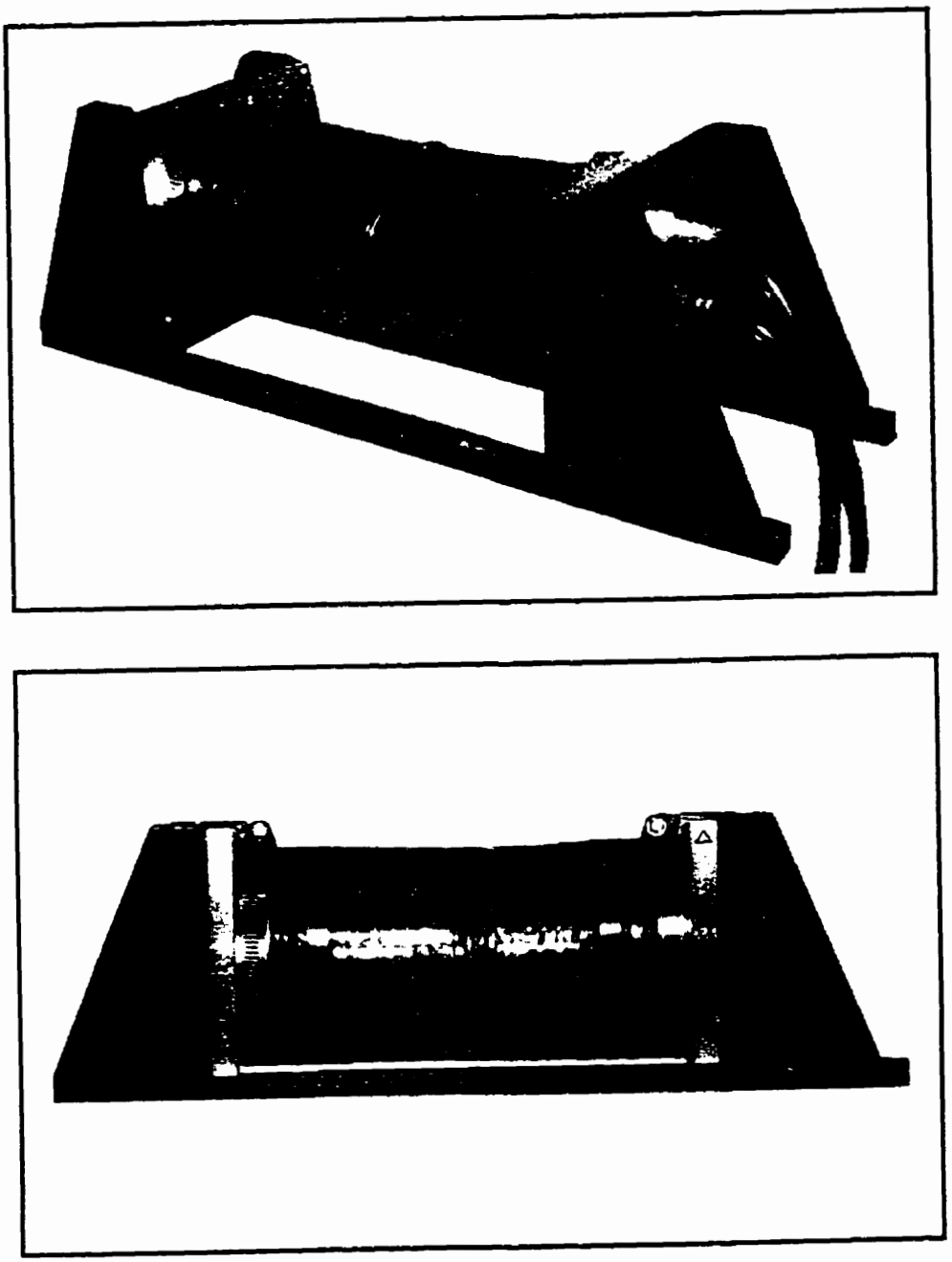

Figure 4-2 Compartment syndrome simulator.

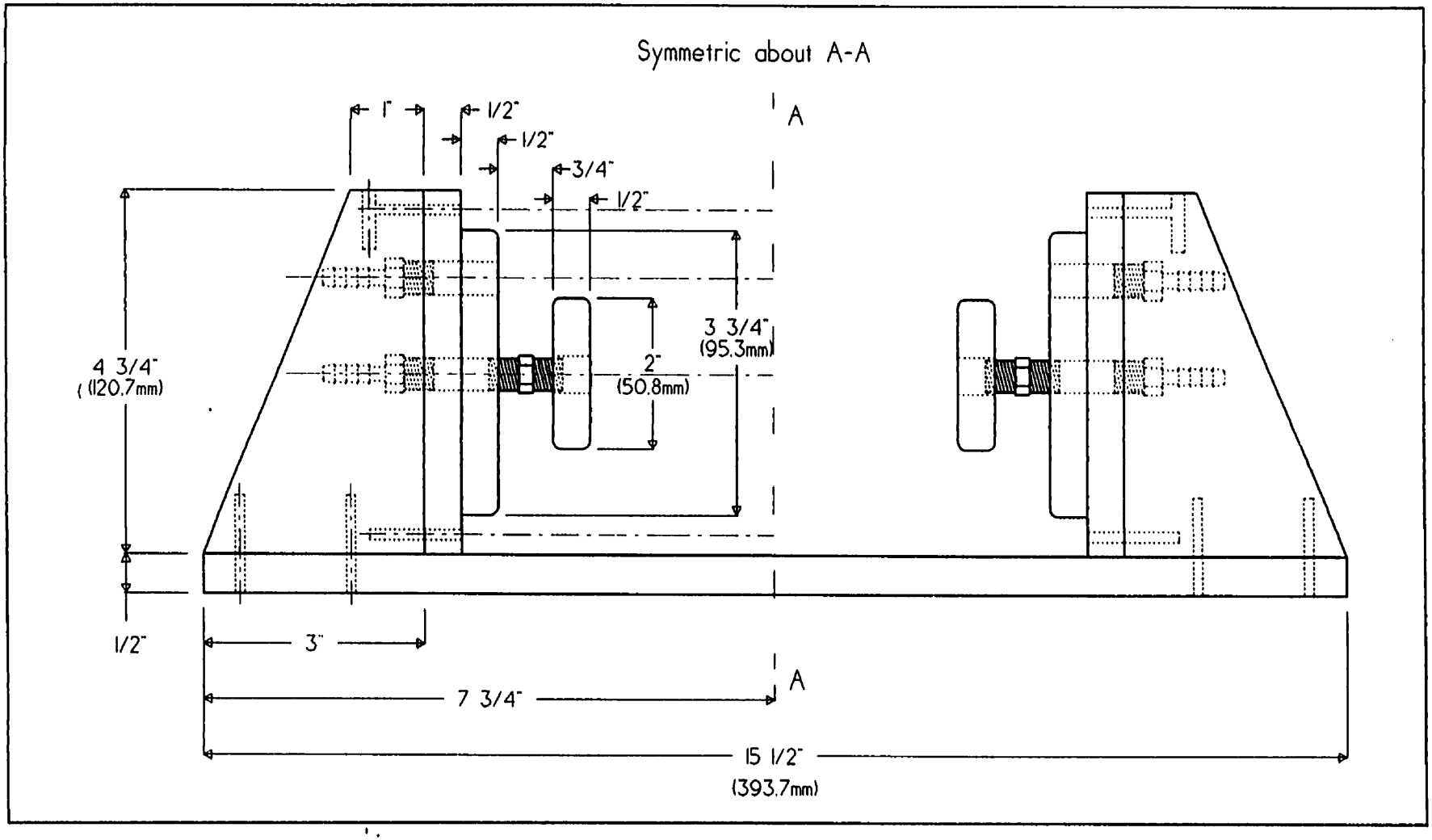

Figure 4-3 Side view drawing of compartment syndrome simulator frame.

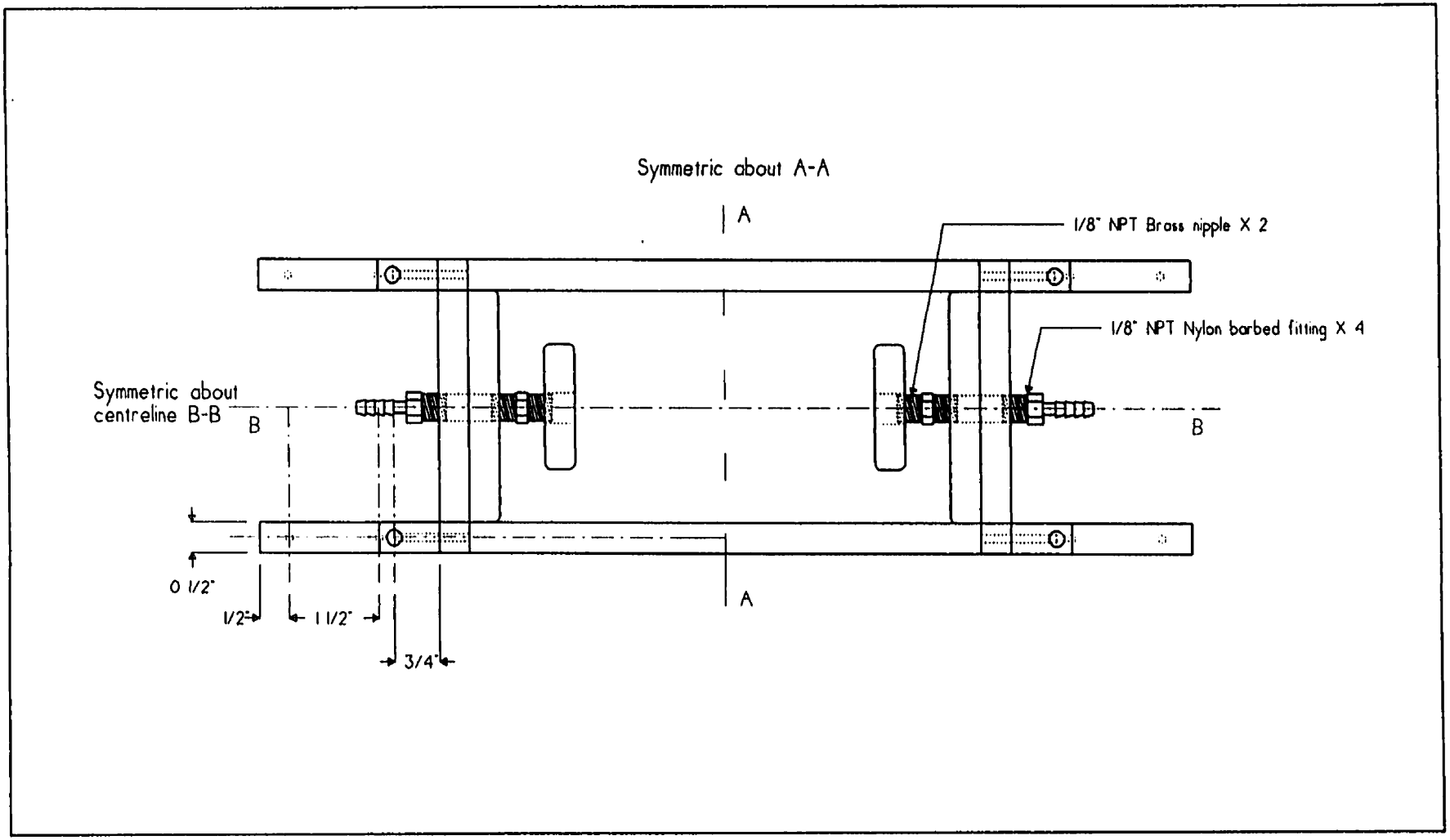

Figure 4-4 Top view drawing of compartment syndrome simulator frame.

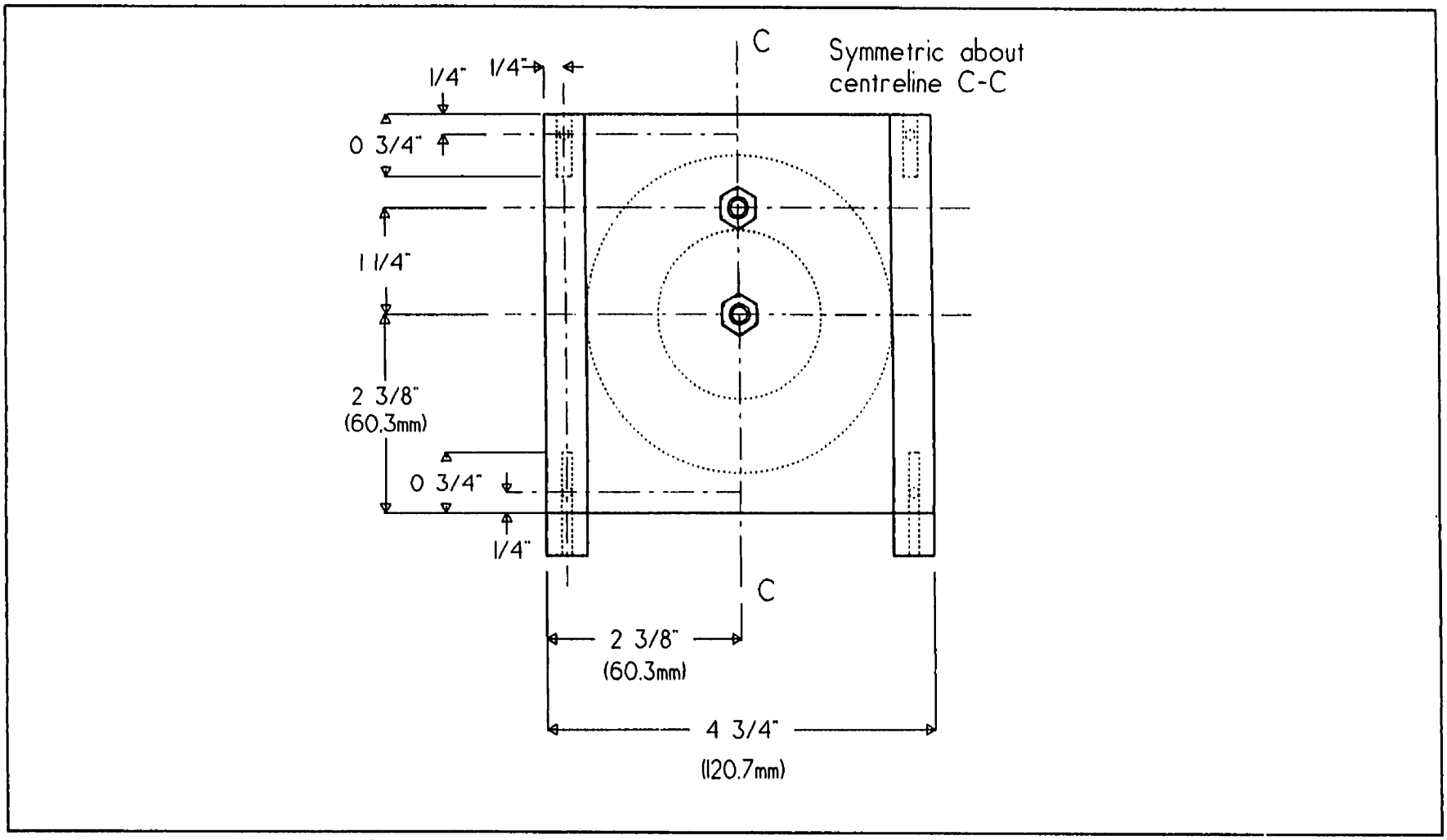

Figure 4-5 Front view drawing of compartment syndrome simulator frame.

Filling and pressurization of the cylinders was achieved through access ports on either side of the model. Pressure in the chambers was measured relative to the centre of the limb compartment and could be varied by raising or lowering the height of the Tygon® tubing (Figure 4-6).

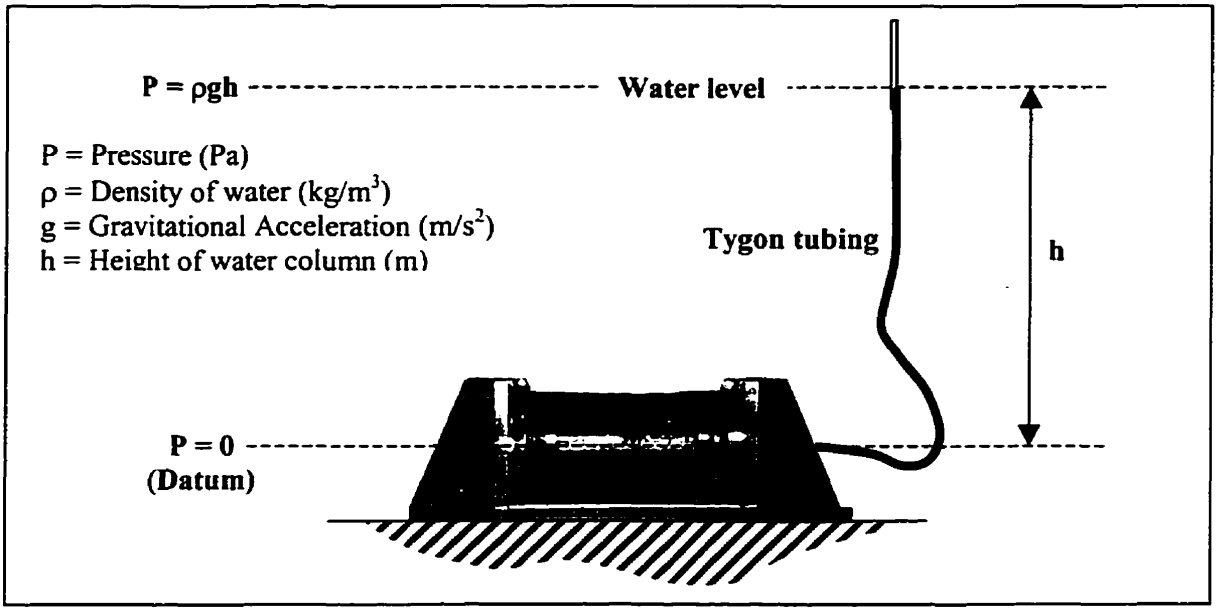

Figure 4-6 Pressurization of the artificial limb compartments.

4.2 Vibrator Stand

The vibrator stand was designed to support the artificial limb and provide it with a variable frequency, repeated impulse stimulus. The stand consisted of a Black and Decker jigsaw (Model 7548) mounted upside down in a wooden speaker cabinet (Figure 4-7). The cabinet stood 26.5cm (10

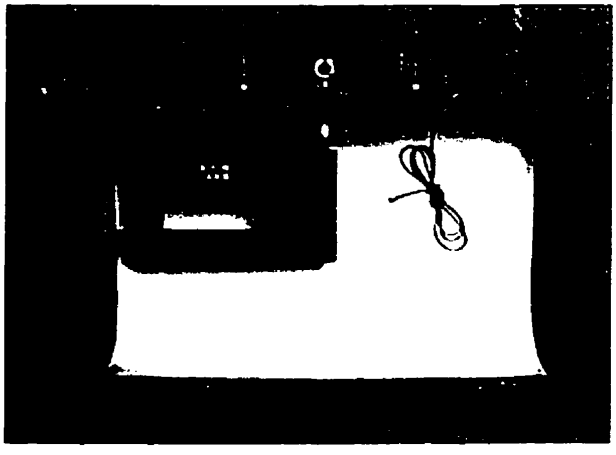

Figure 4-7 Photograph of vibrator stand.

1/2") tall, 44.3cm (17 1/2") long, and 17.5cm (7") wide.

The limb indentor consisted of a plastic CPVC tube 8.3cm (3 1/4") long and 1.6cm (5/8") in diameter, and was connected to the jigsaw with a steel threaded rod. The jigsaw provided sinusoidal actuation of the indentor with a stroke length of 16mm. Actual contact time between the indentor and artificial limb could be varied, but was fixed such that contact only occurred during half of the 16mm stroke length (see Figure 4-8).

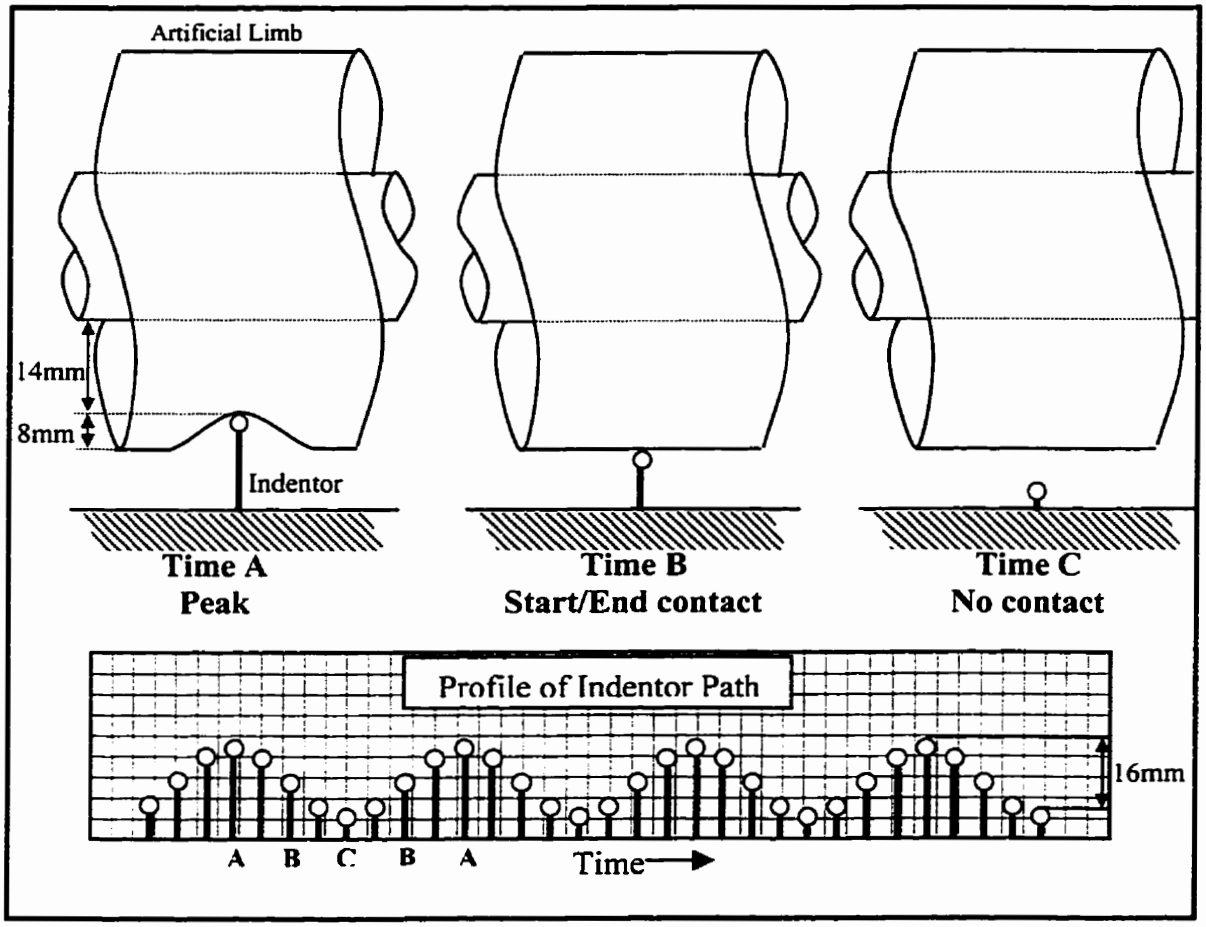

Figure 4-8 Schematic of indentor making contact for only half of the 16mm stroke length.

Speed control was obtained using a Powerstat® variable voltage autotransformer (Model 3PN116B, Superior Electric Co., Bristol, Connecticut). This set-up allowed excitation frequencies to vary from 3 to 50 Hz (strokes per second).

4.3 Indentor-Transducer System

A piezoelectric transducer fastened to the contact surface of the indentor was used to monitor the frequency of excitation. A schematic of the indentor transducer system is shown in Figure 4-9 below.

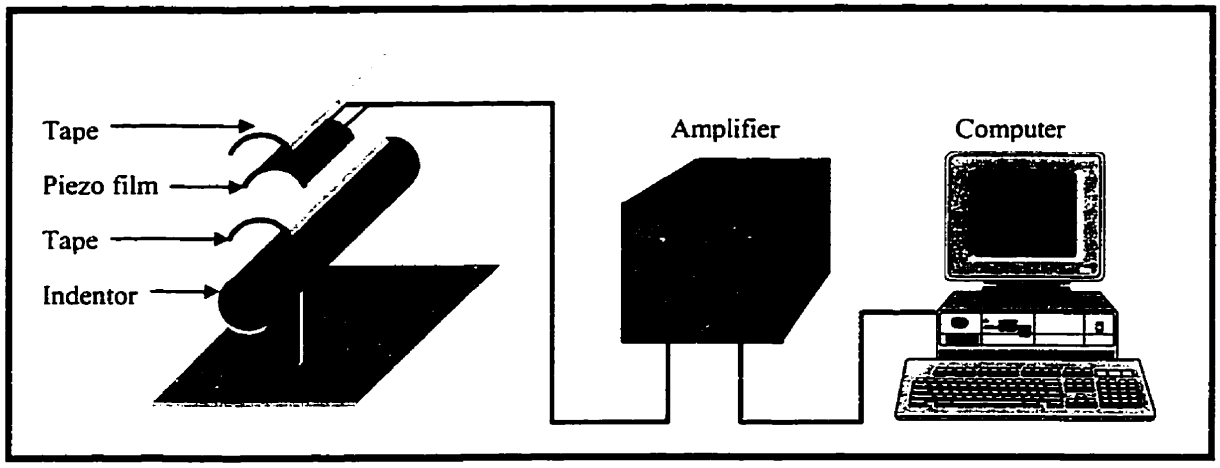

Figure 4-9 Piezoelectric film transducer system.

The piezoelectric film (Part No.: DT1-028K, AMP Inc., Valley Forge, Pennsylvania) was placed between two strips of double-sided foam tape and fastened to the indentor. The foam tape was used to ensure adequate deformation of the film so that it would produce a measurable charge. The charge was amplified using a Precision Conditioning Amplifier (Model 2650, Bruel and Kjaar, Denmark) and recorded using Pentium computer equipped with a DAS-801 A/D (analog to digital) board (Keithley Metrabyte, Cleveland,

Ohio). The amplifier settings were adjusted to provided a signal range of -10 to +10 Volts.

The A/D board was controlled with a custom made program running in Viewdac®, a data acquisition software from Keithley Metrabyte. Figure 4-10 is a screen shot of the program's interface. (A copy of the program can be obtained through Dr. C. Small from the Biomedical Engineering Lab, Department of Mechanical Engineering, Queen's University, Kingston, Ontario)

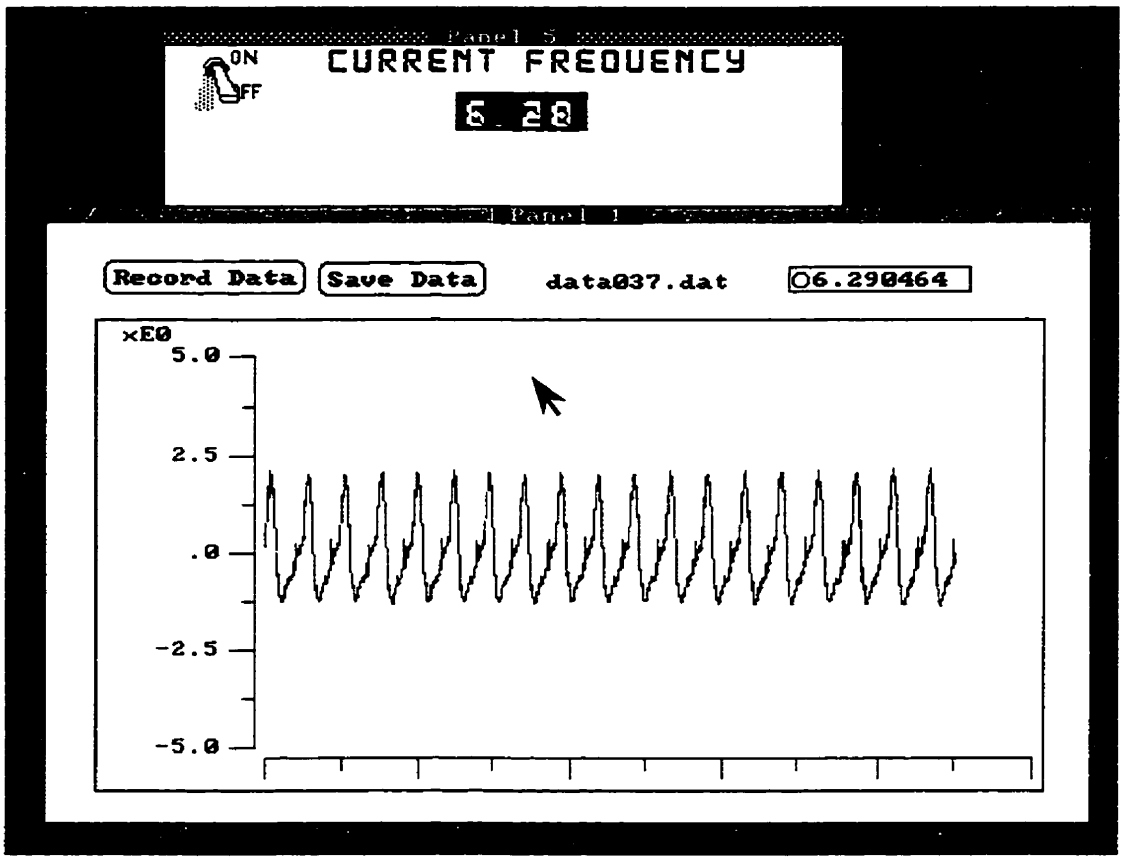

Figure 4-10 Screen shot of data acquisition interface using Viewdac® software. (Vertical axis is voltage (Volts); Horizontal axis is time (Minor unit = 0.5 seconds)

The program was capable of performing in one of two modes: online monitoring, and data collection. The toggle switch on "Panel 5" in Figure 4-10 allowed the user to switch between the two modes of operation. When the toggle switch was set to the "ON" position, the data acquisition system would be in the online monitoring mode. This mode provided continuous monitoring of the indentor frequency and was used when adjusting the speed of the jigsaw. In this mode, the data acquisition program would continuously collect data over half second intervals at a sampling rate of 3003Hz. Each half second interval of data was subjected to a Fast Fourier transform (FFT) analysis. The dominant frequency from the FFT analysis, assumed to be the excitation frequency of the indentor, was then updated on screen every half second as the "CURRENT FREQUENCY" (see "Panel 5" in Figure 4-10).

When the toggle switch was set to the off position, continuous monitoring ceased, and data collection had to be activated manually. In this mode, data collection was performed by "clicking on" the "RECORD DATA" button. This action activated the data acquisition system to collect 3 seconds of data at a sampling rate of 3003 Hz, plot the raw data and report the excitation frequency in "Panel 1" on the screen. The "SAVE DATA" button could then be used to save the data to a text file for further analysis. Filenames starting from "Data001.txt" to "Data999.txt" were assigned sequentially to the saved data and displayed to the right of the "SAVE DATA" button after the file was saved. Alternatively, the user could use the "RECORD DATA" button again to collect a new data series without saving the previous series. The data were used to verify excitation frequencies.

4.4 Ultrasound Machine

Movement of the artificial limb's compartment membrane was monitored with the High Definition Imaging (HDI) 3000 Ultrasound machine (Advanced Technologies Laboratories Canada Inc., Markham, Ontario) used in the Angiodynography Lab at Kingston General Hospital (Figure 4-11a). A linear array ultrasound probe (Model: L7-4 38mm) with an operating frequency of 4MHz was mounted to the frame of the artificial limb with a custom vise as shown in Figure 4-11b (details in Appendix B).

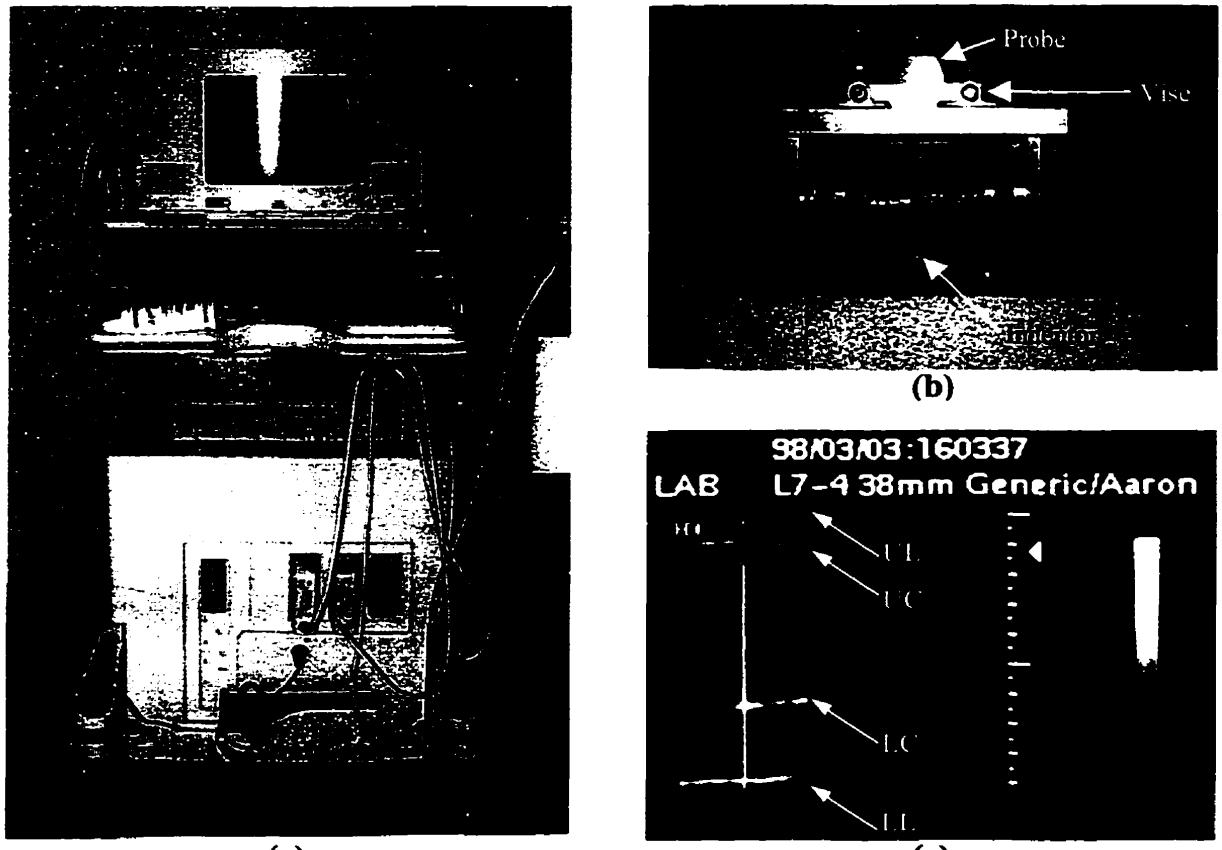

(a) (b) (c)

Figure 4-11 (a) HDI 3000 Ultrasound machine, (b) probe and (c) image. UL = Upper limb/probe contact surface, UC = Upper compartment boundary, LC = Lower compartment boundary, LL = Lower limb surface

A typical ultrasound image of the artificial limb displayed the probe-upper limb contact surface, the upper compartment boundary, the lower compartment boundary, and the lower limb surface (Figure 4-11c). Frozen screen images were "captured" using the ultrasound's printer. The printer featured both normal and "2X" magnification settings. In order to obtain dynamic measurements from these images, the HDI 3000 was operated in either M (Movement) or Doppler modes.

M-Mode was used to measure compartment membrane displacements using a vertical line cursor that could be placed over the ultrasound image where movement was to be monitored (Figure 4-12). The image projected on the cursor was stored and displayed on the screen. A series of these vertical lines collected over time and displayed side by side produced a plot of position versus time for any moving target that was coincident with the cursor. Since the cursor extended over the entire length of the image, both compartment membranes could be monitored at the same time. A "High Definition Zoom" option could be used to magnify one section of the image (i.e. one trace) to twice the normal size.

In Doppler mode, a rectangular cursor was placed over the image of the compartment membrane and the HDI-3000 determined the velocity of the moving target within the sample volume. Velocities were displayed graphically against time (Figure 4-13).

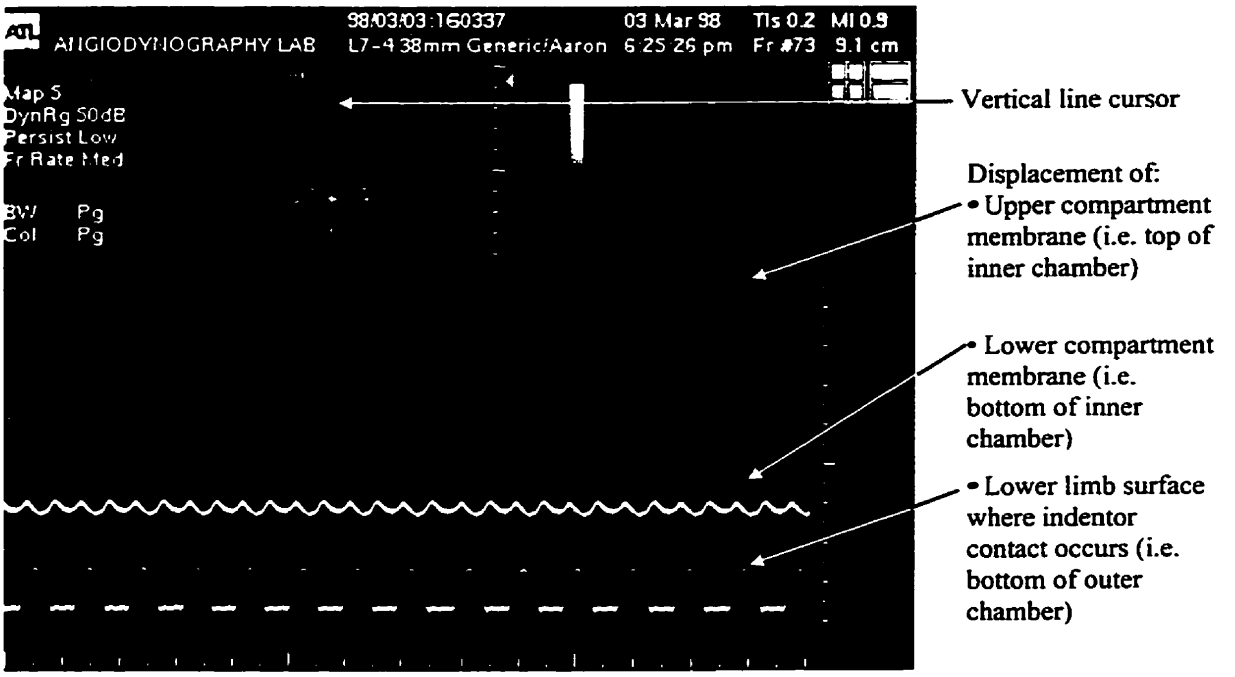

Figure 4-12 Ultrasound image data using M-Mode.

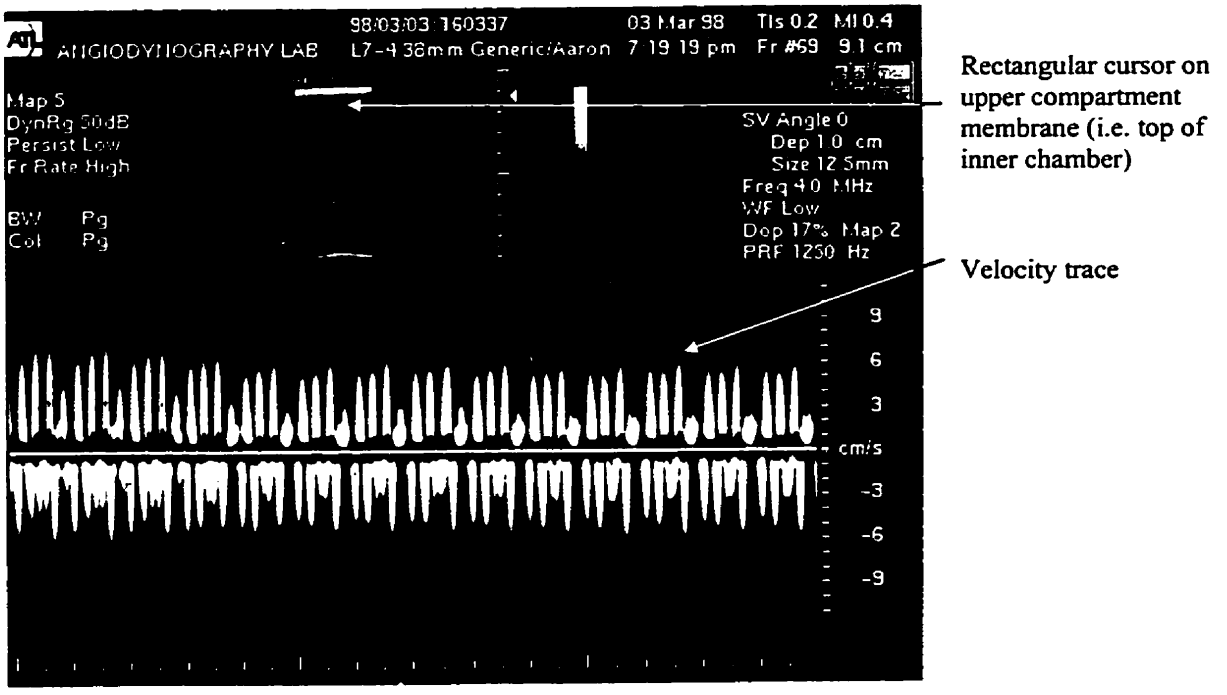

Figure 4-13 Ultrasound image data in Doppler mode.

4.5 Methodology

4.5.1 Experimental Procedure

The experimental procedure is detailed in Figure 4-14.

Experimental Procedure

1. The computer and ultrasound machine were turned on.
2. The data acquisition program was loaded and run.
3. The limb and compartment pressures were lowered to 7mmHg.
4. The ultrasound probe was secured into the vise.
5. A numbered Popsicle® stick was selected from a hat to determine which test (i.e. which combination of variables) was to be performed.
6. The data acquisition was switched to online monitoring mode.
7. The autotransformer was switched on and the jigsaw speed was adjusted until the data acquisition program displayed the desired excitation frequency.
8. The ultrasound's operation mode (Doppler or M-Mode) was selected and the ultrasound controls were adjusted to optimize the on-screen image.
9. The membrane image was magnified with the ultrasound's "HD Zoom" setting and the printer magnification was set to "2X Zoom". (*Note: Magnification was not used in the pilot study.*)
10. Limb and compartment pressures were raised or lowered by adjusting the height of the Tygon tubing (water was added or removed as required).
11. The jigsaw speed was adjusted (if necessary) and the data acquisition program was set to data collection mode.
12. The "COLLECT DATA" button from the data acquisition program was pressed to initiate three seconds of indentor data collection.
13. The moment the indentor data was finished collecting, the ultrasound image was manually frozen on screen (with a "PAUSE" button).
14. If the ultrasound image was not reasonably clear, steps 12 and 13 were repeated If the ultrasound image was clear, or after three attempts to obtain a clear image failed, a hard copy image of the data was printed and the indentor data was saved.
15. Steps 5 through 14 were repeated until all tests were completed.

Figure 4-14 Experimental procedure.

4.5.2 Ultrasound Evaluation

Since access to the time-series data used to generate the display was not available, the quantification of the ultrasound data was performed by measuring, counting, and scoring the ultrasound images. A summary of the information extracted from the Doppler (velocity) and M-Mode (displacement) ultrasound images is shown in Table 4-1.

Variables Extracted from the Ultrasound Images	Units	Type	Doppler	M-Mode
Amplitude Range	cm or cm/sec	Meas/Calc	✓	✓
Peak Negative Amplitude	cm/sec	Measured	✓	✗
Peak Positive Amplitude	cm/sec	Measured	✓	✗
Peaks/Cycle Positive	peaks	Counted	✓	✓
Peaks/Cycle Negative	peaks	Counted	✓	✓
Frequency Positive	Hz	Calculated	✓	✓
Frequency Negative	Hz	Calculated	✓	✓
Repeatability	–	Scored	✓	✓
Clarity	–	Scored	✓	✓
Peak Sharpness	–	Scored	✗	✓
"Frequency Content"	–	Scored	✗	✓

Table 4-1 Data extracted from the ultrasound images

For Doppler images, the positive and negative peak velocities were measured using the scale provided on the image (Figure 4-15). The difference between these two velocities was calculated as the amplitude range. For M-Mode images, the amplitude range was measured directly using the scale provided on the image. In magnified images, the scale was out of the image range and amplitudes had to be measured with a ruler (resolution +/- 0.5mm). The measured amplitudes were subsequently divided by the magnification factor, and compared to the scale of a "non-magnified" printout.

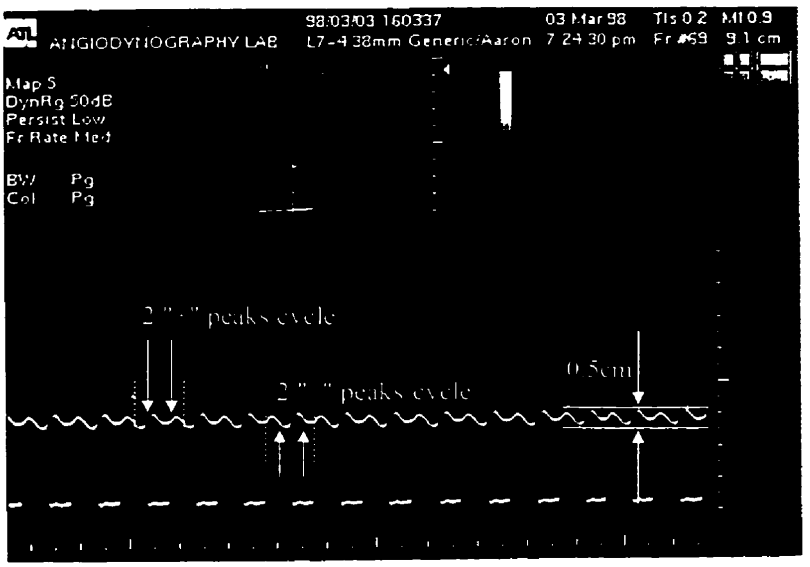

M-Mode

Excitation frequency: 5Hz
Amplitude range = 0.5cm
Peaks/cycle (+) = 2
Peaks/cycle (–) = 2
Frequency (+) = 10 Hz
Frequency (–) = 10 Hz

Scores:	
Clarity	5
Repeatability	5
Frequency Content	3
Peak Sharpness	5

Horizontal axis: 1 unit = 0.1 sec, Vertical axis: 1 unit = 0.5cm

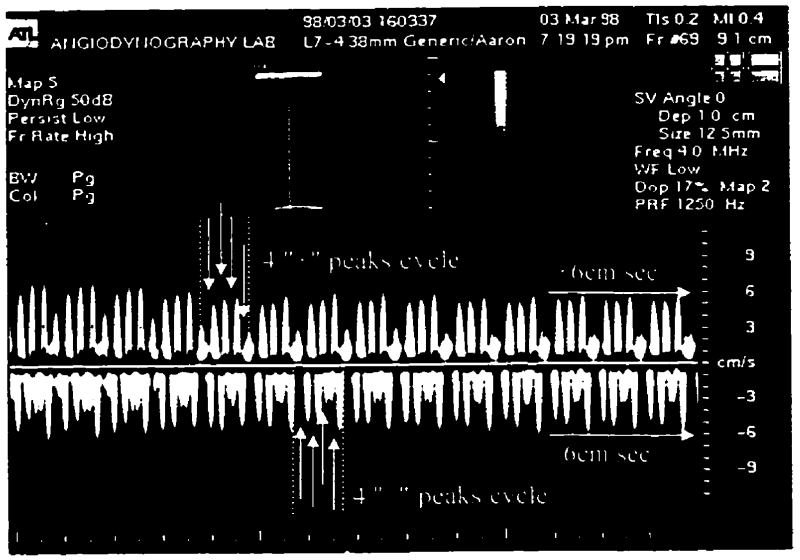

Doppler Mode

Excitation frequency = 5Hz
Amplitude range = 12cm/s
Peak amplitude (+) = 6cm/s
Peak amplitude (–) = –6cm/s
Peaks/cycle (+) = 4
Peaks/cycle (–) = 4
Frequency (+) = 20 Hz
Frequency (–) = 20 Hz

Scores:	
Clarity	5
Repeatability	5

Horizontal axis: 1 unit = 0.1 sec, Vertical axis: 1 unit = 1cm/sec

Figure 4-15 Sample measurements from M-Mode (top) and Doppler (below) images.

If a Doppler or M-Mode image was periodic, the number of positive and negative peaks per cycle was counted. The "peaks per cycle" values were then multiplied by the excitation frequency in order to determine an approximate "frequency" of the membrane.

A scoring system was created to evaluate ultrasound images for their repeatability and clarity. In each case, a score of 1 to 5 was assigned to each image (Table 4-2). Repeatability was defined as a signal's tendency to be periodic. Scores for repeatability varied from 1, for a non-periodic signal, to a score of 5 indicating a very periodic signal. Clarity was defined as the sharpness of an image trace. Clarity scores varied from 1, for thick, blurry (and sometimes missing) traces, to 5 for sharp lined traces with no discontinuities and well defined peaks and troughs.

Table 4-2 Scheme used for scoring ultrasound images

Criteria	Score: 1	3	5
Repeatability	Non-periodic	Somewhat periodic	Very periodic
Clarity	Blurred, thick, or missing	Blurred but distinguishable	Very clear, sharp lines
Peak Sharpness†	Sharp / jagged	Both sharp and smooth	Smooth
"Frequency Content"†	Complex combination of modes	Combination of tw modes	Simple sine wave

† - M-Mode only.

Two additional scores were assigned to the M-Mode data: "frequency content " and "peak sharpness". Sinusoidal complexity was defined as the apparent number of modes of excitation of a given membrane. A score of 1 for sinusoidal complexity indicated a signal exhibiting simple sinusoidal motion and a score of 5 indicated a complex signal with an undetermined number of vibration modes. Peak sharpness was defined as the

smoothness of the M-mode trace. A score of 1 indicated smooth curves throughout the signal and a score of 5 indicated very sharp, jagged or discontinuous peaks.

4.6 Pilot Study Experimental Design

A pilot study was performed to study the effects of the different variables on the mechanical response of the compartment membranes and which measurement technique was best suited to detect these effects. The experimental protocol incorporated three independent variables (nominal limb pressure, differential compartment pressure, and stimulus excitation frequency), two modes of measurement (Doppler and M-Mode), and two locations for measurement (the membrane closest and farthest from the excitation) (Table 4-3).

Table 4-3 List of experimental variables

	Description: Qualitative	**Range**
Variables:		
P_{limb}	Nominal limb pressure	0 – 60 mmHg
ΔP	Differential pressure between compartment and limb	0 – 60 mmHg
f	Excitation frequency	3 – 50 Hertz
Measurement:		
Mode	Displacement or velocity	M-Mode/Doppler
Membrane	Section of membrane to be observed (relative to vibration source)	Closest/Farthest

The pilot study incorporated all three of the apparatus variables and followed a two facto factorial design (Table 4-4). This meant that each variable was assigned a low and high setting, and experimentation was performed for each combination of variable settings. The exception to this was that the excitation frequency, f, was assigned three variable settings instead of two.

Table 4-4 List of experimental variables for the pilot study

Variable	Settings:			
	Low	Med.	High	Units
P_{limb}	7	-	37	mmHg
ΔP	0	-	30	mmHg
f	5	10	15	Hertz

The low limb pressure setting of 7mmHg corresponded to normal interstitial pressure; the higher setting of 37mmHg was selected arbitrarily. The choice of 0 and 30 mmHg for the limb-compartment differential pressure corresponded to the normal and symptomatic pressures of lower limb compartment syndromes. The selection of excitation frequencies was based on the inability of the jigsaw to perform well under 5 Hertz and preliminary observations of poorly resolved ultrasound image data with frequencies above 15 Hertz.

The different combinations of all the independent variables resulted in a total of 12 possible test conditions. The complete pilot study consisted of 36 tests because the test conditions had to be performed once for each M-Mode measurement, and twice for each Doppler measurement (a separate test for each measurement location). All 36 tests wer performed in random order. Repeated measurements were not performed for the pilo study.

The data from the pilot study (Chapter 5) were used to determine the combination of variables and measurements that best differentiated the mechanical response of the normal and pressurized compartments. The results from the pilot study were used to specify the limb pressure, excitation frequency, measurement mode, and measurement location to be used for the second test procedure.

4.7 Pressure Dependence Study Experimental Design

The second study used only one independent variable; compartment pressure. All other apparatus and measurement variables including limb pressure, excitation frequency, measurement mode and membrane were fixed (Table 4-5).

Table 4-5 List of experimental variables for the pressure dependence study

Variable:	Settings:
Apparatus:	
ΔP	0 - 45 mmHg
P_{limb}	7 mmHg
f	5 Hertz
Measurement:	
Mode	M-Mode
Location	Closest

Compartment pressures were varied between 0 and 45mmHg (relative to P_{limb}) at 3mmHg intervals. These values were chosen because they represented the typical compartment pressures found in normal to symptomatic compartments. The limb pressure was fixed at 7 mmHg. This value was chosen because it was within the range of normal compartment pressures. The settings for frequency, measurement mode, and membrane were chosen for the clarity of the ultrasound images they provided. Three M-Mode images were obtained for each compartment pressure setting to obtain a total of 48 ultrasound images.

In order to improve the precision of the measurements taken from the M-Mode images, the ultrasound's High Definition Zoom (HD Zoom) option was used. This option magnified the portion of the ultrasound image of greatest interest (in this case the membrane closest to the excitation frequency). The image was further magnified by

selecting the "2X Zoom" option on the ultrasound's printer. The combination of these two options obtained a magnification of 4X the normal image size (and 2.35X the actual size).

4.8 Summary

The artificial limb, vibrator stand and ultrasound machine were used to simulate the diagnosis of compartment syndromes in a human limb. The pilot study was designed to obtain information on the different experimental variables (P_{limb}, ΔP, f, and measurement mode & location) and how each one affected the simulator and the data collection systems. This information was used in designing the second study, which focused on the effects of compartment pressure. The results from the pressure dependence study were critical for determining the feasibility of the "mechanical stimulus" diagnostic technique.

Chapter 5: Results

The pilot study results gave a generalized overview of how the experimental variables affected the compartment syndrome simulator as shown in the ultrasound images. The pressure dependence study described the specific relationship between compartment pressures and displacement amplitudes of the compartment membrane subjected to the vibratory stimulus. The pressure-displacement relationship was compared to the stiffness-displacement relationship of a spring-mass-damper system.

5.1 Pilot Study Results

Twelve M-Mode and twenty-four Doppler images were produced from the pilot study. The measurements and scores described in Table 4-1 (i.e. amplitude range, clarity scores, etc.) were organized in tables designed to draw comparisons between normal and pressurized compartment data (Table 5-1). The pilot study ultrasound images can be found in Appendix C. Highlights of the pilot study results are categorised here with respect to each of the study's experimental variables.

Variable: Amplitude Range (cm or cm/sec)									
		M-Closest		M-Farthest		D-Closest		D-Farthest	
Plimb	Freq	ΔP=0	30	0	30	0	30	0	30
7	5	0.5	0.25	0.75	0.25	34.5	14	8.25	12
	10	1.5	0.5	1	0.5	X	33	X	34
	15	1.75	1	1	X	115	70	X	77.5
37	5	0.5	0.13	0.13	0.13	28	16	15	15
	10	0.5	0.5	0.5	0.5	70	80	X	110
	15	1.25	0.38	0.38	0.38	140	90	165	60

Variable: Peaks/Cycle Positive									
		M-Closest		M-Farthest		D-Closest		D-Farthest	
Plimt	Freq	ΔP=0	30	0	30	0	30	0	30
7	5	2	2	2	2	4	4	8	4
	10	3	2	X	3	X	2	X	2
	15	1	2	1	1	1	2	X	2
37	5	2	5	2	X	2	5	2	5
	10	1	3	1	2	1	2	X	2
	15	1	2	1	2	1	2	3	2

Variable: Peak Velocity Negative (cm/sec)									
		M-Closest		M-Farthest		D-Closest		D-Farthest	
Plimb	Freq	ΔP=0	30	0	30	0	30	0	30
7	5					-23	-6.5	-3.8	-5.5
	10					X	-15	X	-20
	15					-55	-40	X	-43
37	5					-10	-7	-7	-8
	10					-30	-40	X	-55
	15					-80	-40	-80	-35

Variable: Peaks/Cycle Negative									
		M-Closest		M-Farthest		D-Closest		D-Farthest	
Plimt	Freq	ΔP=0	30	0	30	0	30	0	30
7	5	2	3	2	2	2	4	7	4
	10	2	2	3	3	X	2	X	2
	15	1	2	1	X	1	2	X	2
37	5	2	5	2	X	2	5	2	5
	10	1	3	1	2	1	2	X	2
	15	1	2	1	2	1	2	3	2

Variable: Peak Velocity Positive (cm/sec)									
		M-Closest		M-Farthest		D-Closest		D-Farthest	
Plimb	Freq	ΔP=0	30	0	30	0	30	0	30
7	5					12	7.5	4.5	6.5
	10					X	18	X	14
	15					60	30	X	35
37	5					18	9	8	7
	10					40	40	X	55
	15					65	50	85	25

Variable: Frequency Positive (Hz)									
		M-Closest		M-Farthest		D-Closest		D-Farthest	
Plimt	Freq	ΔP=0	30	0	30	0	30	0	30
7	5	10	10	10	10	25	20	40	20
	10	30	20	X	30	X	20	X	20
	15	15	30	15	15	15	30	X	30
37	5	10	25	10	X	10	25	10	25
	10	10	30	10	20	10	20	X	20
	15	15	30	15	30	15	30	45	30

Table 5-1 Tabulated data from pilot study. Each table represents one parameter. M indicates M-Mode. D indicates Doppler mode. X indicates no data due to poor image or signal quality. Blank box indicates that these measurements did not apply.

Variable:		Frequency Negative (Hz)							
		M-Closest		M-Farthest		D-Closest		D-Farthest	
Plimb	Freq	ΔP=0	30	0	30	0	30	0	30
7	5	10	15	10	10	20	20	35	20
	10	30	20	X	30	X	20	X	20
	15	15	30	15	X	15	30	X	30
37	5	10	25	10	X	10	25	10	25
	10	10	30	10	20	10	20	X	20
	15	15	30	15	30	15	30	45	30

Variable:		Peak Shapness Score							
		M-Closest		M-Farthest		D-Closest		D-Farthest	
Plimt	Freq	ΔP=0	30	0	30	0	30	0	30
7	5	5	5	5	5				
	10	3	2	3	3				
	15	1	1	1	2				
37	5	4	5	5	5				
	10	5	2	4	2				
	15	3	2	3	3				

Variable:		Repeatability Score							
		M-Closest		M-Farthest		D-Closest		D-Farthest	
Plimb	Freq	ΔP=0	30	0	30	0	30	0	30
7	5	5	4	5	4	4	5	5	5
	10	3	3	1	3	1	5	1	5
	15	5	5	5	5	3	5	1	5
37	5	5	4	5	4	5	5	5	5
	10	5	5	5	5	5	4	2	3
	15	3	5	2	5	4	5	5	5

Variable:		Clarity Score							
		M-Closest		M-Farthest		D-Closest		D-Farthest	
Plimt	Freq	ΔP=0	30	0	30	0	30	0	30
7	5	5	5	5	5	2	4	3	5
	10	4	4	3	4	1	4	1	5
	15	5	5	5	3	2	3	1	5
37	5	5	5	5	5	5	5	5	5
	10	5	5	5	3	5	5	1	2
	15	5	4	5	5	2	5	5	5

Variable:		"Frequency Content" Score							
		M-Closest		M-Farthest		D-Closest		D-Farthest	
Plimb	Freq	ΔP=0	30	0	30	0	30	0	30
7	5	3	3	4	3				
	10	2	4	1	2				
	15	4	2	4	4				
37	5	4	3	4	3				
	10	2	1	2	2				
	15	2	2	1	3				

Table 5-1 Tabulated data from pilot study (cont'd). Each table represents one parameter. M indicates M-Mode. D indicates Doppler mode. X indicates no data due to poor image or signal quality. Blank box indicates that these measurements did not apply

5.1.1 Membrane and Mode

M-Mode images generally exhibited well defined, easy to interpret traces whereas the Doppler images were sometimes clear, but other times uninterpretable. These results reflected the difficulty involved in obtaining good Doppler readings from the ultrasound equipment. The difference between Doppler and M-Mode image quality was noted quantitatively in their respective "clarity" scores (Table 5-2). The clarity and repeatability scores from both the M-Mode and Doppler images were usually better for the closest membrane. Sample M-Mode and Doppler images with high and low clarity scores are shown in Figure 5-1.

Average Clarity and Repeatability Scores								
Mode-Membrane:	M-Closest		M-Furthest		D-Closest		D-Furthest	
Patm Freq	ΔP=0	ΔP=30	0	30	0	30	0	30
Clarity	4.8		4.4		3.6		3.6	
Repeatability	4.3		4.1		4.3		3.9	

Table 5-2 Average clarity and repeatability scores for pilot study data

SAMPLE M-MODE IMAGES

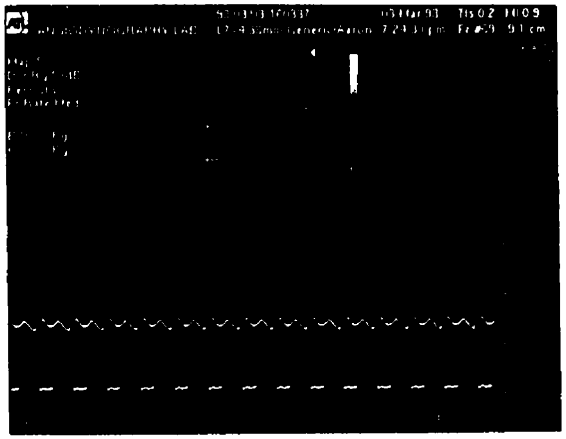

(a) Good quality M-Mode image

Clarity: 5

Repeatability: 5

Frequency Content: 3

Peak Sharpness: 5

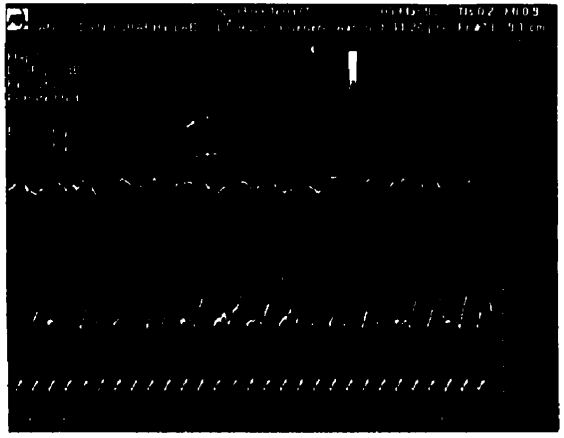

(b) Poor quality M-Mode image

Clarity: 4

Repeatability: 3

Frequency Content: 3

Peak Sharpness: 3

SAMPLE DOPPLER IMAGES

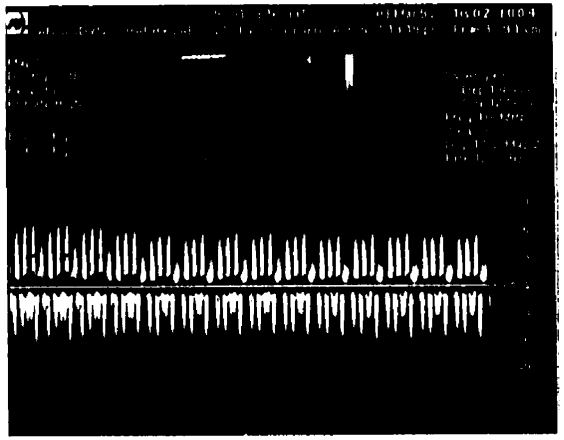

(c) Good quality Doppler image

Clarity: 5

Repeatability: 5

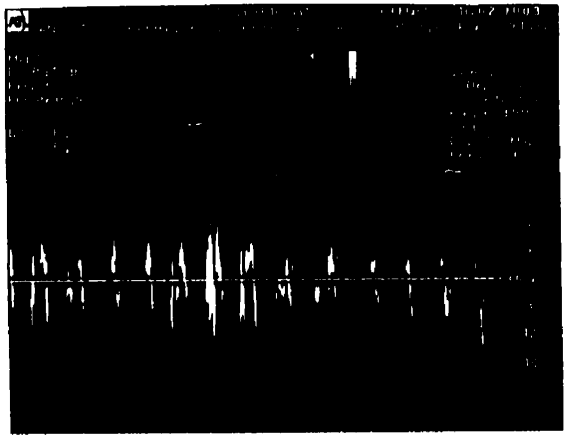

(d) Poor quality Doppler image

Clarity: 1

Repeatability: 1

Figure 5-1 Sample pilot study images - comparison of M-Mode and Doppler images. Clarity and repeatability scores for M-Mode images were generally better then Doppler images. Displacement (M-Mode) amplitudes of the farthest membrane (top line of each M-Mode image) were generally less then those of the closest membrane (middle line of each M-Mode image).

The clear Doppler images tended to be symmetrical in amplitude about the zero axis (see Figure 5-1c). This symmetry made it possible to reduce the number of parameters considered in the analysis. The three amplitude parameters (i.e. peak positive velocity, peak negative velocity, and peak to peak velocity) were all considered equivalents as a result of this symmetry. Similarly, any pair of "signed" parameters (e.g. positive peaks per cycle, negative frequency) could be reduced to one.

The (M-Mode) displacement amplitudes of the membrane closest to the vibration source were usually higher then the displacement amplitudes of the membrane farthest from the vibration (see Figure 5-1a and b). Velocities between the closest and farthest membrane did not usually change.

5.1.2 Compartment Pressures

Increases in compartment pressure generally decreased the amplitudes of both M-Mode and Doppler images; sharply in the M-Mode images (Figure 5-2). Compartment pressure also increased the number of "peaks/cycle" and the "frequency" of both Doppler and M-Mode images. These effects were attributed to the tightening of the compartment walls (simulated fascia) causing them to increase their natural resonant frequency and decrease their amplitudes much like the behaviour of a guitar string.

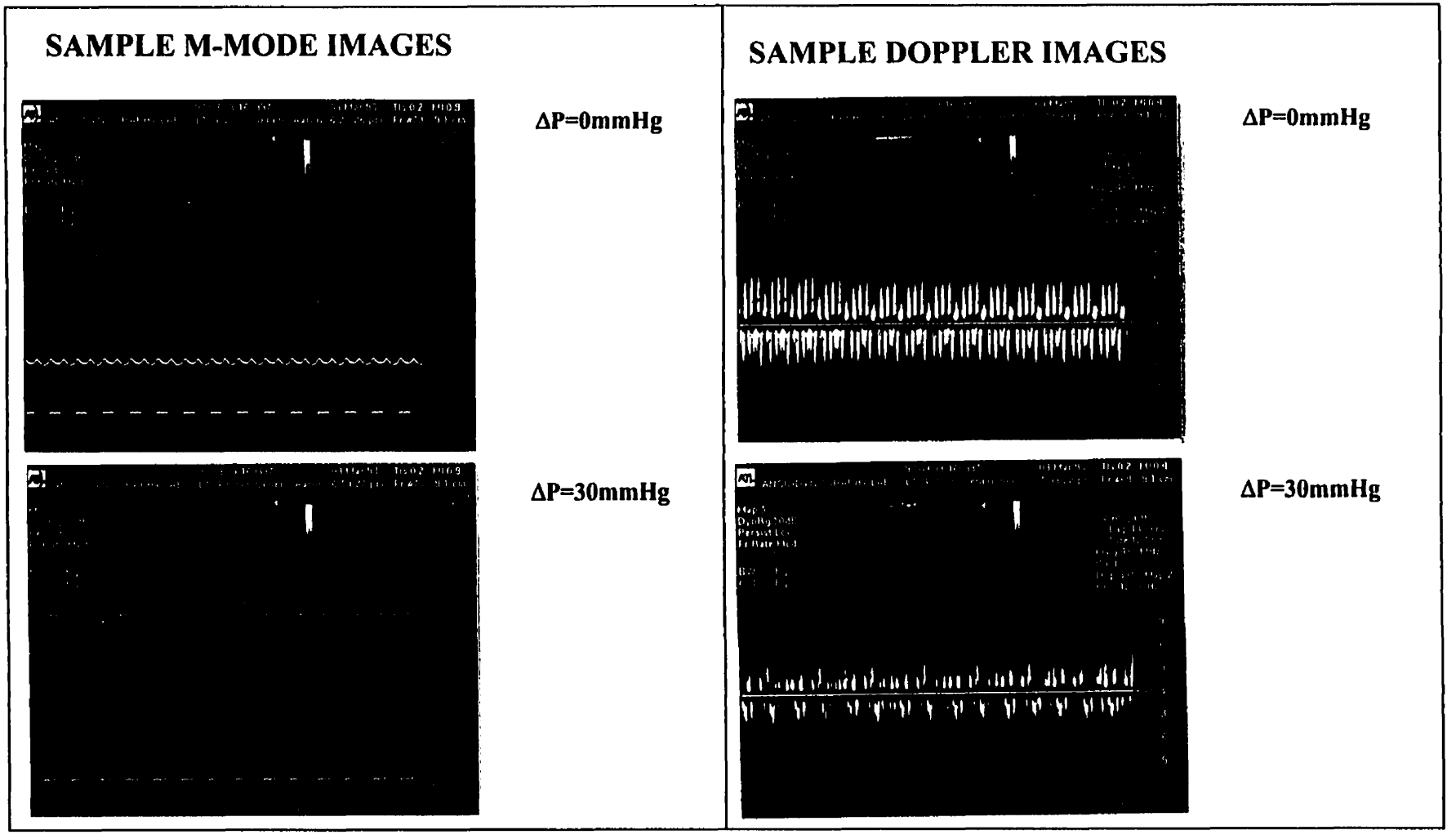

Figure 5-2 Sample pilot study images - effects of compartment pressure (ΔP). Amplitudes generally decreased in both M-Mode and Doppler images with increases in compartment pressures. "Peaks/cycle" and the " Frequency" generally increased in both Doppler and M-Mode images with increases in compartment pressures. Clarity and repeatability scores generally improved with increased compartment pressure

The clarity and repeatability scores generally improved with compartment pressure. It was concluded that this was likely caused by "loose" and "sloppy" behaviour when there was insufficient tension in the compartment walls.

5.1.3 Limb Pressures

Changes in limb pressure had little effect on the results when the trans-membrane pressures were held constant. The only notable difference was a decrease in the repeatability and clarity scores at lower limb pressures. This may have been caused by the "sloppier" movement of the limb at lower pressures affecting the compartment motion.

5.1.4 Excitation Frequency

Increases in excitation frequencies caused increased amplitudes and "frequencies" of both the M-Mode and Doppler images. This was expected – more excitation produced more movement (Figure 5-3). The increased frequency content was noted by sharper displacement peaks at higher excitation frequencies and was reflected quantitatively in the "peak sharpness" scores.

The number of "peaks per cycle" decreased with increasing excitation frequency. This was probably because, at low excitation frequencies, motion corresponded to the membrane's natural frequency whereas at high excitation frequencies, the membrane motion corresponded closer to the excitation frequencies.

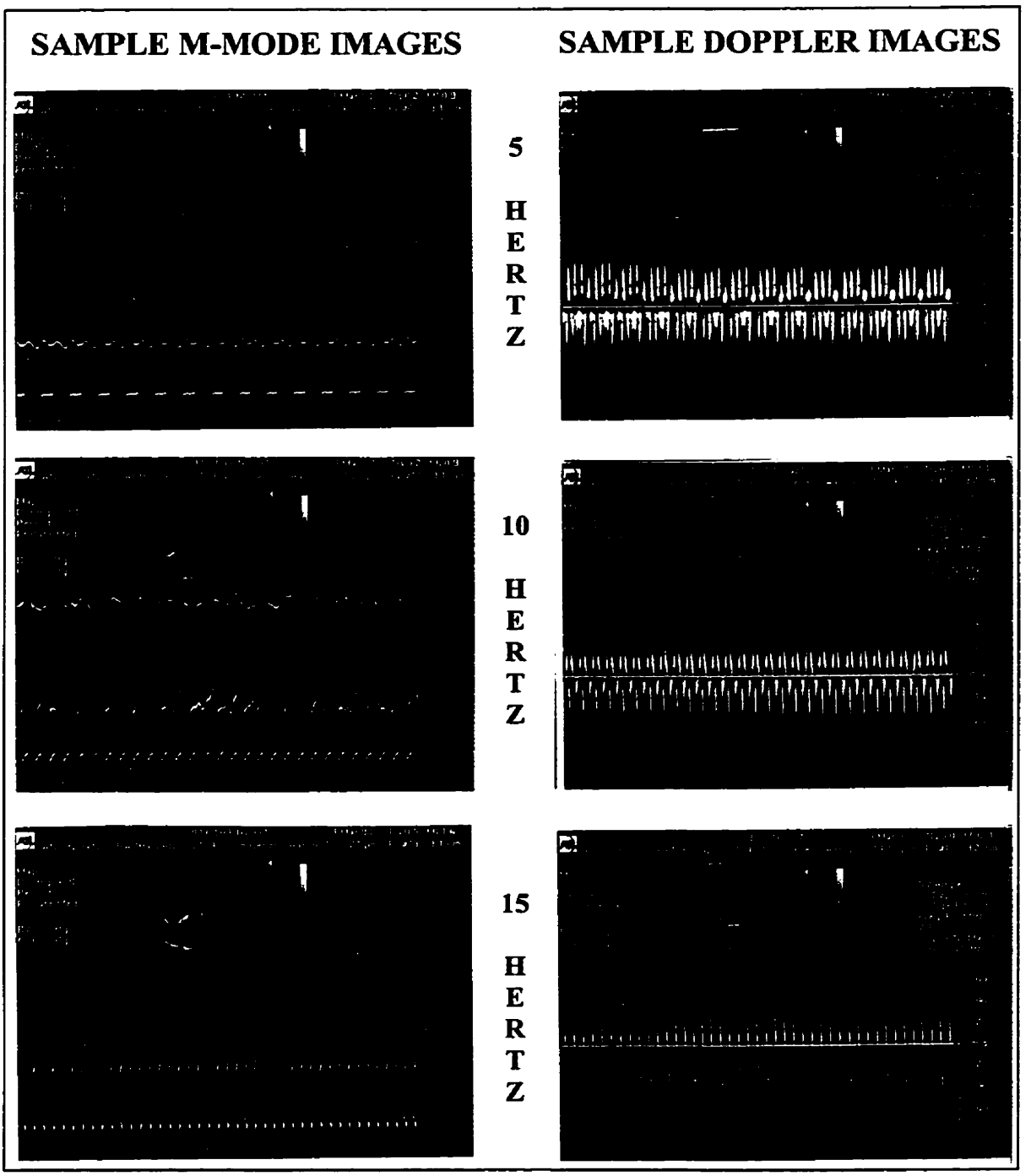

Figure 5-3 Sample pilot study images - effects of excitation frequency (*f*). As excitation frequencies increased: Displacement (M-Mode) and velocity (Doppler) amplitudes increased , M-Mode and Doppler "Peaks/cycle" decreased, M-Mode and Doppler "Frequency" increased, M-Mode peak sharpness scores decreased. Clarity and repeatability scores were highest at *f*=5 Hertz and lowest when *f*=10 Hertz.

Repeatability and clarity scores decreased with increasing excitation frequencies. This was attributed to the ultrasound machine's limited ability to measure high frequency movements. The ultrasound machine was designed to monitor low frequency signals (i.e. heart rates at ≈1-2 Hz) and did not perform well when measuring high frequency vibration. The horizontal resolution of the high frequency signals was limited by the manufacturer's options of preset time scales.

It was noted that the ultrasound images produced with a 10 Hertz vibration frequency were consistently lower then those with a 5 or 15 Hertz frequency. This anomaly was attributed to the complex movement patterns observed in the membranes stimulated at a frequency of 10 Hertz. It was hypothesized that this complex movement may have been the result of the resonant frequency of the simulator or one of its components being close to 10 Hertz.

5.2 Pilot Study Conclusions

The pilot study was designed to combine all the different experimental variables and determine which ones had any effect on the data and how. The effects of changing compartment pressures on the data were of particular interest since these changes would become the basis for a non-invasive diagnostic technique for compartment syndromes. Conclusions regarding the effects of the other variables (including nominal limb pressure, excitation frequency, measurement mode, and membrane) helped determine what set-ups

were to be used in the second study. A summary of the findings can be found in Table 5-3.

The pilot study results confirmed the hypothesis that compartment pressures within the physiological range of 0-30mmHg had a measurable effect on the membrane motion. Specifically, increased compartment pressures caused: decreased membrane displacements, decreased membrane velocities, increased clarity and repeatability scores, and (at higher nominal limb pressures) an increase in the "peaks/cycle" and "frequency" parameters. Since the range of 0 to 30mmHg worked successfully in the pilot study, it was reused in the pressure dependence study.

Table 5-3 Summary of pilot study findings

	AS:				
	Compartment Pressure (ΔP)	**Limb Pressure (P_{limb})**	**Excitation Frequency (f)**	**Membrane**	**Measurement Mode**
	CHANGED FROM:				
	0 ↓ 30	**7 ↓ 37**	**5 ↓ 15**	**Closest ↓ Farthest**	**M-Mode ↓ Doppler**
Parameters:	**THE FOLLOWING PARAMETERS:**				
Amplitudes †	Decreased	X	Increased	Decreased [A]	NA
Peaks/Cycle †	Increased [B]	X	Decreased	X	NA
Frequency †	Increased [B]	X	Increased	X	NA
Repeatability	Increased	Increased [C]	Decreased [D]	Decreased	Decreased
Clarity	Increased	Increased [C]	Decreased [D]	Decreased	Decreased
Peak Sharpness [A]	X	X	Decreased	X	NA
Frequency Content [A]	X	X	X	X	NA

X - no change, † - includes positive and negative aspects due to symmetry across the horizontal (time) axis, A - M-Mode only, B - Only when P_{limb}=30mmHg, excludes Doppler mode measurements of upper membrane, C - Doppler mode only, D - Clarity and repeatability scored high when f=5Hertz, low when f=15Hertz, and lowest when f=10Hertz.

The clarity and repeatability scores were usually better for the M-Mode images (average 4.6 and 4.2 respectively) compared to Doppler (average 3.6 and 4.1 respectively). The displacement amplitudes of the closest membrane were higher, clearer and more repeatable than those of the farther membrane. Therefore, M-Mode imaging of the membrane closest to the excitation was used for the second study.

Increased nominal limb pressures did not affect membrane motion at a given trans-membrane pressure, but did improve Doppler image quality. M-Mode images were not affected.

Membrane displacement, velocity, and "Frequency" increased with higher excitation frequencies whereas the "Peaks/cycle" decreased. Low frequency excitation produced better ultrasound images in both the Doppler and M-Modes. Therefore, frequencies near 5Hertz were used in further testing.

5.3 Pressure Dependence Study Results

The displacement amplitudes measured from each of the ultrasound images are given in Table 5-4. The average and standard deviation of the displacement amplitudes as measured from the ultrasound images were divided by the magnification factor to give membrane displacement amplitudes. A plot of the membrane displacement amplitude versus the compartment pressure shows that the amplitude of the membrane vibration decreased with increasing pressure (Figure 5-4).

ΔP (mmHg)	IMAGE MEASUREMENTS					MEMBRANE DISPLACEMENT	
	Image Amplitude (mm)			Average	Std Dev.	Average	Std Dev.
	TEST 1	TEST 2	TEST 3			(÷ ZOOM FACTOR OF 2.35)	
0	4.5	7.5	5.5	5.83	± 1.53	2.48	± 0.65
3	5.5	6.5	7	6.33	± 0.76	2.70	± 0.33
6	5	5.5	5	5.17	± 0.29	2.20	± 0.12
9	3	3.5	3	3.17	± 0.29	1.35	± 0.12
12	2	2.5	4.5	3.00	± 1.32	1.28	± 0.56
15	2	2	1.5	1.83	± 0.29	0.78	± 0.12
18	1.5	2	1.5	1.67	± 0.29	0.71	± 0.12
21	1.5	1.5	X	1.50	± 0.00	0.64	± 0.00
24	1.5	1	1.5	1.33	± 0.29	0.57	± 0.12
27	1	1	1	1.00	± 0.00	0.43	± 0.00
30	1.5	1	1	1.17	± 0.29	0.50	± 0.12
33	1	1	1	1.00	± 0.00	0.43	± 0.00
36	1	1	1.5	1.17	± 0.29	0.50	± 0.12
39	1.5	1	1	1.17	± 0.29	0.50	± 0.12
42	1	1	1	1.00	± 0.00	0.43	± 0.00
45	1	1	1	1.00	± 0.00	0.43	± 0.00

Table 5-4 Displacement amplitudes from main study

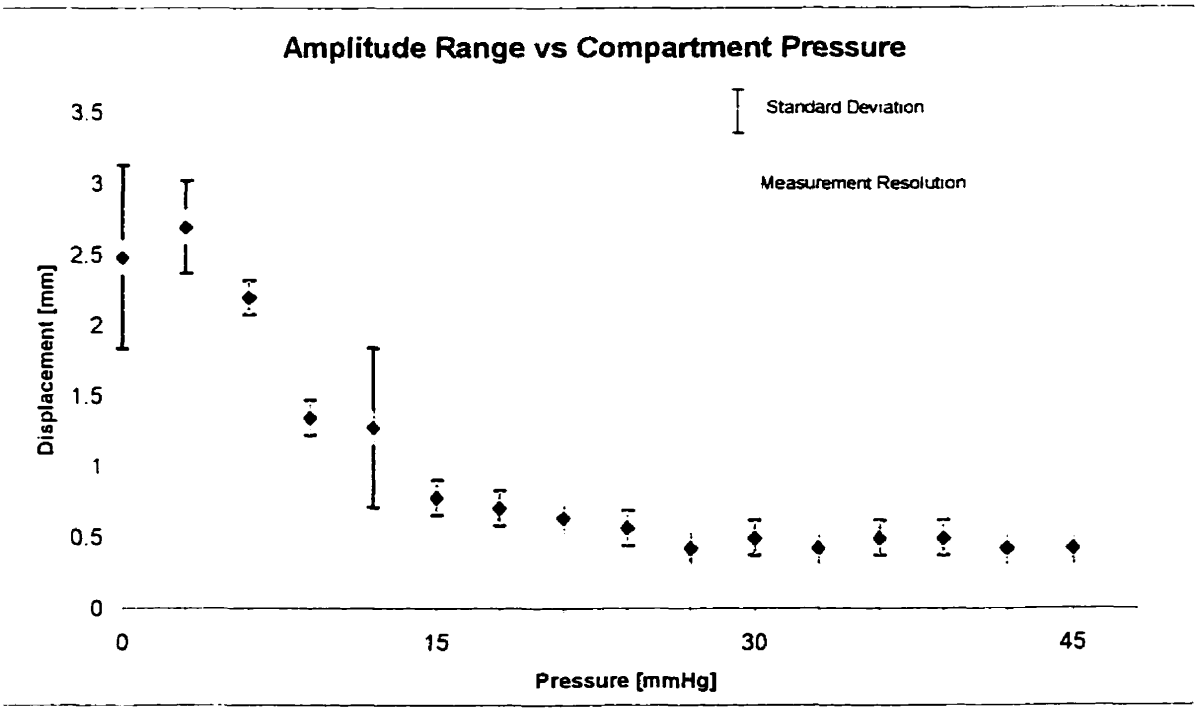

Figure 5-4 Displacement amplitude vs. compartment pressure plot.

The data seemed to divide themselves naturally on either side of the 15mmHg pressure mark. Amplitudes in the low pressure range were higher in magnitude and variability. The high variability was attributed to poor reproducibility of the ultrasound images. In comparison, amplitudes in the high pressure range tended to decay to approximately 0.5mm. These amplitudes were expected to decay towards 0mm, however measurements incorporated the thickness of the ultrasound trace which defined the ultrasound's image resolution and hence the lower limit of 0.5mm. As a consequence of the asymptotic relationship shown in Figure 5-4, a displacement amplitude measured with ultrasound could only predict artificial limb compartment pressures below 15mmHg. Amplitude displacements in the 0.5mm range would only indicate that the pressure is elevated, but not to what degree. However, the simple fact that the ultrasound measurements can differentiate between low and high pressure compartments may be all that is needed in a clinical setting.

5.4 Compartment Membrane Modelling

The compartment membrane was modelled as a second-order mass-spring-damper system subjected to a sinusoidal force (Figure 5-5). It was hypothesized that the compartment pressure increased tension in the compartment membrane thereby changing the system overall "stiffness" (k).

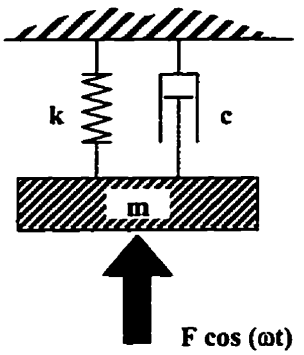

The amplitude of displacement is defined as:

$$x_{max} = \frac{F}{\sqrt{\left(k - m\omega^2\right)^2 + (c\omega)^2}}$$

where,
x is the position of the mass [m]
m is the mass [kg]
c is the damping coefficient [N s / m]
k is the spring constant [N/m]
F is the amplitude of the vibration stimulus[N].
ω is the vibration frequency [rad / s], and
t is time [s]

Figure 5-5 Mass-spring-damper system.

A regression analysis was performed using the equation from Figure 5-5 to produce a line of "best fit" for the pressure dependence study data (Figure 5-6; details of regression in Appendix E). The regression equation was a good approximation to the experimental data indicating that increasing compartment pressure is analogous to increasing the systems overall "stiffness".

5.5 Summary

The pilot study results proved that changes in the mechanical response of a compartment membrane can be measured with ultrasound, and strengthened the hypothesis that compartment pressures change the mechanical response of its compliant boundaries. The pressure dependence study confirmed that hypothesis and helped to characterize the pressure-displacement relationship.

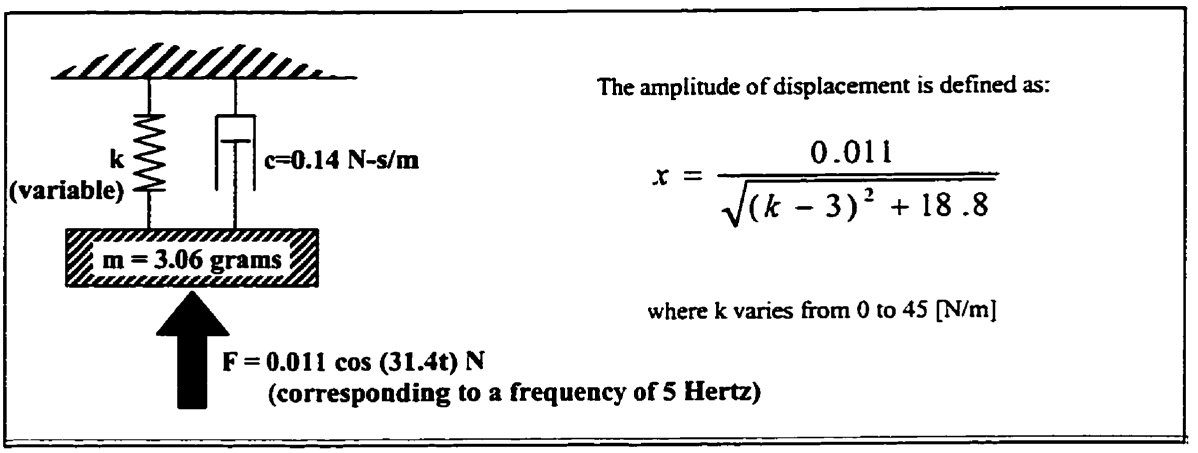

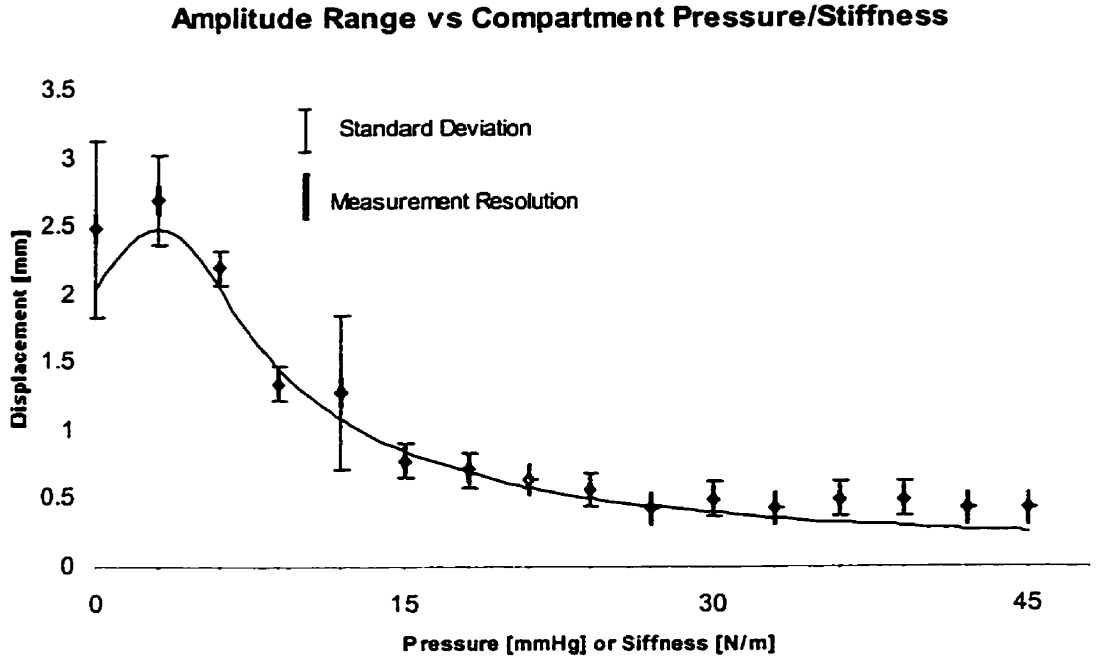

Figure 5-6 Experimental data and equation from regression analysis (Note: k≡ΔP, trans-membrane pressure, see Appendix E for details).

Chapter 6: Discussion & Conclusions

Three pertinent conclusions can be drawn from this study. First, the velocities and displacements of a vibrating membrane can be measured non-invasively using ultrasound imaging. Second, the experimental data have shown that a relationship exists between the pressure in a flexible walled compartment and its mechanical response to vibration. Third, in the simulator, the relationship between displacement amplitude and compartment pressure was found to be decaying, similar to the response of a second order, spring-mass-damper model with variable stiffness. These conclusions are based on a simplified model of compartment syndromes. The mechanical model only mimicked one aspect of compartment syndromes: a compartment with flexible walls of low extensibility inside a second compartment at a different hydrostatic pressure. The model did not account for the shapes and material properties of the fluids, tissues and bones both within and surrounding compartment syndromes. However, the three conclusions do provide some insight for the future use of a mechanical response technique for diagnosing compartment syndromes.

The use of ultrasound imaging to detect differences in mechanical behaviour was an extremely important element of this study. Non-invasiveness was the most critical element of this work; the ultrasound machine's success in monitoring membrane motion proved that a "mechanical response diagnosis" could be a non-invasive diagnosis. The ability of ultrasound to detect fascial borders in humans has been documented [1], and was attempted informally in the ultrasound lab. The images from these experiments show that the displacement and velocities of human fascia can also be monitored with ultrasound.

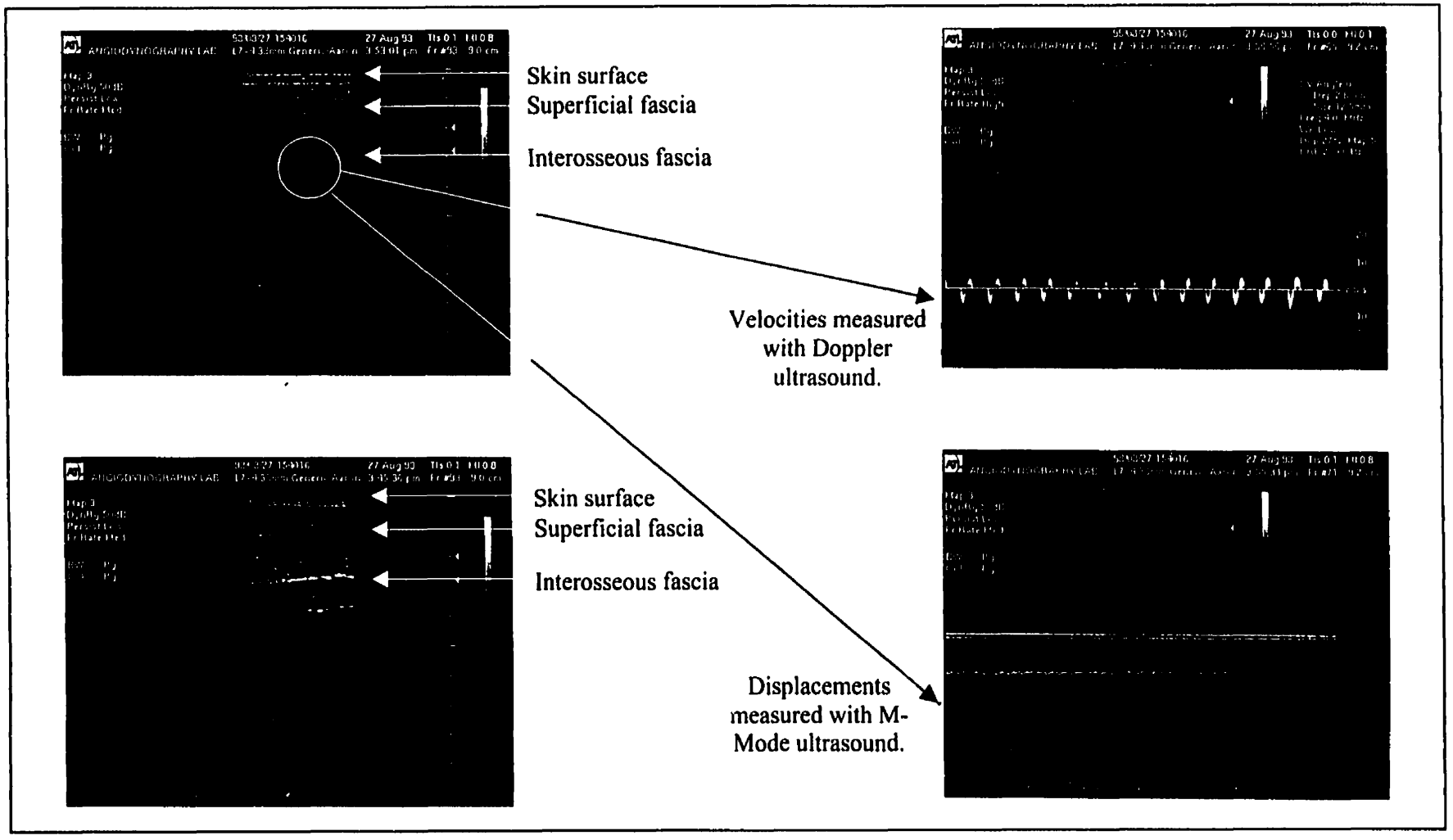

Figure 6-1 Ultrasound images of human fascia. Left: Two ultrasound images showing the superficial and interosseous fascia in the anterior compartment of a human leg. Top Right : Doppler image recording velocities of the interosseous fascia while the limb was being "tapped" by hand. Bottom left: M-Mode image showing the displacement of the same.

(Figure 6-1). The successful use of ultrasound to monitor membrane motion both in the experimental model and human limbs supports the credibility of using the "mechanical response technique" for the non-invasive diagnosis of compartment syndromes.

The experimental data show that the mechanical behaviour of a flexible walled compartment under vibratory stimulus does change with compartment pressure. The analytical model suggests that the increased tension in the membrane walls due to rising pressures increases the natural frequency of the compartment membranes. In clinical compartment syndromes, fascia becomes stretched by excess tissue fluids and becomes stiffer. However, unlike the experimental model, the fascia would probably exhibit a more damped response due to surrounding tissues preventing excessive motion. It remains to be seen if the changes in fascial mechanical response can be detected using ultrasound.

In this study, the parameter used to define mechanical response was displacement amplitude as measured from M-Mode images. This parameter was chosen because the ultrasound's time series data was inaccessible and the M-Mode images were the clearest and easiest to interpret. However, the success of the spring-mass-damper model demonstrates that other forms of mechanical response such as natural frequencies might also change with pressure. Such tests might be better conducted using a non-sinusoidal vibratory stimulus, such as an impulse function or a train of short pulses. Frequency response parameters may be useful in estimating compartment pressures non-invasively in humans and should be considered in further research.

In summary, the compartment syndrome simulator has demonstrated that compartment pressures change the mechanical response of a compartment, and these changes can be detected non-invasively with ultrasound imaging. If these two assertions remain true for clinical compartment syndromes, then the "mechanical response procedure" has the potential of becoming the elusive non-invasive diagnosis for compartment syndromes.

Chapter 7: Recommendations

Further development of the "mechanical response" diagnostic technique should include the development of a more accurate compartment syndrome simulator, consideration of different mechanical stimuli, investigation of the effect of probe placement, and improved data collection and analysis.

Experimentation on an improved mechanical model would help determine if the changes in mechanical response due to pressure are detectable in clinical compartment syndromes. The new model could be an improvement over the current mechanical model, or one of the many animal, human, or cadaveric models presented in the literature. In the former case, the new model design should consider modelling the variety of tissues and geometries involved in compartment syndromes.

It is possible that different mechanical stimuli may produce better results for different pressures and or compartments. These effects should be considered in future research. Stroke length, waveform (e.g. sinusoidal, square, sawtooth, impulse), and frequency are amongst the variables that could be considered in a new mechanical stimulator. Clinical research should also be performed to determine if any of these variables have any (negative) effects on the condition of the patient subjected to them.

Changes in probe placement could alter the effects of the mechanical stimulus and/or the compartment response. Research should be carried out to study these effects and determine if they are pertinent to the diagnostic procedure. The effects of probe

placement were not considered in this study because the probe was not moved throughout any of the experimental procedures. However, in clinical use, ultrasound probes are held by hand; thus introducing a new variable to be considered.

Accessing the time series ultrasound data would eliminate the need to interpret the ultrasound image data. Access to this data would increase measurement accuracy and allow the use of signal analysis tools to construct frequency spectra and determine different types of response. Alternatively, the audio signal from the HDI-3000 or a hand-held acoustic Doppler machine could provide a secondary access to analog data.

References

1. Brahim F, Zaccardelli W. Ultrasound Measurement of the Anterior Leg Compartment. American Journal of Sports Medicine 1986; 14:300-302.

2. Breit GA, Gross JH, Watenpaugh DE, Chance B, Hargens AR. Near-Infrared Spectroscopy for Monitoring of Tissue Oxygenation of Exercising Skeletal Muscle in a Chronic Compartment Syndrome Model. The Journal of Bone and Joint Surgery 1997; 79-A:838-843.

3. Chidgey LK, Szabo RM, Kolack B. Effects of Elevation on Nerve Function in an Acute Upper Extremity Nerve Compression Model. Journal of Orthopaedic Research 1989; 7:783-791.

4. Cook TC, Brown D, Roe J. Hypokalemia, Hypophosphatemia, and Compartment Syndrome of the Leg After Downhill Skiing on Moguls. Journal of Emergency Medicine 1993; 11:709-715.

5. Gall WE, Burr JW, Wright CB. Noninvasive Evaluation and Correlation of Hemodynamics in "Compartment Syndrome". Surgical Forum 1989; 29:222-224.

6. Gao L, Parker KJ, Lerner RM, Levinson SF. Imaging of the Elastic Properties of Tissue A Review. Ultrasound in Medicine and Biology 1996; 22:959-977.

7. Gershuni DH, Gosink BB, Hargens AR, Gould RN, Forsythye JR, Mubarak SJ, et al. Ultrasound Evaluation of the Anterior Musculofascial Compartment of the Leg Following Exercise. Clinical Orthopaedics and Related Research 1982; 167:185-190.

8. Good LP. Compartment Syndrome A Closer Look at Etiology, Treatment. AORN Journal 1992; 56:904-911.

9. Hargens AR, Romine JS, Sipe JC, Evans KL, Mubarak SJ, Akeson WH. Peripheral Nerve-Conduction Block by High Muscle Compartment Pressure. The Journal of Bone and Joint Surgery 1979; 61-A:192-200.

10. Heppenstall R, Sapega AA, Scott R, Shenton D, Park YS, Maris J, et al. An Experimental and Clinical Study of Muscular Energy Metabolism Using Phosphorus Nuclear Magnetic Resonance Spectroscopy. Clinical Orthopaedics and Related Research 1988; 226:138-155.

11. Jones WG, Perry MO, Bush HLJ. Changes in Tibial Venous Blood Flow in the Evolving Compartment Syndrome. Archives of Surgery 1989; 124:801-804.

12. Landi A, De Santis G, Torricelli P, Colombo A, Bedeschi P. CT in Established Volkmann's Contracture in Forearm Muscles. Journal of Hand Surgery 1989; 14-B:49-52.

13. Matsen FA, Mayo KA, Krugmire RB, Jr., Sheriden GW, Kraft GH. A Model Compartment Syndrome in Man with Particular Reference to the Quantification of Nerve Function. The Journal of Bone and Joint Surgery 1977; 59-A:648-653.

14. Matsen FA, Rorabeck CH. Compartment Syndromes. Instructional Course Lectures 1989; 38:463-472.

15. Mubarak SJ, Hargens AR. Acute Compartment Syndromes. Surgical Clinics of North America 1983; 63:539-565.

16. Petrik ME, Stambough JL, Rothman RH. Posttraumatic Gluteal Compartment Syndrome A Case Report. Clinical Orthopaedics and Related Research 1988; 231:127-129.

17. Phillips JH, Mackinnon SE, Beatty SE, Lee Dellon A, O'Brien J.P. Vibratory Sensory Testing in Acute Compartment Syndromes: A Clinical and Experimental Study. Plastic and Reconstructive Surgery 1987; 79:796-801.

18. Present DA, Nainzedeh NK, Ben-Yishay A, Mazzara JT. The Evaluation of Compartment Syndromes Using Somatosensory Evoked Potentials in Monkeys. Clinical Orthopaedics and Related Research 1993; 287:276-285.

19. Qvarfordt P, Christenson JT, Eklof B, Ohlin P, Saltin B. Intramuscular Pressure, Muscle Blood Flow, and Skeletal Muscle Metabolism in Chronic Anterior Tibial Compartment Syndrome. Clinical Orthopaedics and Related Research 1983; 179:284-290.

20. Robinson D, On E, Halperin N. Anterior Compartment Syndrome of the Thigh in Athletes Indications for Conservative Treatment. Journal of Trauma 1992; 32:183-186.

21. Rorabeck CH. Compartment Syndromes. In: Jupiter JB, Browner BD, Levine AM, Trafton PG, editors. Skeletal Trauma. Toronto: W. B. Saunders Company, 1992:285-309.

22. Rorabeck CH, Clarke KM. The Pathophysiology of the Anterior Tibial Compartment Syndrome: An Experimental Investigation. Journal of Trauma 1978; 18:299-304.

23. Russell WL, Apyan PM, Burns PR. An Electronic Technique for Compartment Pressure Measurement Using the Wick Catheter. Surgery, Gynecology and Obstetrics 1985; 161:173-175.

24. Sheriden GW, Matsen FA, Krugmire RB, Jr. Further Investigations on the Pathophysiology of the Compartment Syndrome. Clinical Orthopaedics and Related Research 1977; 123:266-270.

25. Steinberg BD, Gelberman RH. Evaluation of Limb Compartments With Suspected Increased Interstitial Pressure A Noninvasive Method for Determining Quantitative Hardness. Clinical Orthopaedics and Related Research 1994; 300:248-253.

26. Styf J, Korner L, Suurkula M. Intramuscular Pressure and Muscle Blood Flow During Exercise in Chronic Compartment Syndrome. The Journal of Bone and Joint Surgery 1987; 69-B:301-305.

27. Vukanovic S, Hauser H, Wettstein P. CT Localization of Myonecrosis for Surgical Decompression. American Journal of Radiology 1980; 135:1298-1299.

28. Willey RF, Corall RJM, French EB. Non-Invasive Method for the Measurement of Anterior Tibial Compartment Pressure. Lancet 1982; 1:595-596.

29. ATL Canada Inc., HDI 3000 Reference Manual, Markham, Ontario.

Appendix A - Criteria for Evaluating New Diagnostic Techniques

Noninvasive:
The procedure does not require any invasive procedures (i.e. penetration of the skin)

Repeatable / Continuous measurements:
The procedure can be easily repeated or used for continuously monitoring so a suspect compartment can be monitored over time.

Early diagnosis:
The procedure will diagnose the compartment syndrome before any neurological or muscular deficits occur.

Specific to compartment syndromes:
The procedure will rule out all other possible (differential) diagnoses.

Specific to affected compartment:
The procedure will specify which compartment is effected by the compartment syndrome.

Sensitive to compartment syndromes:
The procedure will have a good chance of detecting a compartment syndrome if there is one there. (i.e. it will not "miss" a compartment syndrome, no false negatives.)

Diagnosis of all compartments:
The procedure will be able to diagnose all of the major compartments subjected to compartment syndromes. Specifically the four lower leg compartments and the three forearm compartments.

No risk to patient:
The procedure will not put any additional risk to the patient's condition.

Easily interpreted:
The results will be easy to interpret so that a "Go / No go" diagnosis can be made quickly and confidently. Quantitative results are preferable.

Portability:
The procedure can be carried out at the patient's bedside if necessary.

Inexpensive:
The procedure's capital and operating costs are not excessive (especially in view of the need for repeated measurements).

Appendix B - Detailed Drawings of Apparatus

B1.0 ASSEMBLY OF FRAME AND VISE

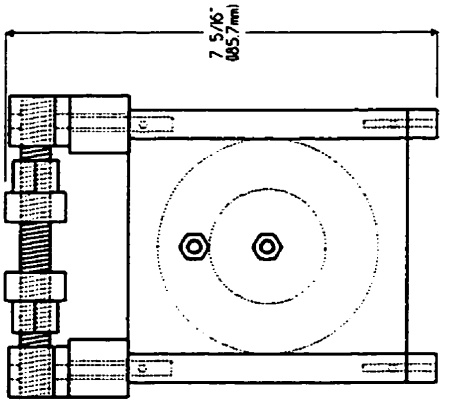

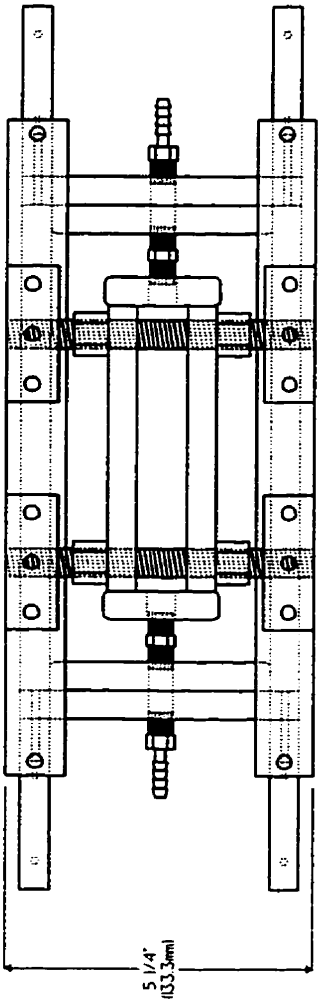

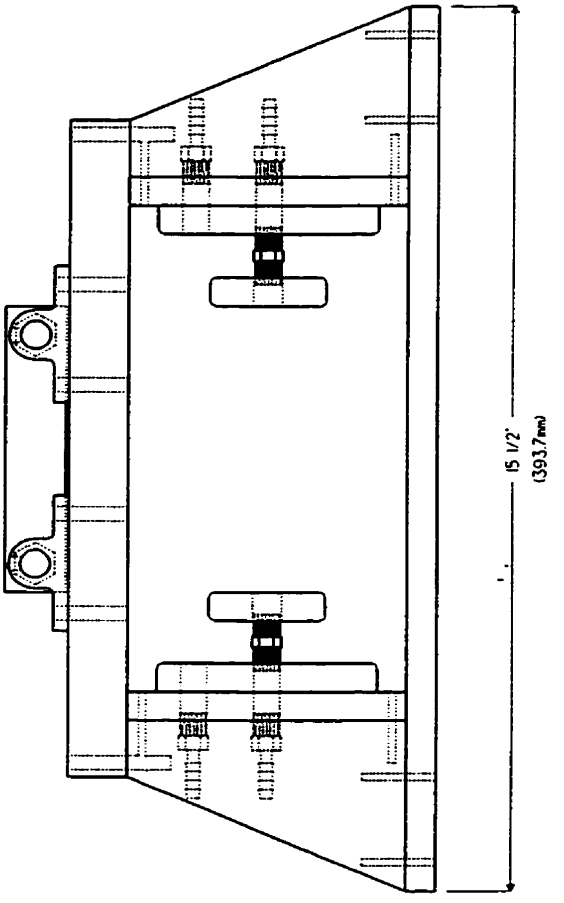

B2.0 COMPARTMENT SYNDROME SIMULATOR FRAME

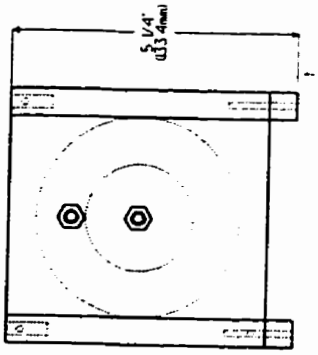

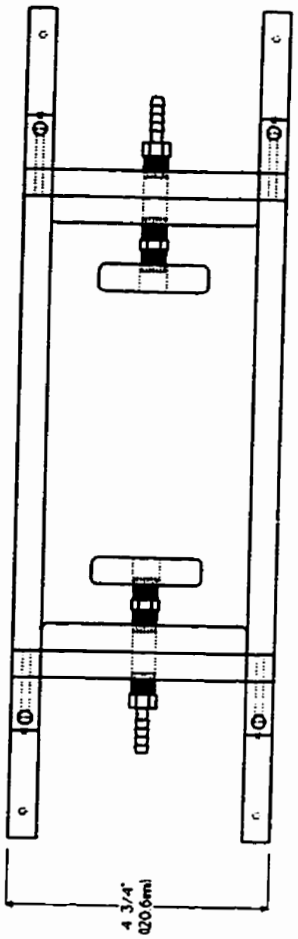

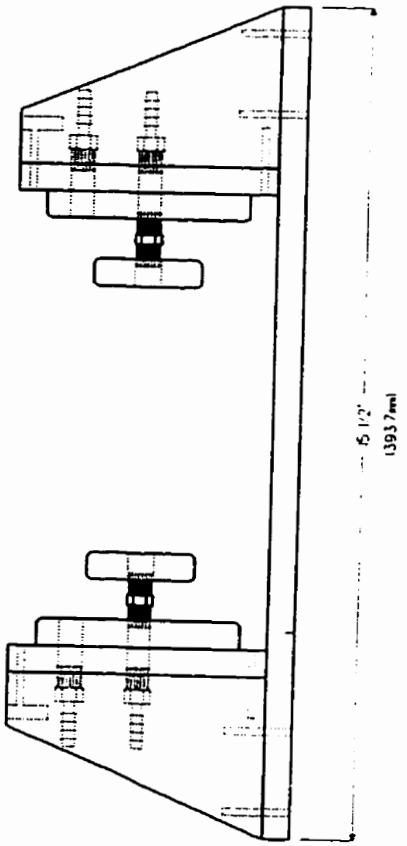

B2.1 FRAME ASSEMBLY DRAWING

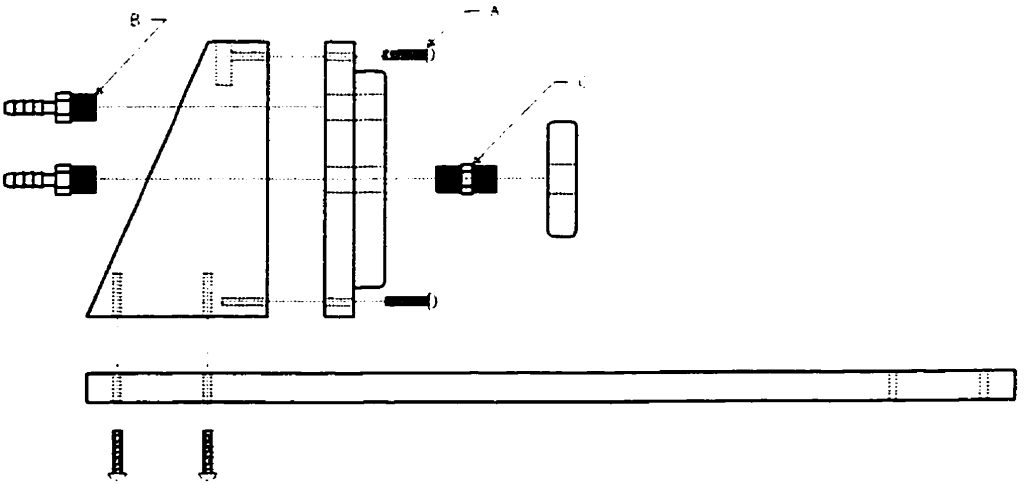

Component	Description	Quantity
A. Screw	8/32 X 3/4"	16
B. Barbed nylon	Cole-Parmer	4
Fitting	P/N: E-06465-10	
C. Brass nipple	Canadian Tire	2
	P/N: 63-4609-0	
NOT SHOWN		
Baby bottle liner	Platex 227mL/8oz.	1
Milk bag	Diameter = 3 3/4"	1
	Length = 8 1/2"	
Hose clamp	Canadian Tire	2
	P/N: 63-2125-2	
Hose clamp	Canadian Tire	2
	P/N: 63-2119-8	
Bicycle rim tape	Width = 1/2" thick	
	(Hose clamp seal)	

B2.2 FRAME BASE

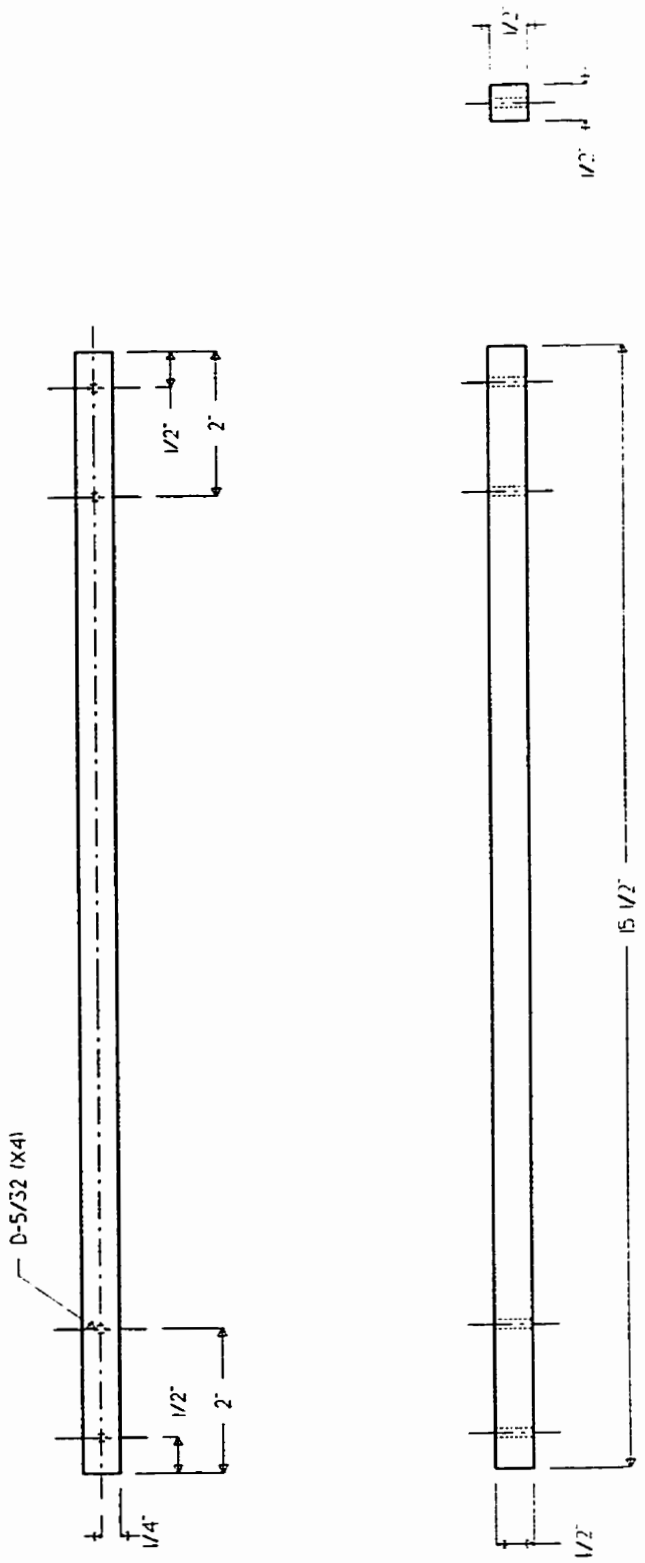

B2.3 FRAME BRAKETS

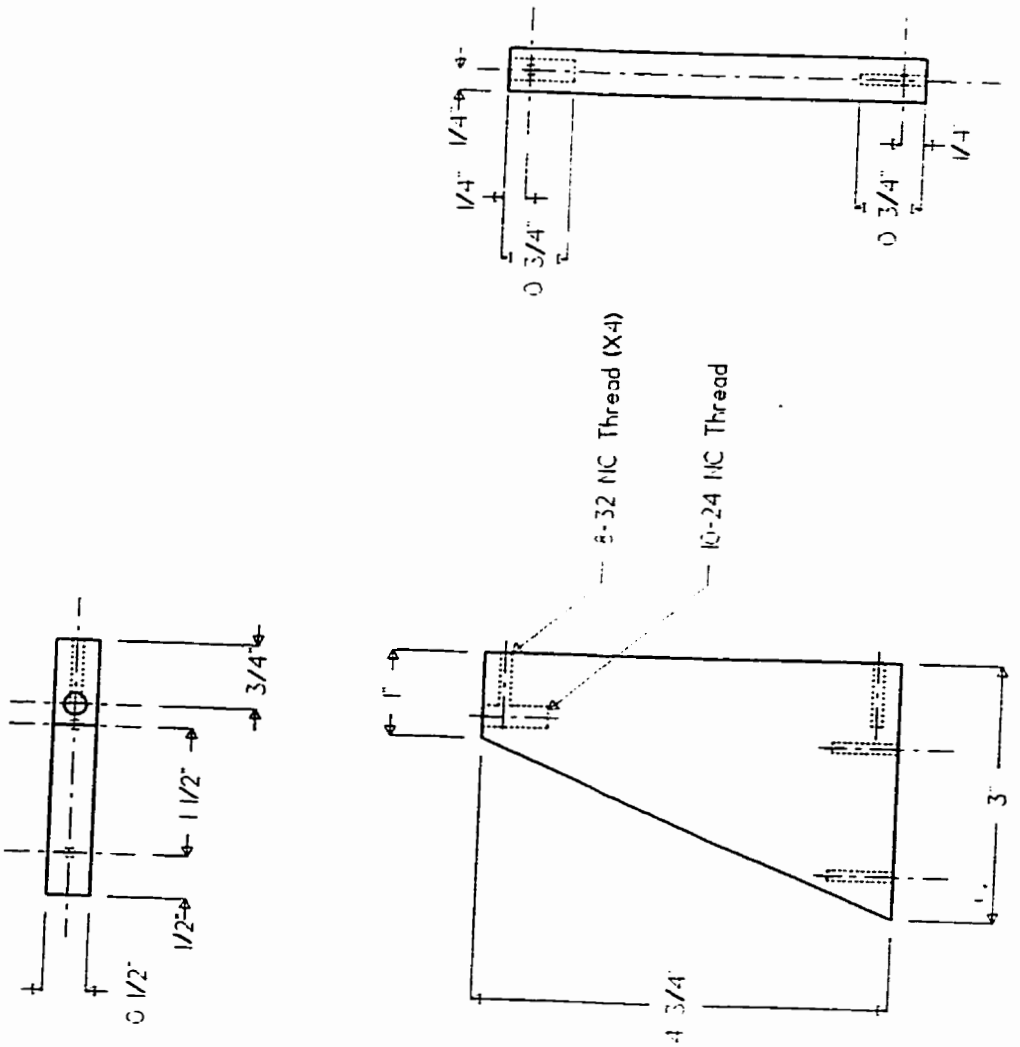

B2.4 "LIMB" PLATE

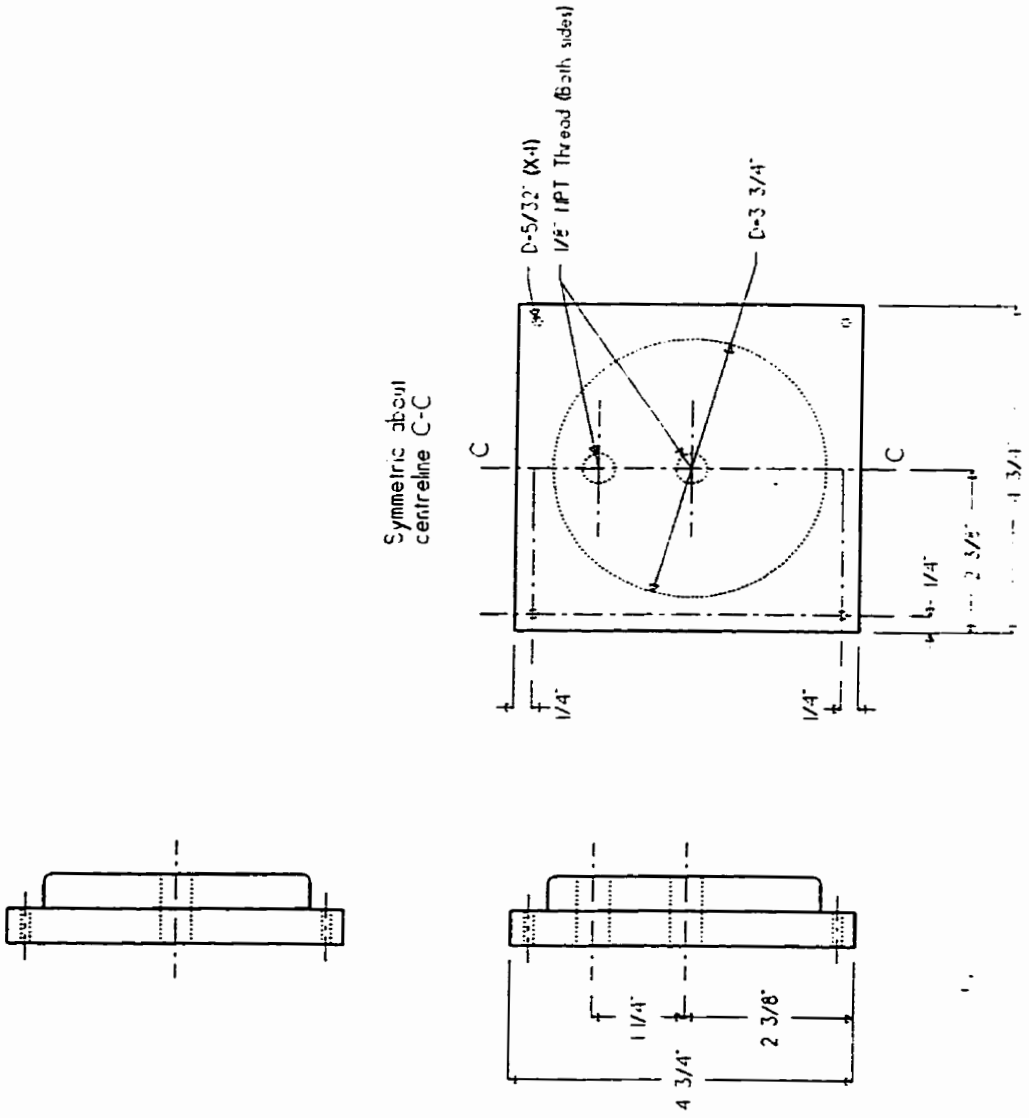

B2.5 "COMPARTMENT PLATE"

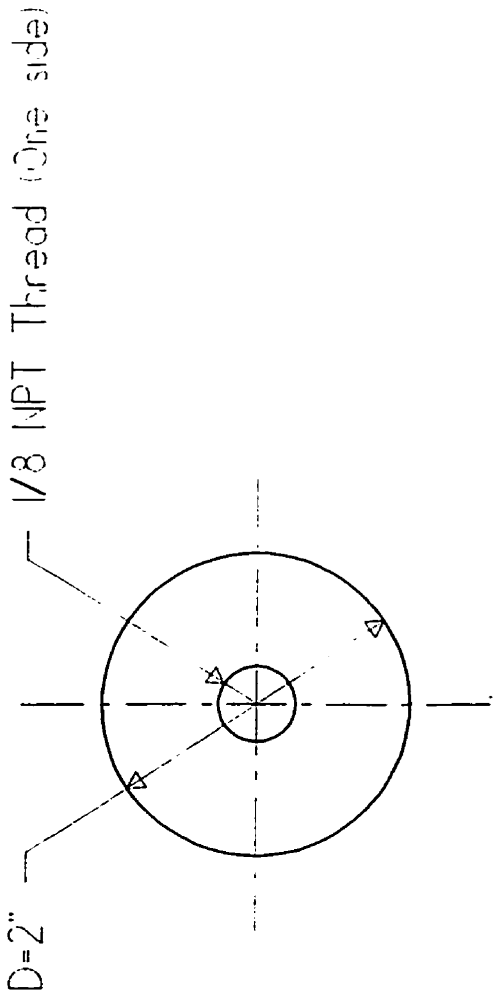

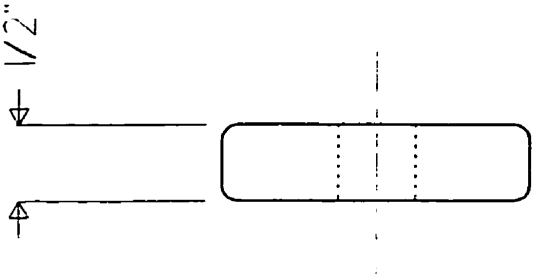

B3.0 ULTRASOUND PROBE VISE

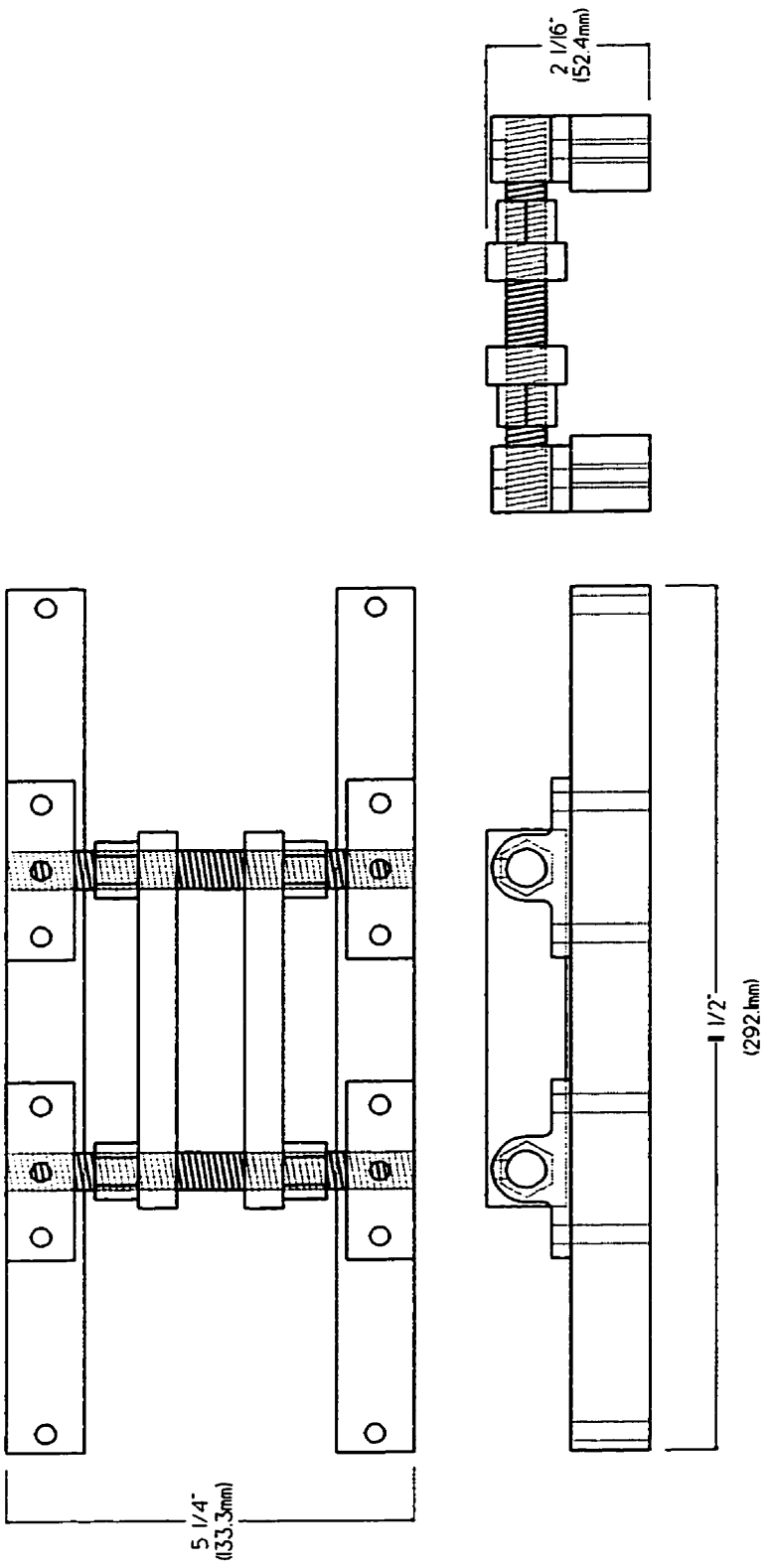

B3.1 VISE ASSEMBLY DRAWING

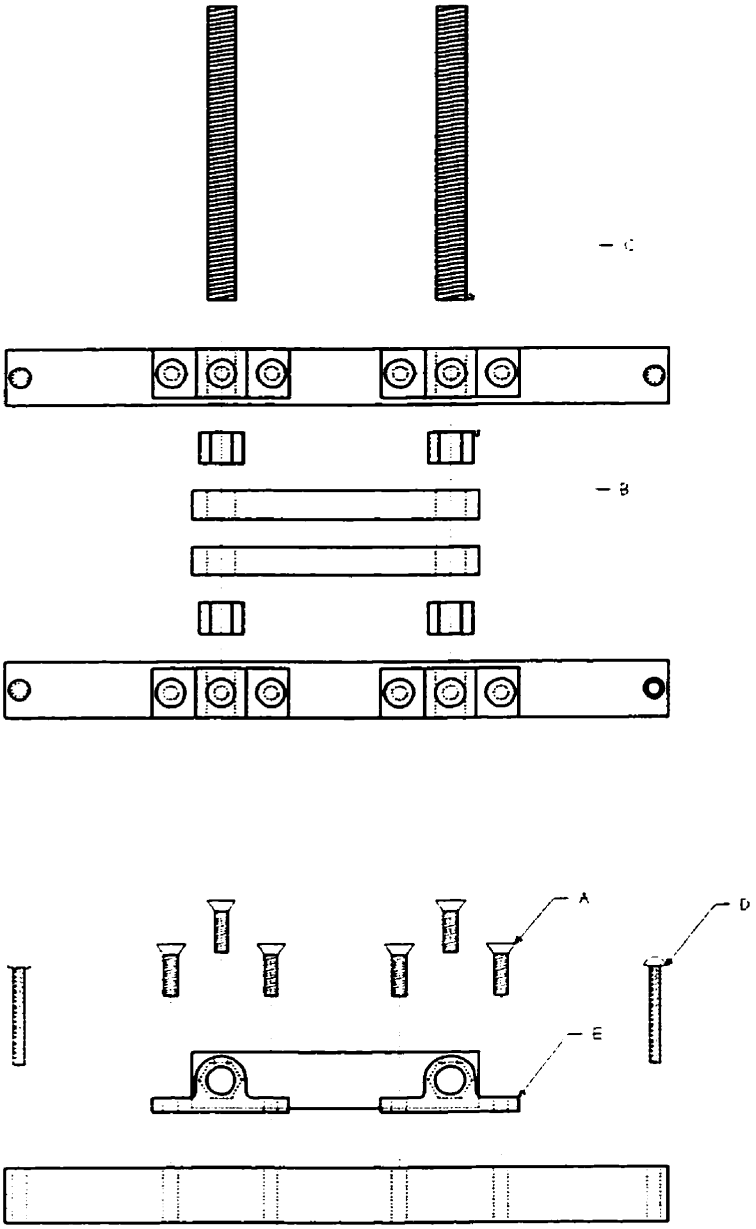

Component	Description	Quantity
A. Screw	1/4-20 X 3/4"	12
B. Nut	1/2-13	4
C. Threaded rod	1/2-13 X 5 1/4"	2
D. Screw	10-24 X 1 3/4"	4
E. Bearing sleeve	Canadian Tire	4
	P/N: 56-0606-6	

B3.2 VISE BASE

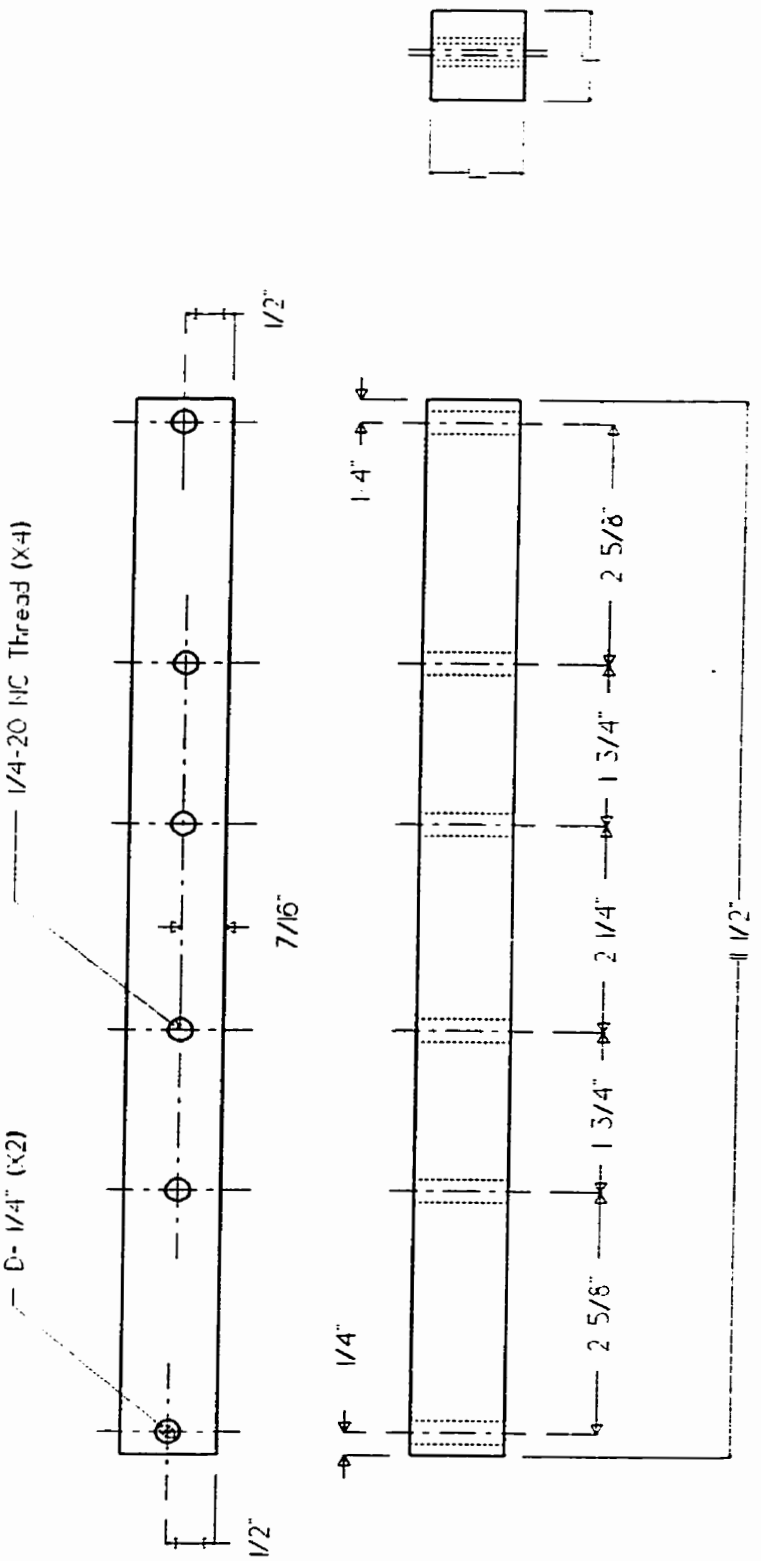

B3.3 VISE BEARINGS

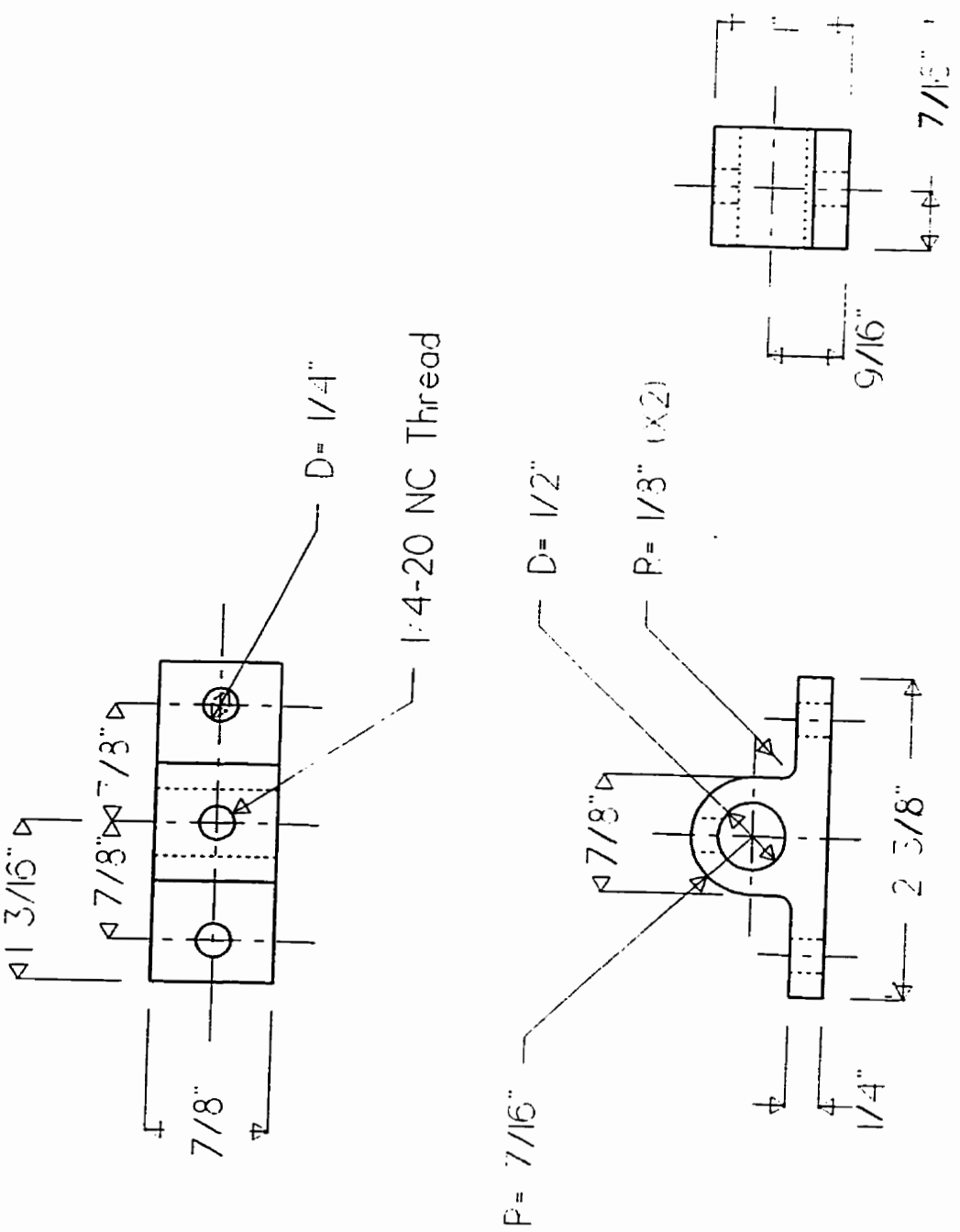

B3.4 VISE BRACKETS

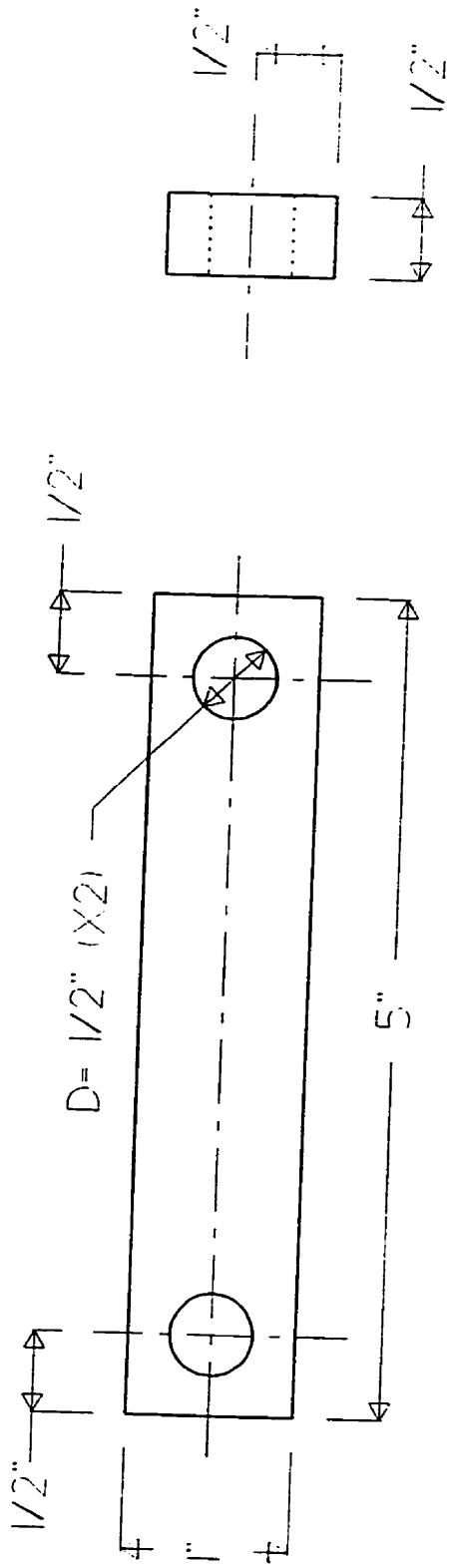

Appendix C - Pilot Study Ultrasound Images

PILOT STUDY DATA: M-Mode, f=5Hertz

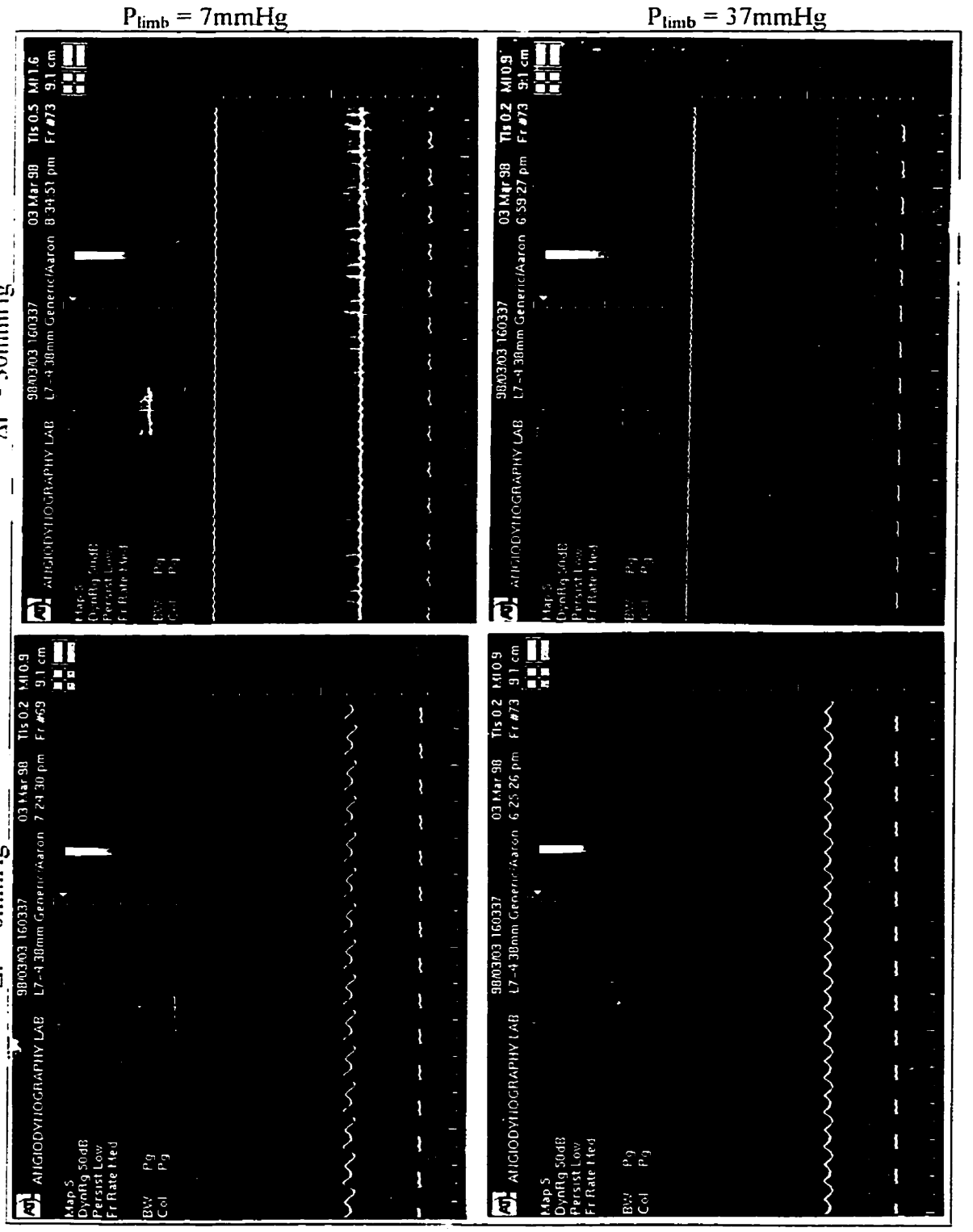

PILOT STUDY DATA: M-Mode, f=10Hertz

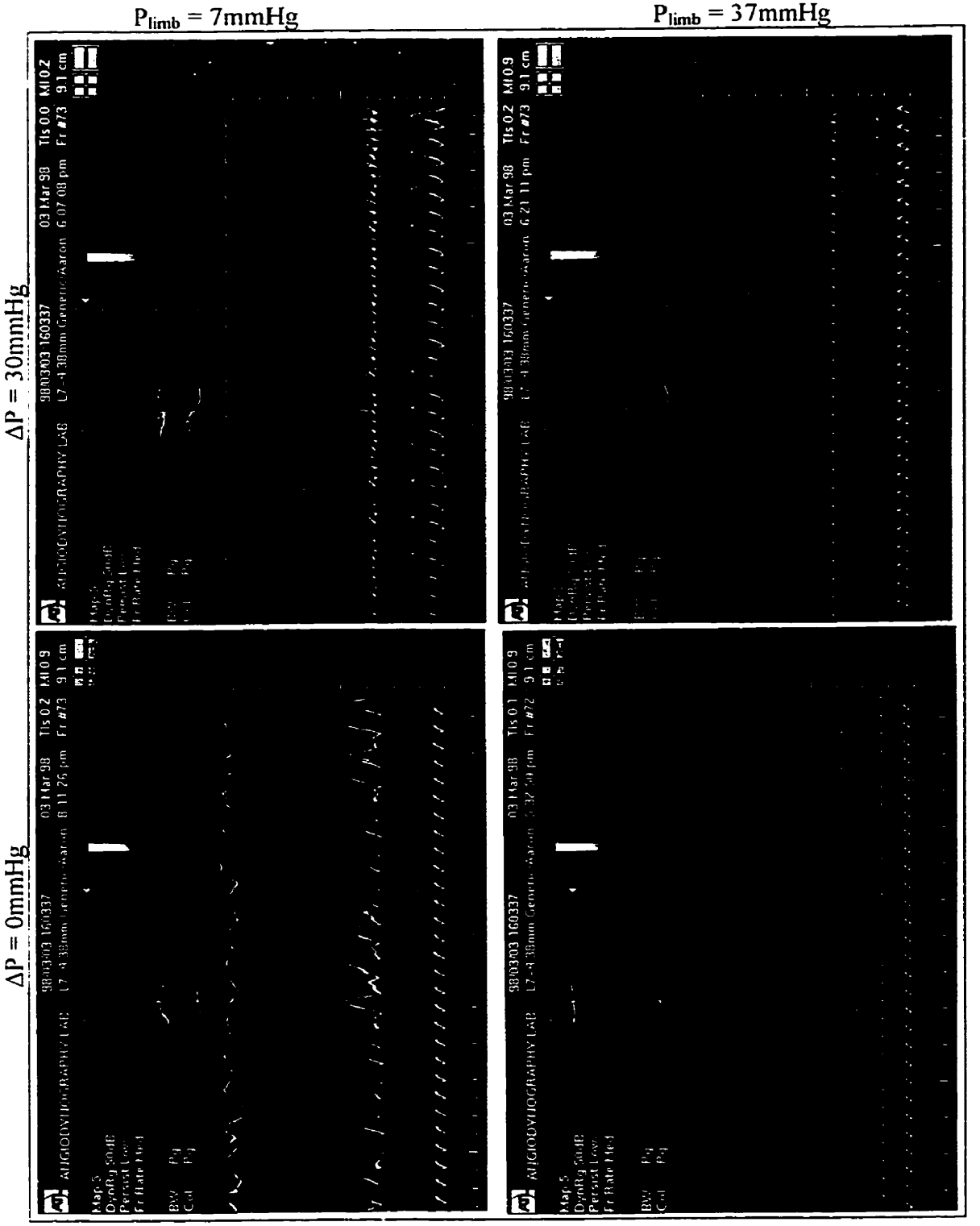

PILOT STUDY DATA: M-Mode, f=15Hertz

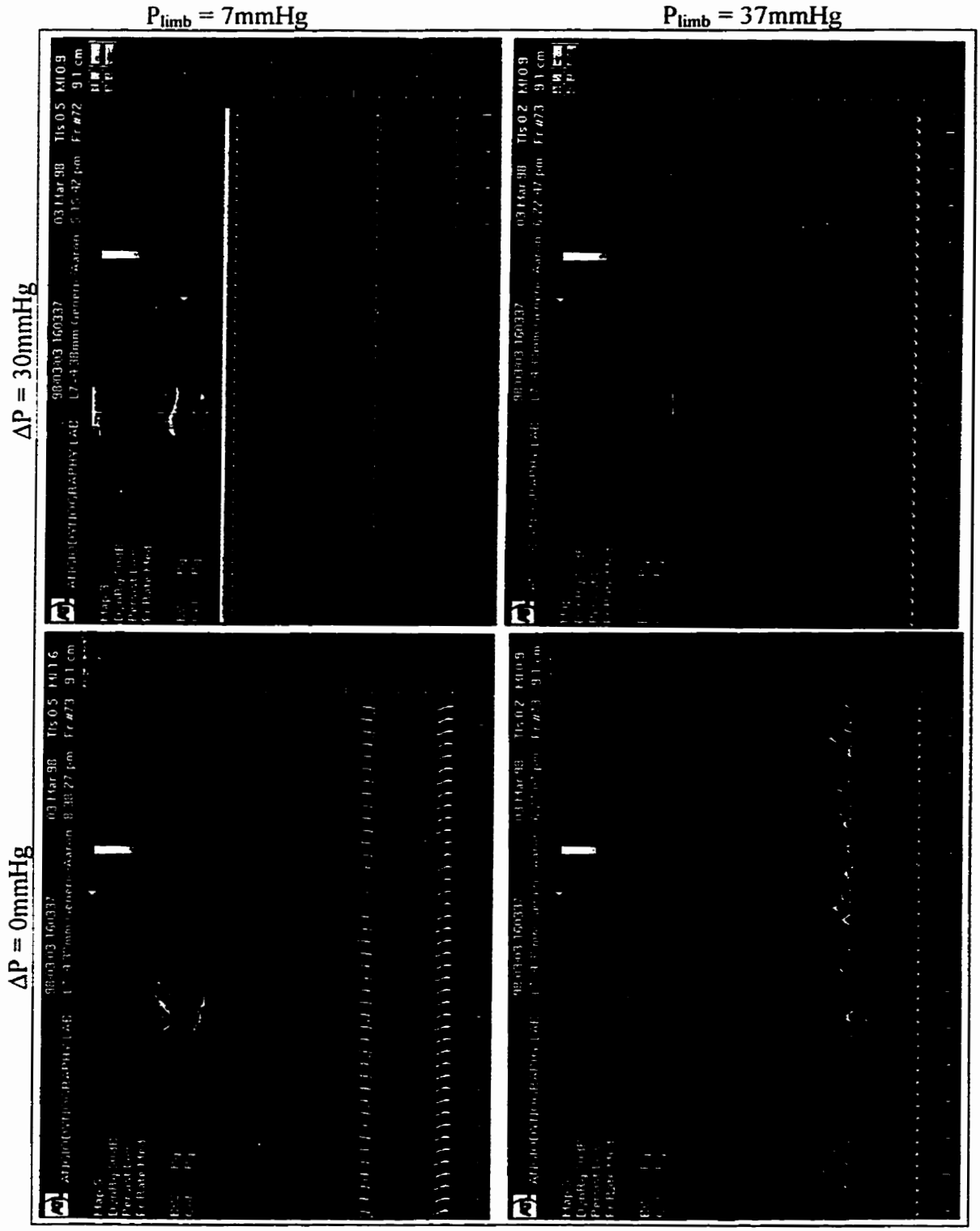

PILOT STUDY DATA: Doppler Mode, f=5Hertz, Closest Membrane

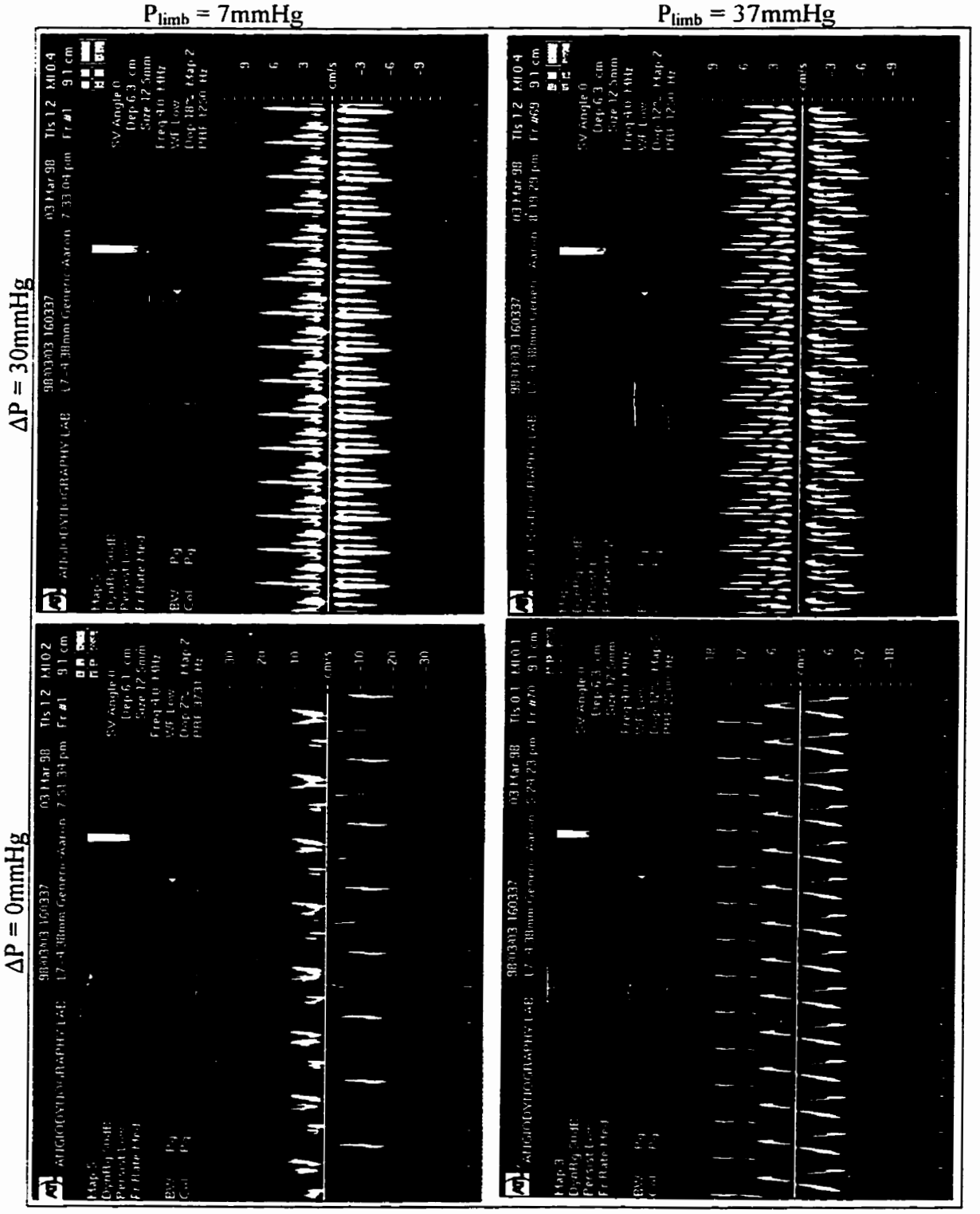

PILOT STUDY DATA: Doppler Mode, f=10Hertz, Closest Membrane

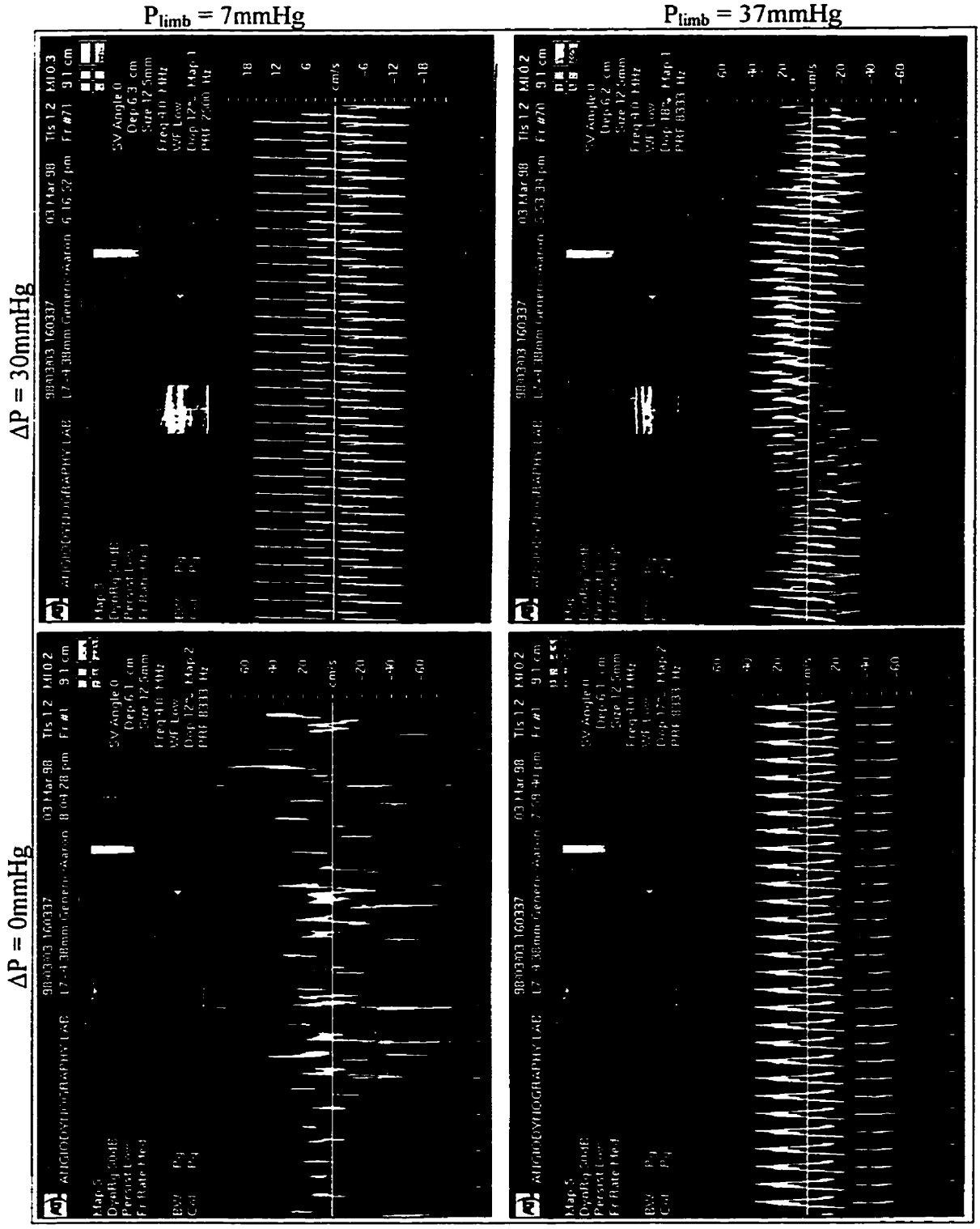

PILOT STUDY DATA: Doppler Mode, f=15Hertz, Closest Membrane

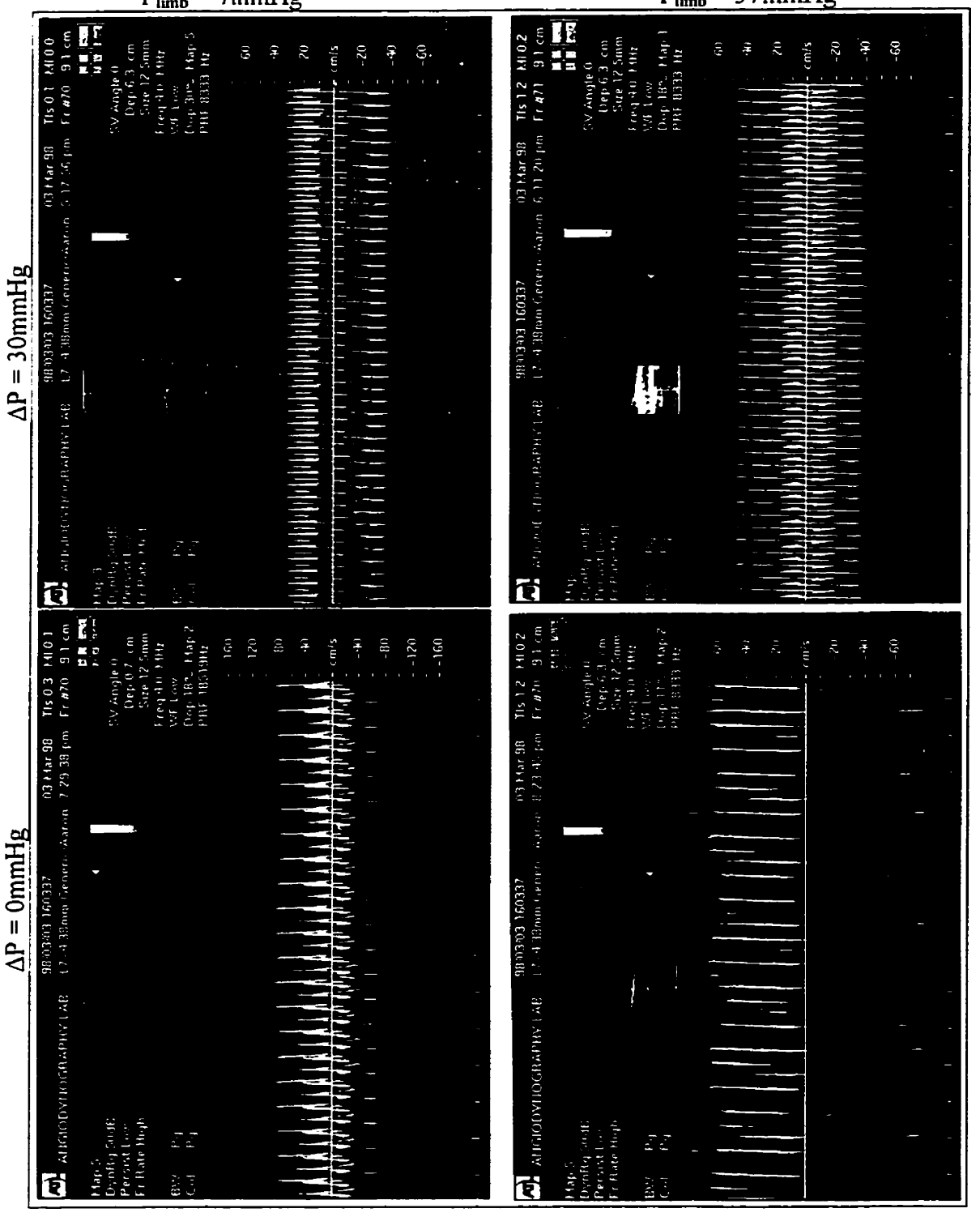

PILOT STUDY DATA: Doppler Mode, f=5Hertz, Furthest Membrane

P_{limb} = 7mmHg

P_{limb} = 37mmHg

ΔP = 30mmHg

ΔP = 0mmHg

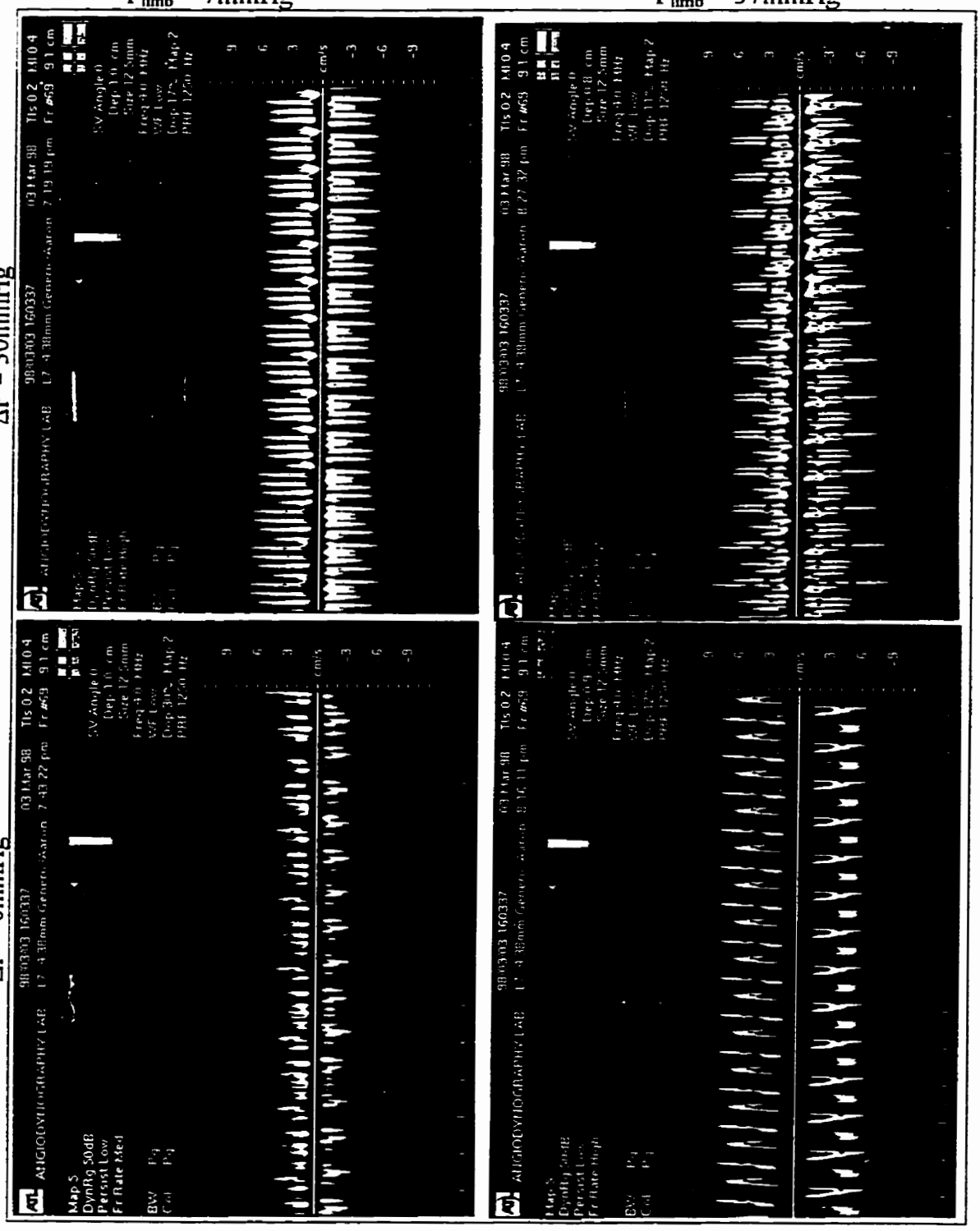

PILOT STUDY DATA: Doppler Mode, f=10Hertz, Furthest Membrane

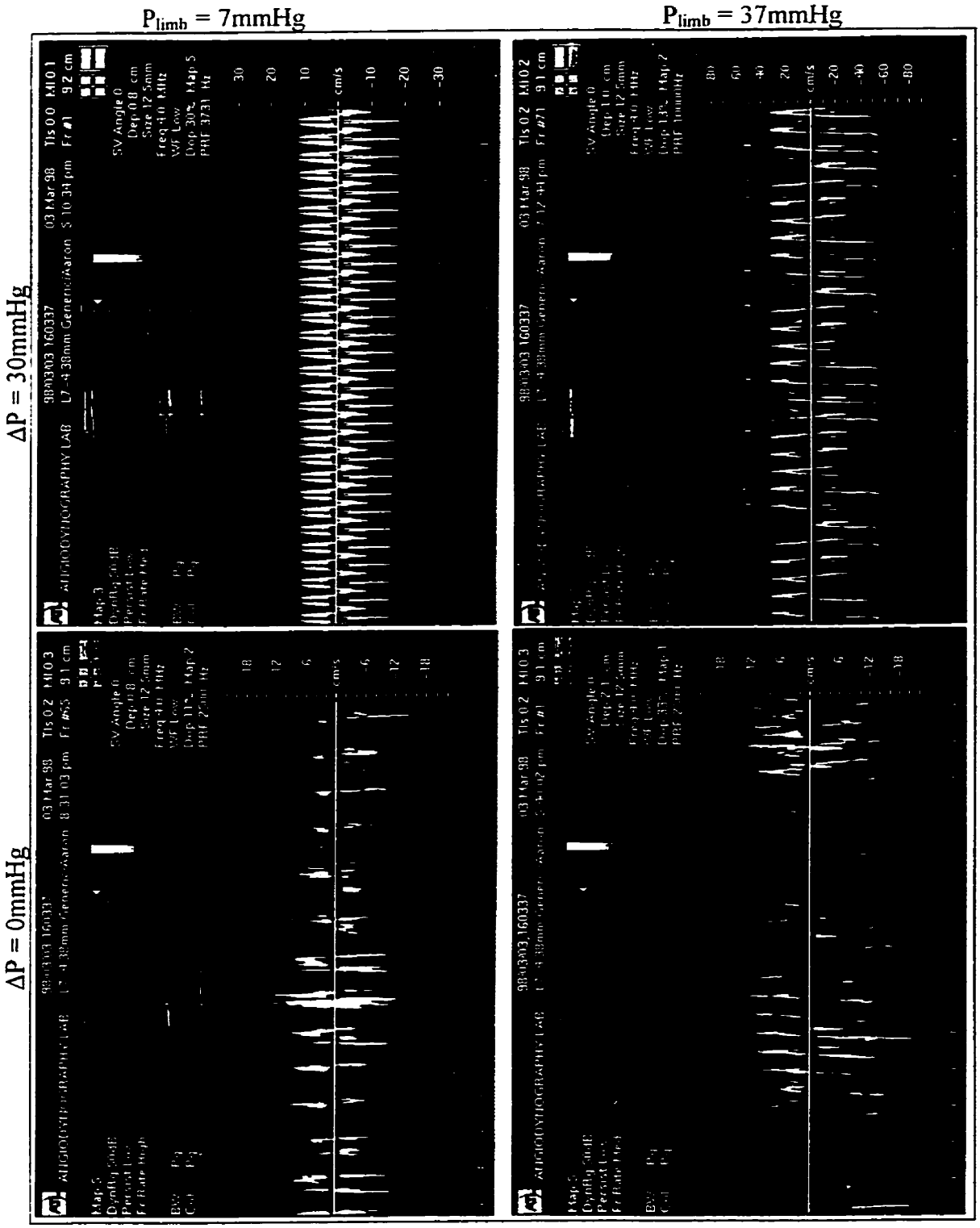

PILOT STUDY DATA: Doppler Mode, f=15Hertz, Furthest Membrane

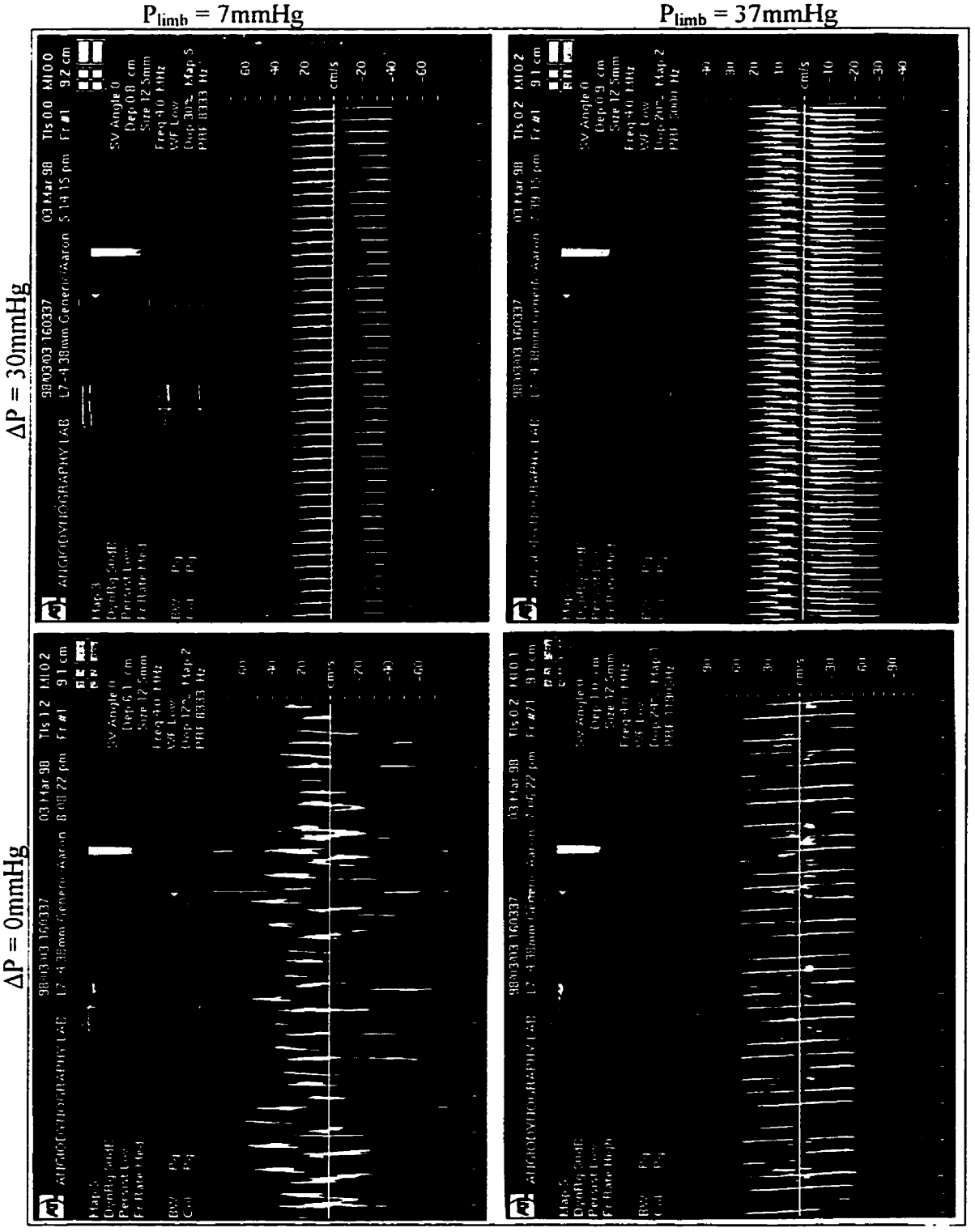

Appendix D - Sample Pressure Dependence Study Ultrasound Images

MAIN STUDY DATA

$\Delta P = 45mmHg$

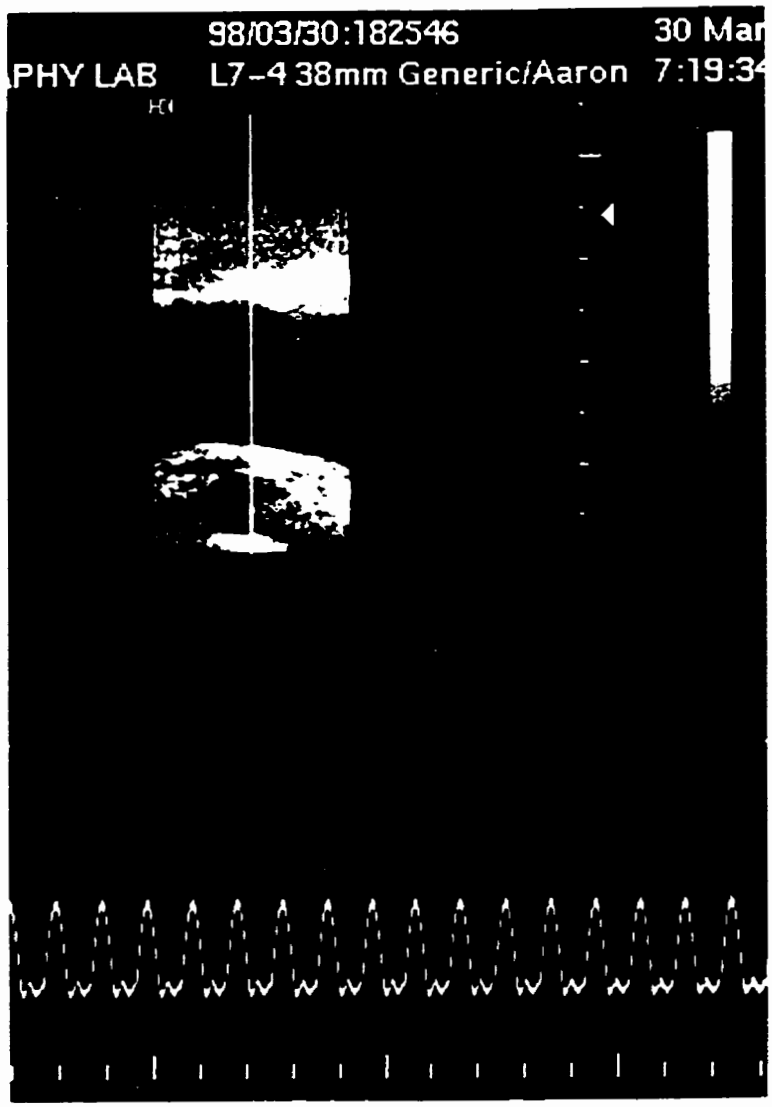

MAIN STUDY DATA

ΔP = 42mmHg

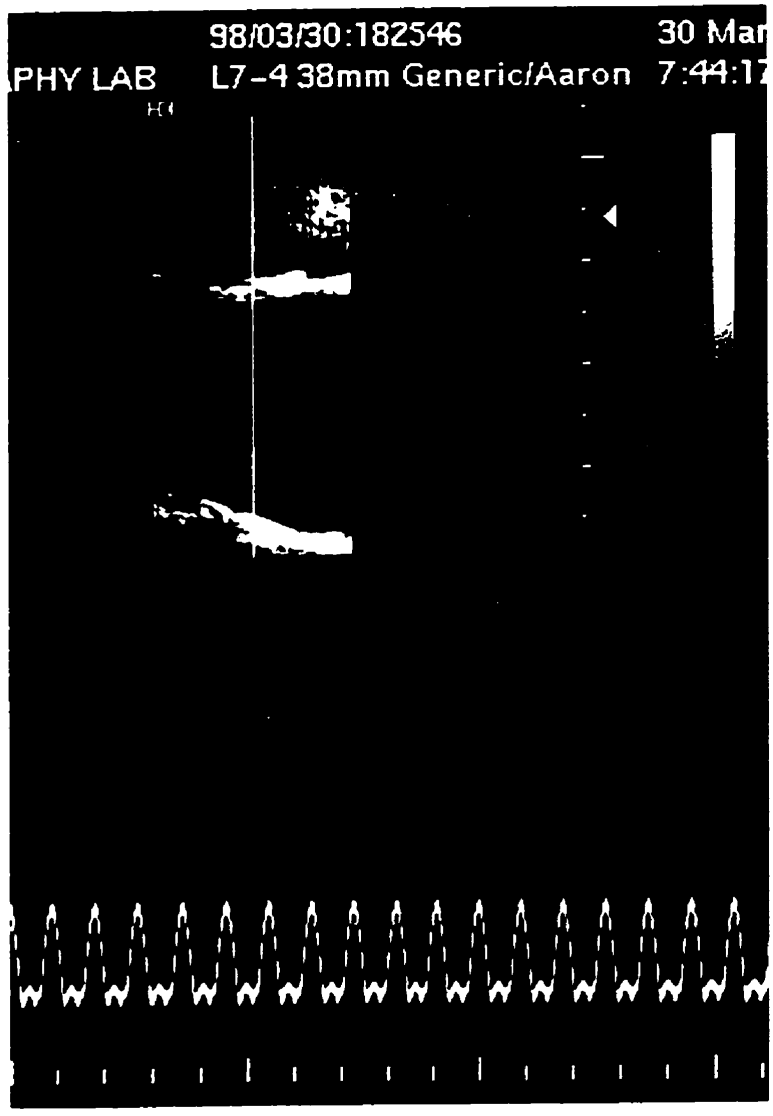

MAIN STUDY DATA

ΔP = 39mmHg

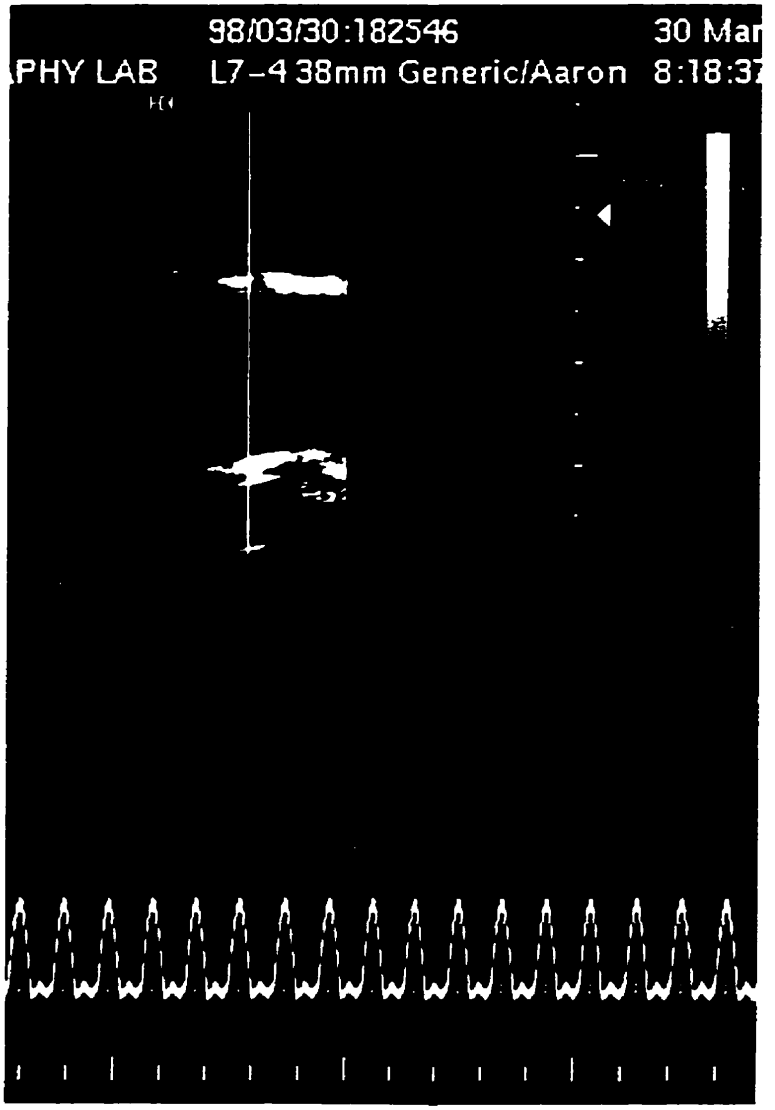

MAIN STUDY DATA

ΔP = 36mmHg

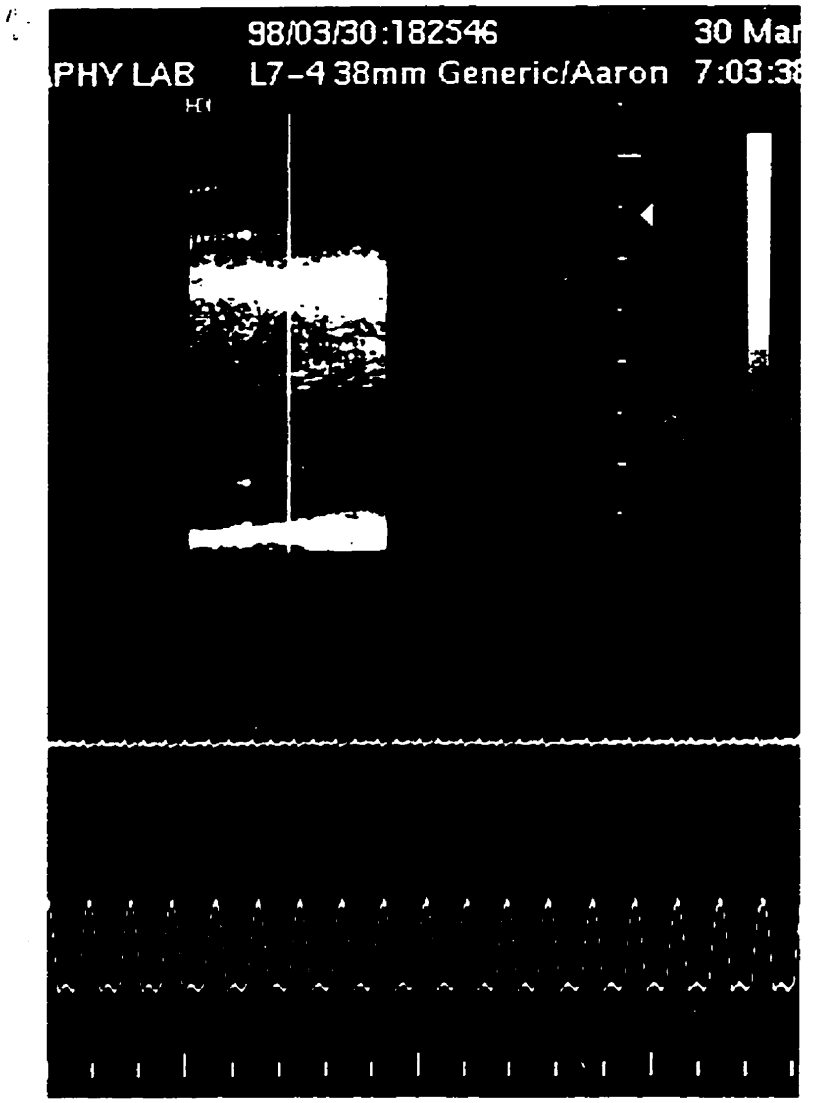

MAIN STUDY DATA

ΔP = 33mmHg

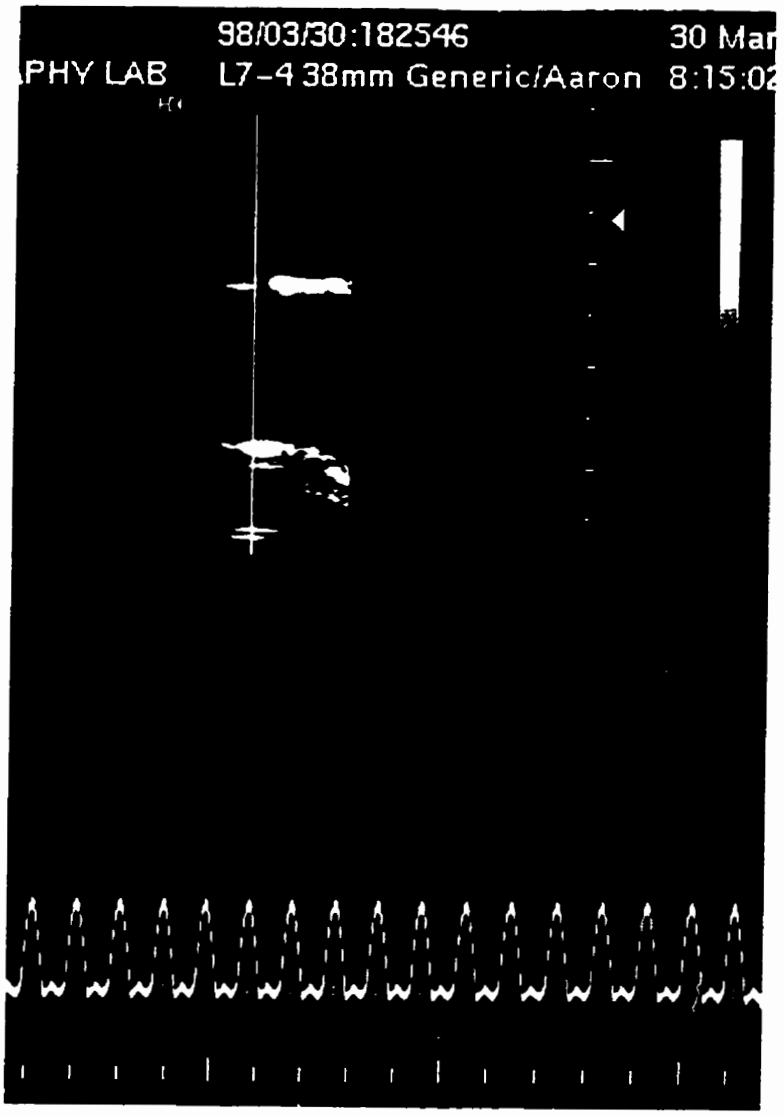

MAIN STUDY DATA

ΔP = 30mmHg

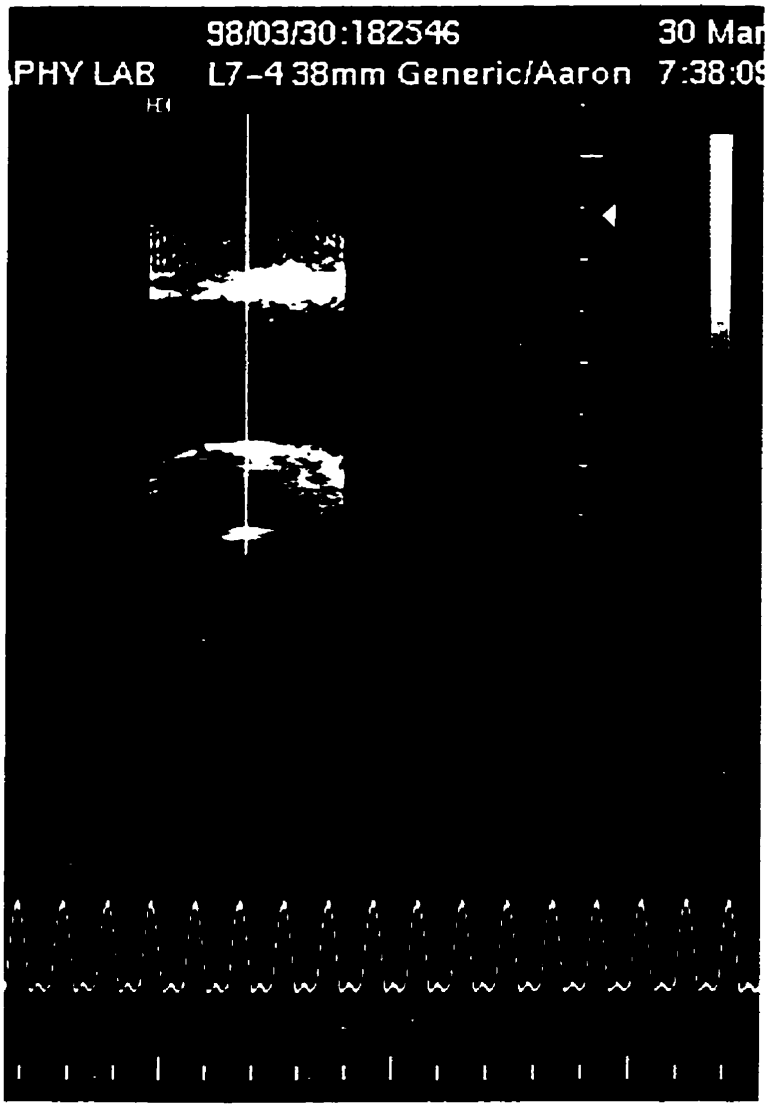

MAIN STUDY DATA

ΔP = 27mmHg

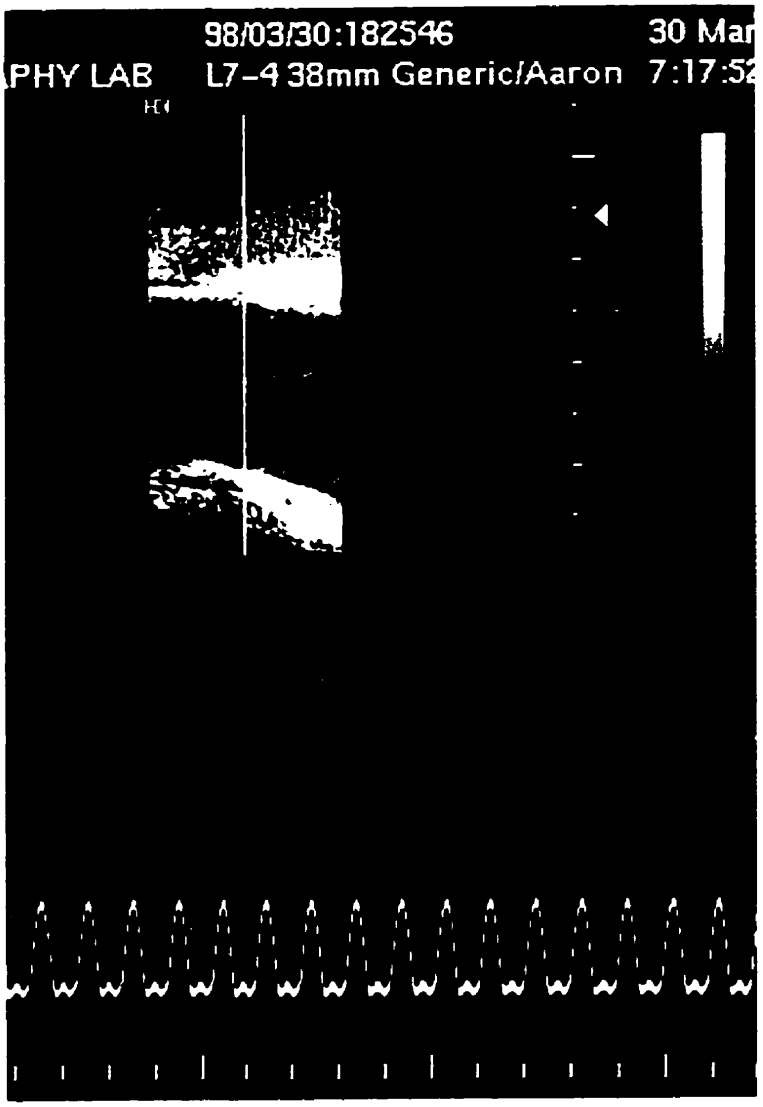

MAIN STUDY DATA

ΔP = 24mmHg

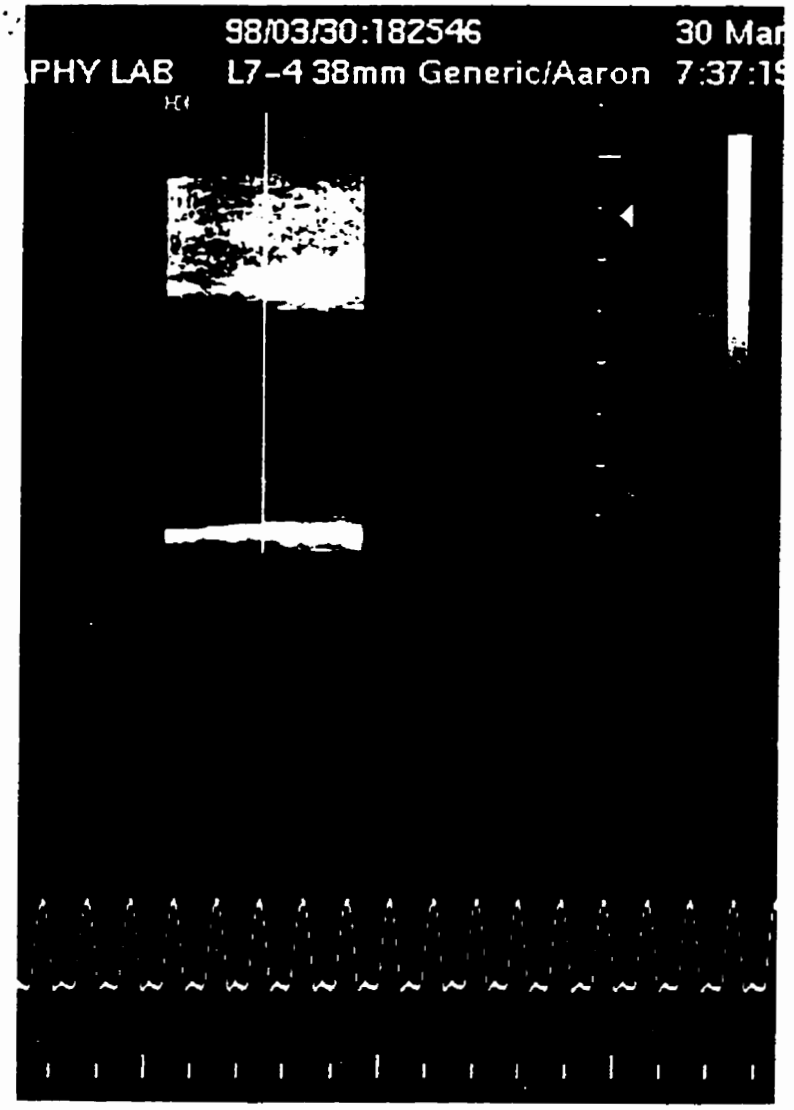

MAIN STUDY DATA

ΔP = 21mmHg

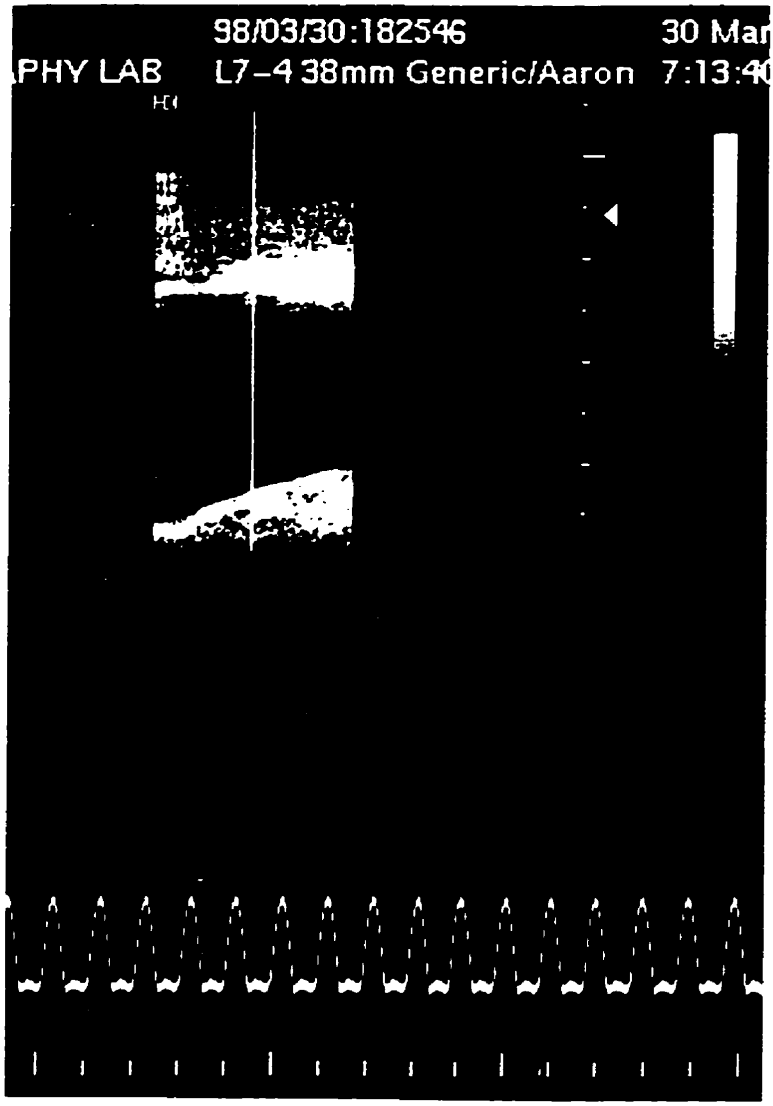

MAIN STUDY DATA

ΔP = 18mmHg

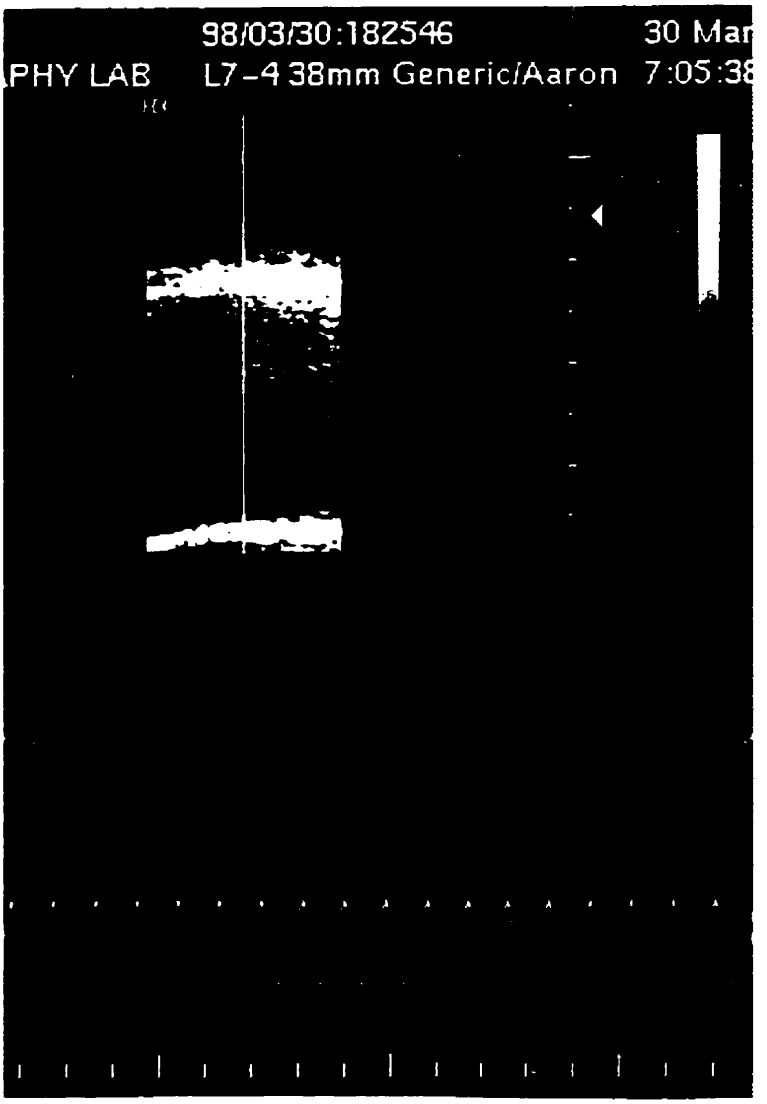

MAIN STUDY DATA

ΔP = 15mmHg

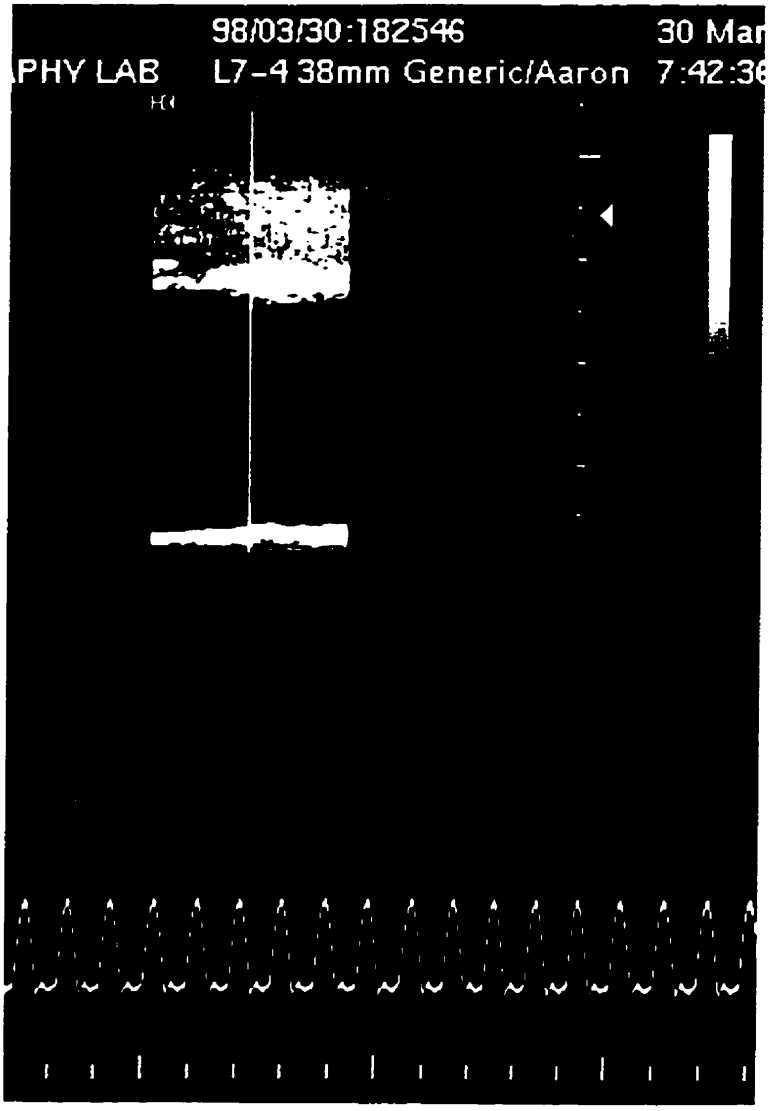

MAIN STUDY DATA

$\Delta P = 12mmHg$

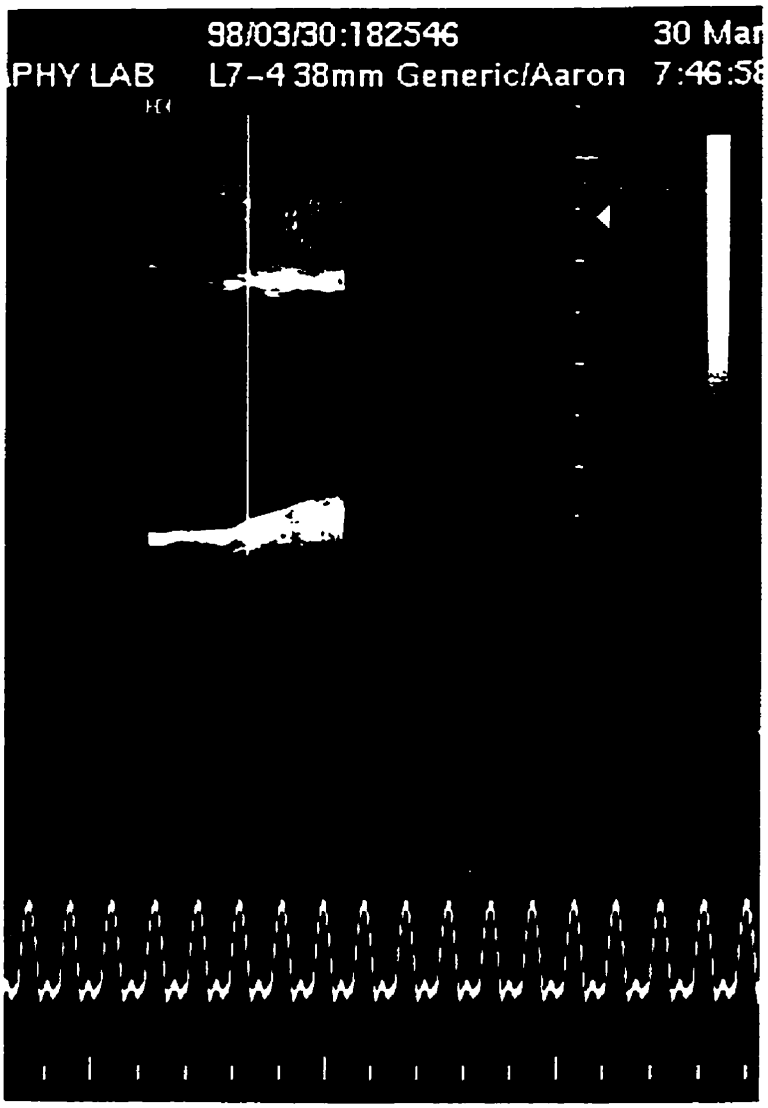

MAIN STUDY DATA

ΔP = 9mmHg

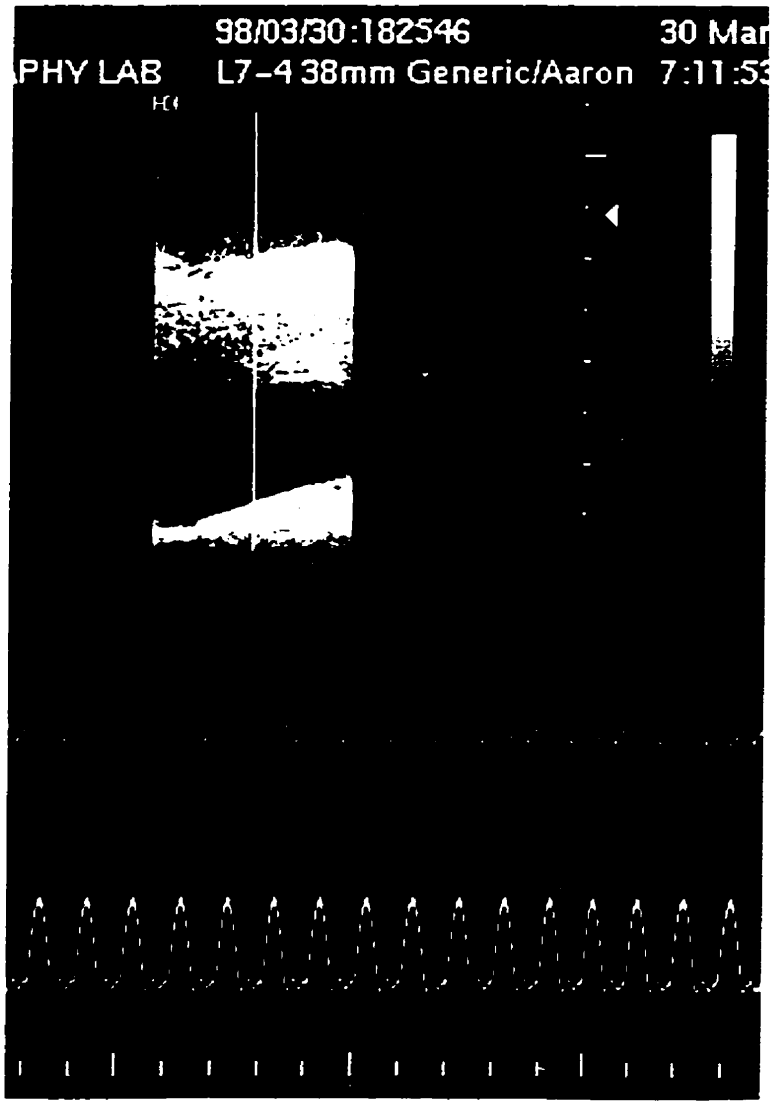

MAIN STUDY DATA

ΔP = 6mmHg

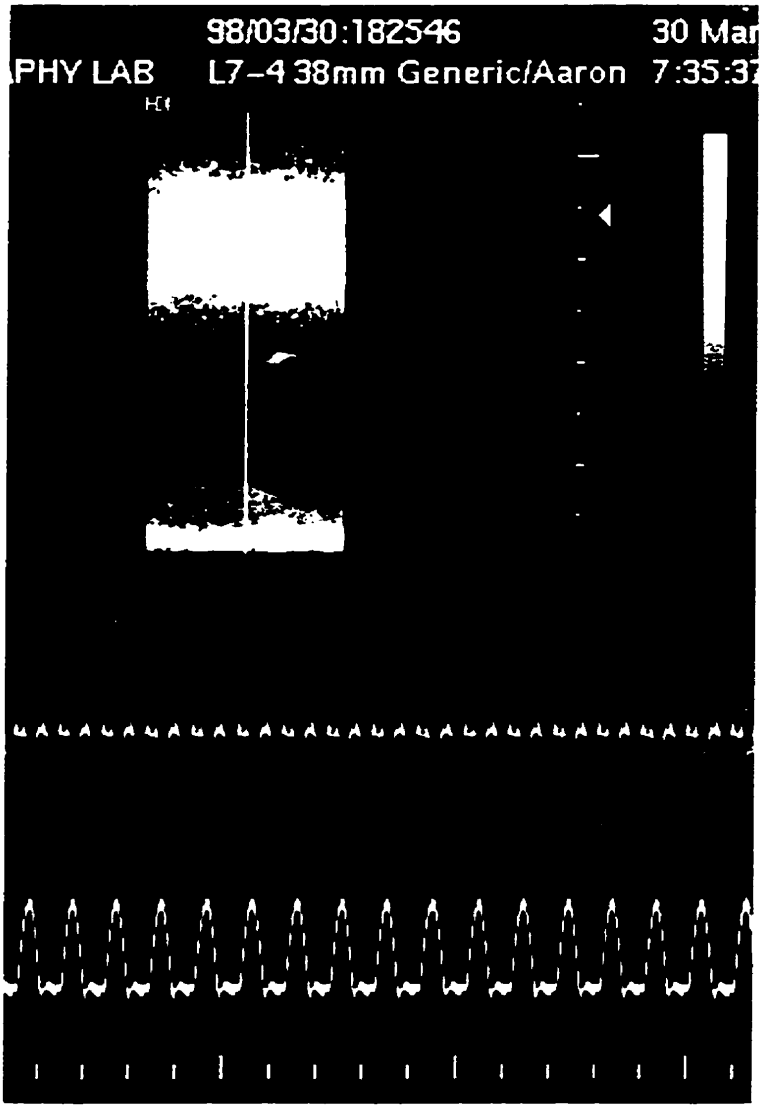

MAIN STUDY DATA

ΔP = 3mmHg

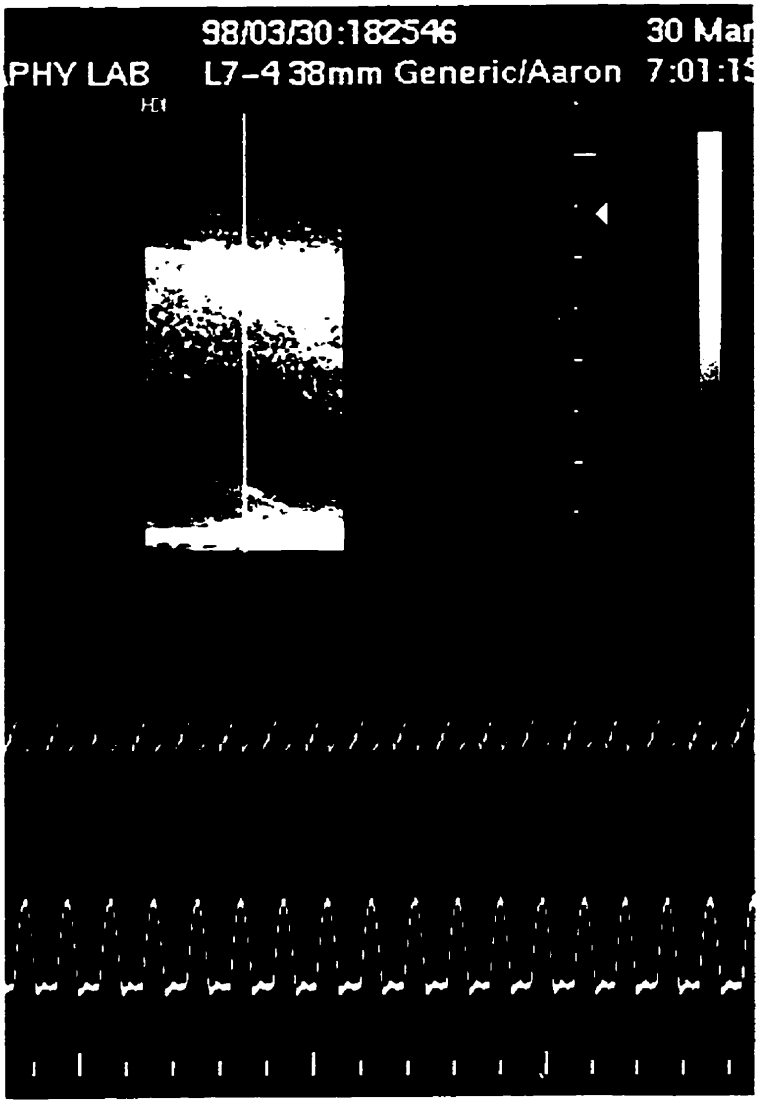

MAIN STUDY DATA

ΔP = 0mmHg

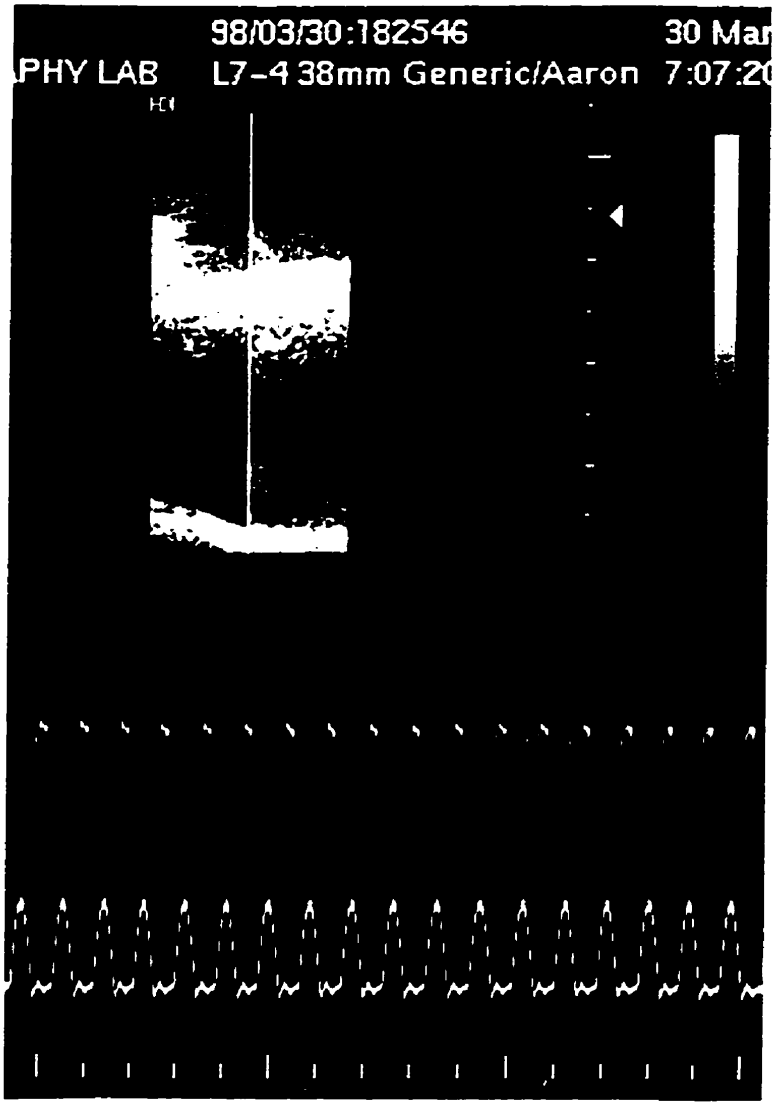

Appendix E - Regression Analysis for Second Order Model

A typical mass-spring-damper system is analyzed by dissecting the components of the system and doing a "force balance" on the mass.

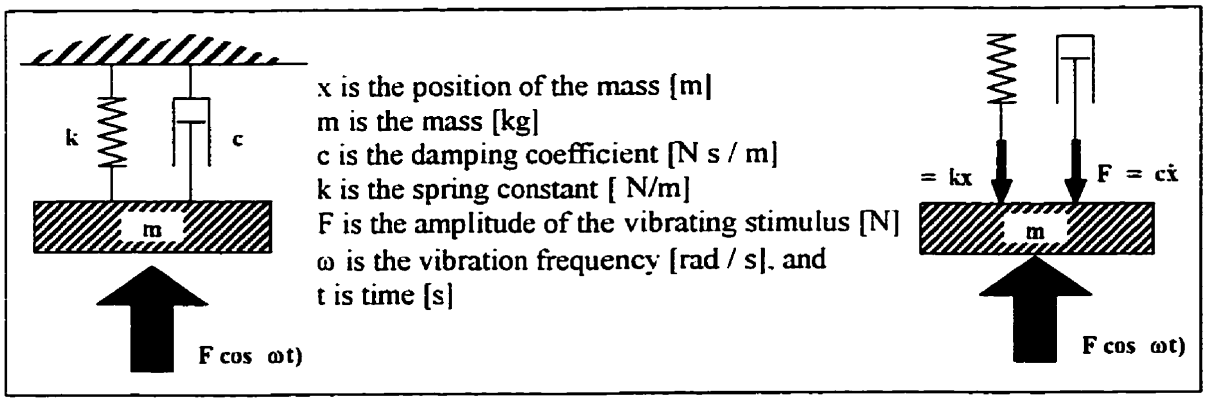

- **The force balance yields:**

$$\sum F = ma$$

$$F\cos(\omega t) - F_s - F_d = ma$$

$$F\cos(\omega t) - kx - c\dot{x} = m\ddot{x}$$

$$m\ddot{x} + c\dot{x} + kx = F\cos(\omega t)$$

- **The solution to this differential equation is:**

$$x = x_{max}\cos(\omega t - \phi)$$

where,

$$x_{max} = \frac{F}{\sqrt{\left(k - m\omega^2\right)^2 + \left(c\omega\right)^2}} \qquad \text{(Equation 1)}$$

(ϕ is the phase angle, and describes the lag between the forcing function and the system's response).

- **Equation 1 can be rewritten as:**

$$\frac{1}{x_{max}^2} = C_1 k^2 + C_2 k + C_3 \qquad \text{(Equation 2)}$$

where,

$$C_1 = \frac{1}{F^2} \qquad C_2 = -\frac{2m\omega^2}{F^2} \qquad C_3 = \frac{m^2\omega^4}{F^2} + \frac{c^2\omega^2}{F^2}$$

(Note that C_1, C_2, and C_3 must be positive, negative, and positive respectfully.)

- **Finally, the regression analysis can be used to "fit" n data pairs (k_i, x_i) to Equation 2 by solving the following matrix equation:**

$$\begin{bmatrix} \sum_{i=1}^{n} k_i^4 & \sum_{i=1}^{n} k_i^3 & \sum_{i=1}^{n} k_i^2 \\ \sum_{i=1}^{n} k_i^3 & \sum_{i=1}^{n} k_i^2 & \sum_{i=1}^{n} k_i^1 \\ \sum_{i=1}^{n} k_i^2 & \sum_{i=1}^{n} k_i^1 & \sum_{i=1}^{n} k_i^0 \end{bmatrix} \begin{bmatrix} C_1 \\ C_2 \\ C_3 \end{bmatrix} = \begin{bmatrix} \sum_{i=1}^{n} \frac{k_i^2}{x_i^2} \\ \sum_{i=1}^{n} \frac{k_i}{x_i^2} \\ \sum_{i=1}^{n} \frac{1}{x_i^2} \end{bmatrix}$$

where, k_i is the measured stiffness, and
x_i is the measured displacement

Assuming $\Delta P_i \equiv k_i$ and $\omega/2\pi = f = 5$ Hertz the regression analysis can be performed with the pressure dependence study data to obtain the equation and plot below:

$$x_{max} = \frac{1}{\sqrt{-1324P^2 + 201897P - 651945}}$$

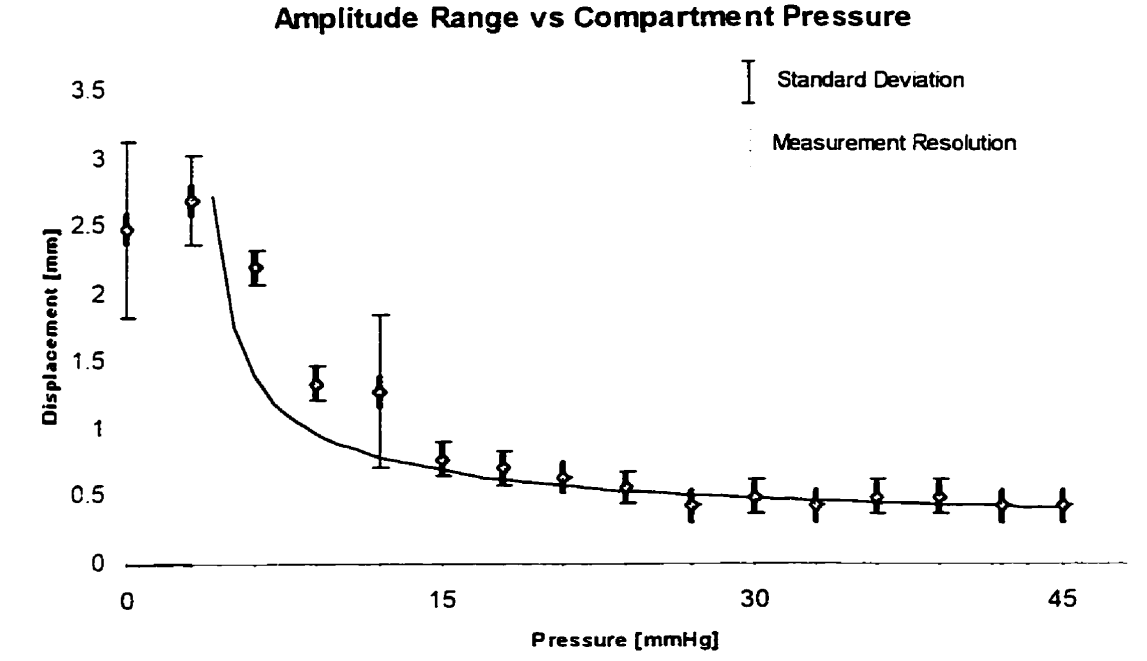

Plot of regression analysis equation against the pressure dependence study data

The values of C_1, C_2 , and C_3, were used to calculate the following "equivalent" parameters:

$$F = 0.0275\sqrt{-\bar{1}}\ N$$

$$m = -0.0775\ kg$$

$$c = 2.53\sqrt{-\bar{1}}\ Ns/m$$

Since these parameters did not have any meaningful sense, several subsequent regressions were performed with each regression eliminating the data pairs corresponding

to the "highest" pressure setting of the last. This elimination of data continued until the extracted parameters (F, m, and c) were all positive values. Finally, the following regression equation and plot was obtained:

$$x_{max} = \frac{1}{\sqrt{8566P^2 - 51660P - 238886}}$$

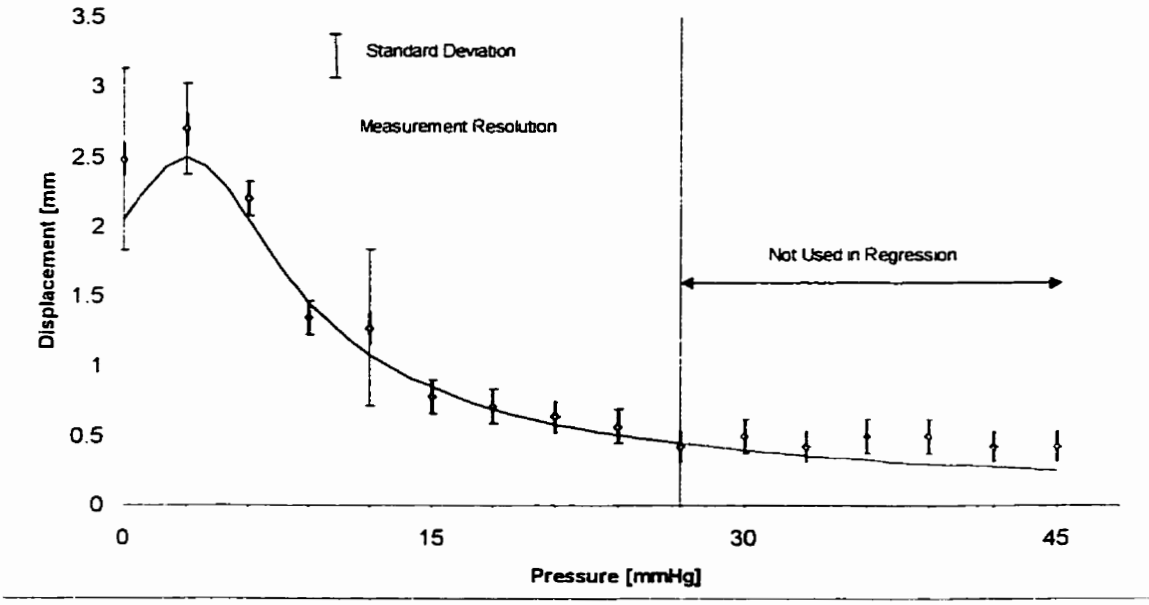

Plot of regression equation against the pressure dependence study data.

This regression gave the following "equivalent" parameters:

F = 0.0108 N

m = 0.00306 kg

c = 0.138 Ns/m

IMAGE EVALUATION
TEST TARGET (QA-3)

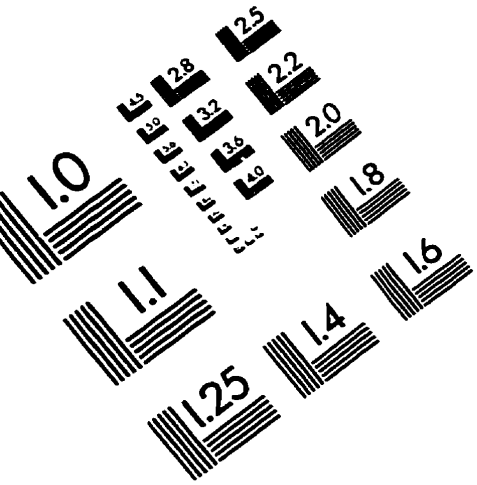

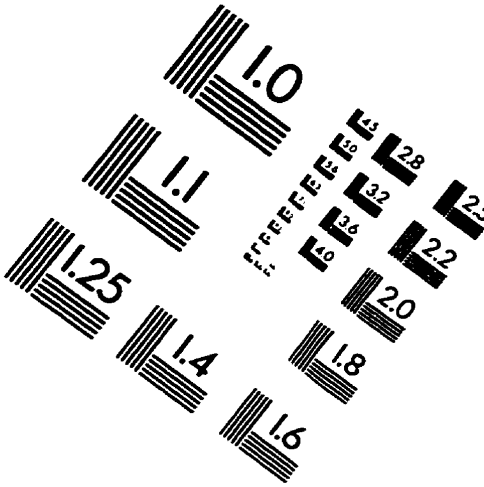

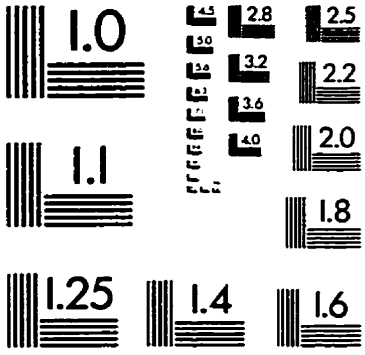

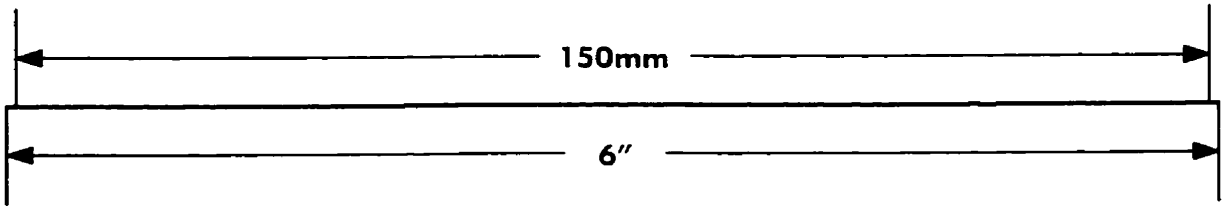

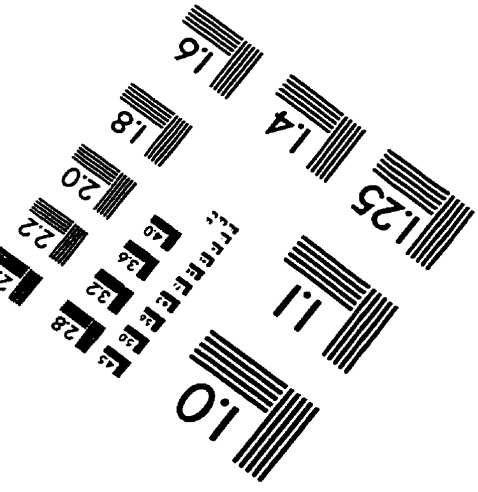

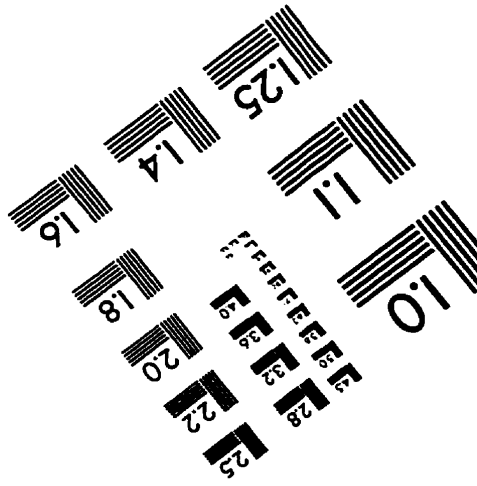

APPLIED IMAGE . Inc
1653 East Main Street
Rochester, NY 14609 USA
Phone: 716/482-0300
Fax: 716/288-5989